NOTE TO USERS

Université d'Ottawa · University of Ottawa

Université d'Ottawa · University of Ottawa

FACULTÉ DE ÉTUDES SUPÉRIEURES ET POSTDOCTORALES

FACULTY OF GRADUATE AND POSTDOCTORAL STUDIES

Valbona CELO

AUTEUR DE LA THÈSE - AUTHOR OF THESIS

Ph.D. (Chemistry)

GRADE - DEGREE

Department of Chemistry

FACULTÉ, ÉCOLE, DÉPARTEMENT - FACULTY, SCHOOL, DEPARTMENT

TITRE DE LA THÈSE - TITLE OF THE THESIS

Abiotic Pathway of Mercury Methylation in the Aquatic Environment

D. Lean

DIRECTEUR DE LA THÈSE - THESIS SUPERVISOR

CO-DIRECTEUR DE LA THÈSE - THESIS CO-SUPERVISOR

EXAMINATEURS DE LA THÈSE - THESIS EXAMINERS

J. Blais

R. Burke

H. Hintelmann

P. Mayer

J.-M. De Koninck, Ph.D.

LE DOYEN DE LA FACULTÉ DES ÉTUDES SUPÉRIEURES ET POSTDOCTORALES

DEAN OF THE FACULTY OF GRADUATE AND POSTDOCTORAL STUDIES

ABIOTIC PATHWAYS OF MERCURY METHYLATION IN THE AQUATIC ENVIRONMENT

Valbona Celo

Thesis submitted to the
Faculty of Graduate and Postdoctoral Studies
University of Ottawa
in partial fulfillment of the requirements for the
Ph.D. degree in the

Ottawa-Carleton Institute of Chemistry

Thèse soumise à
Faculté des études supérieures et postdoctorales
Université d'Ottawa
en vue de l'obtention du doctorat

L'Institut de chimie d'Ottawa-Carleton

Dr. David Lean
Research Supervisor

Valbona Celo
Ph.D. Candidate

Your file Votre référence
ISBN: 0-494-01679-5
Our file Notre référence
ISBN: 0-494-01679-5

To my sons, Erdit and Patrick for the greatest joy and love they bring in every day of my life

Abstract

This thesis studies the chemical reactions of mercury in different oxidations states with several natural methyl-donors present in the aquatic environment. The importance of the abiotic pathway of mercury methylation was assessed by a thorough examination of the kinetics of these reactions in various experimental conditions, relevant to environmental situations. The amount of methylmercury formed in the course of the chemical reactions studied herein shows that the abiotic mercury methylation can be a very significant source of this compound in the environment.

The thesis comprises three main chapters which describe the reactions of three major methyl-donors: methyl iodide, methycobalamine and methyl tin compounds with mercury. Reaction of mercuric ions with methyl iodide yields HgI^+ and HgI_2 as inorganic products and MeOH as the only organic product. The reaction kinetics are biphasic and the reaction rate decreases with pH, increases with temperature and the reaction stops in the presence of complexing agents such as iodide ions. Meanwhile, the reaction of $Hg^0_{(aq)}$ with methyl iodide yields 1.1% methylmercury which is a relatively high yield for environmental reactions. We show that the role of methyl iodide in the geochemical cycle of mercury in the aquatic environment is two-fold: it promotes the formation of compounds such as HgI^+ and HgI_2 which are less reactive towards chemical and biological methylation and it methylates Hg^0 which is present when Hg^{2+} is reduced by reducing agents found in the aquatic environment.

The reaction of mercuric ions with methylcobalamine is studied using methylaquacobaloxime as a model compound. The mechanism is an electrophilic attack of Hg^{2+} to the Co-C bond. It results in the cleavage of this bond and formation of Hg-C bond in the structure of methyl mercury. The reaction is first order to mercury and methylcobaloxime concentration and the value of the second-order rate constant is $k = (6.8 \pm 0.2)\ M^{-1}\ s^{-1}$ at 21.1°C, at a pH of 1.5 and an ionic strength of 0.030 M (HNO_3). The reaction rate decreases with pH, and increases with temperature and ionic strength .The yield of methyl mercury formation is as high as 75%. The presence of chloride

completely shuts down the reaction. So, abiotic methylation of mercury by methylcobalamin could be a source of methylmercury formation in fresh waters which have low pH and low chloride concentrations.

Reactions of mercuric ions with mono-, di and tri methyl tin chloride are fast and the yields of methylmercury at pH 10 and in the presence of 1M KCl were 80, 82 and 75% respectively. The rate constants increase significantly with the number of methyl groups in the structure of the methyl tin compounds. For reaction of mono-, di- and trimethyl tin chlorides with mercuric ions at 20°C, a pH of 10 and in 1M KCl, the rate constants were 15.9 ± 0.6 M^{-1} s^{-1}, 1.68 ± 0.03 M^{-1} s^{-1} and 0.084 ± 0.002 M^{-1} s^{-1} respectively. The reaction rates were significantly affected from the hydrolysis of methyltin compounds: increasing the pH significantly increases the rate constants. Also, the rate constants depend on mercury speciation: $HgCl_2$ is almost non-reactive and $HgCl_3^-$ reacts almost two times faster then $HgCl_4^{2-}$, with rate constants being k_{HgCl3} = 1.0 ± 0.1 M^{-1} s^{-1} and k_{HgCl4} = 0.46 ± 0.04 M^{-1} s^{-1} respectively. We show that the presence of methyltin compounds in sea water is a source of abiotic methylation of inorganic mercury.

Résumé

La présente thèse examine les réactions chimiques du mercure en différents états d'oxydation avec plusieurs donneurs naturels de méthyle présents dans le milieu aquatique. L'importance du parcours abiotique de la méthylation de mercure a été évaluée à travers d'un examen approfondi des cinétiques de ces réactions dans plusieurs conditions expérimentales, pertinentes aux situations environnementales. Le taux de méthyle de mercure formé durant les réactions chimiques étudiées montre que le parcours abiotique de la méthylation de mercure peut être une source importante de ce composé dans l'environnement.

La thèse comprend trois chapitres majeurs qui décrivent les réactions de trois principaux donneurs de méthyle: méthyle d'iode, méthyle cobalamine et des composés de méthyle d'étain avec du mercure. Les réactions des ions du mercure avec le méthyle d'iode produisent HgI^+ et HgI_2 comme produits inorganiques et MeOH comme l'unique produit organique. Les cinétiques de la réaction sont biphasiques et la vitesse de la réactions diminue avec le pH, augmente avec la température et la réaction s'arrête en présence des agents complexants tel que des ions d'iodure. Entre-temps, la réaction de $Hg^0_{(aq)}$ avec le méthyle d'iode produit 1.1 % de méthyle de mercure, un rendement qui est considéré relativement élevé pour des réactions environnementales. Nous montrons que le rôle du méthyle d'iode dans le cycle géochimique du mercure dans le milieu aquatique est double: il favorise la formation des composés tels que HgI^+ et HgI_2 qui sont moins réactifs vers la méthylation chimique et biologique et il méthyle Hg^0 qui est présent lorsque Hg^{2+} est réduit par des agents réducteurs présents dans le milieu aquatique.

La réaction des ions mercuriques avec le méthyle de cobalamine est étudiée en utilisant le methylaquacobaloxime comme composé de modèle. Le mécanisme est une attaque électrophile de Hg^{2+} sur la liaison Co-C. Ceci a comme conséquence le fendage de cette liaison, et la formation de la liaison Hg-C dans la structure du méthyle de mercure. La réaction est du premier ordre en fonction du mercure et de la concentration du methyle cobaloxime, et la valeur de la constante de vitesse du second ordre est k =

(6.8 ± 0,2) M^{-1} s^{-1} à 21.1°C, à un pH de 1.5 et une concentration ionique de 0.03 M (HNO_3). La vitesse de la réaction diminue avec le pH, et augmente avec la température et la concentration ionique. Le rendement de la formation du méthyle de mercure est aussi élevé que 75%. La présence du chlorure arrête la réaction complètement. Donc, la méthylation abiotique du mercure par le methyl cobalamine peut être une source de la formation de méthyle de mercure dans les eaux fraîches qui ont un pH bas et une faible concentration en chlorure.

Les réactions des ions mercuriques avec le mono-, bi- et tri- méthyle du chlorure d'étain sont rapides et le rendement du méthyle de mercure à un pH de 10 et en presence de KCl 1M étaient de 80, 82 et 75% respectivement. Les constantes de vitesse augmente de manière significative avec le nombre des groupes méthyliques dans la structure des composés de methyle d'étain. Pour les réactions du mono-, bi- et tri- méthyle du chlorure d'étain avec les ions mercuriques à 20°C, à un pH de 10 et en présence du KCl 1M, les constantes de vitesse étaient 15.9 ± 0.6 M^{-1} s^{-1}, 1.68 ± 0.03 M^{-1} s^{-1} et 0.084 ± 0.002 M^{-1} s^{-1} respectivement. Les vitesses des réactions ont été sensiblement affectées par le l'hydrolyse des composés de méthyle d'étain: une augmentation de pH affecte d'une manière significative les constantes de vitesse. Par ailleurs, les constantes de vitesse dépendent sur la spéciation du mercure: $HgCl_2$ est quasiment non-réactif et $HgCl_3^-$ réagit presque deux fois plus vite que $HgCl_4^{2-}$, avec des constantes de vitesse k_{HgCl3} = 1.0 ± 0.1 M^{-1} s^{-1} et k_{HgCl4} = 0.46 ± 0.04 M^{-1} s^{-1} respectivement.

Acknowledgements

Firstly, I would like to express my sincere thanks to my supervisors Dr. Susannah Scott and Dr. David Lean for their scientific, financial, and moral support throughout the completion of this thesis. They were always there for me with encouraging words and fresh ideas which helped me to carry on.

Much thanks also to the many other researchers, and grad students, who have been a great source of support and pleasant friendship along the way. Thanks to Tagenine Alladin, Marcel Beaudoin, Jonathan Holmes, Susan Winch, Nelson O'Driscoll... and the list goes on.

I need to thank my parents who have always encouraged and supported me to go forward in the long and exciting course of science and taught me to find the endless beauty of this road.

My final (and largest) thanks are to my husband, Dritan Celo. Thank you for putting up with me in my good and bad days, for being with me in every step and helping me to move forward. You are my greatest moral support, my adviser, and my partner in every sense.

This research was supported by NSERC Strategic Grant to Dr. Susannah Scott and Dr. David Lean, and OGS, SAD and Excellence scholarships to Valbona Celo

Table of Contents

CHAPTER 2

Experimental

CHAPTER 3

Abiotic Methylation of Aqueous Mercury by Methyl Iodide

CHAPTER 4

Reaction of Mercuric Ions with Methylcobaloxime

CHAPTER 5

Rates and mechanisms of mercury methylation by methyltin compounds

CHAPTER 6

Thesis Conclusions and Claims to Original Research

List of Figures

CHAPTER 2

CHAPTER 3

CHAPTER 4

CHAPTER 5

List of Tables

CHAPTER 1

CHAPTER 3

CHAPTER 4

CHAPTER 5

Chapter 1

General Introduction

1.1. Thesis rationale

The organomercurials known to be present in the aquatic environment are methyl-, ethyl- and phenylmercury. Amongst these compounds, methylmercury is the most abundant and also the most toxic form of mercury in the environment, while the levels of ethylmercury in natural waters are normally very low. Also, methylmercury is the only mercury compound that is bioaccumulated and biomagnified in the food chain. It represents up to 95% of total mercury in top predators, while no ethylmercury is found in fish of any trophic level.

The main sources of methylmercury in the aquatic environment are considered to be atmospheric deposition[1,2] and terrestrial runoff, especially from wetlands.[3,4] The relatively high levels of methylmercury found in sediments, biota and water require that other sources of methylmercury need to be identified. The internal processes, i.e., natural methylation of inorganic mercury in the water column and sediments should provide a significant contribution to the overall burden of methylmercury in the aquatic environment.[5]

The first demonstration of natural conversion of inorganic mercury to methylmercury was provided by Jensen and Jernelov, in 1969.[6] Although many studies

have already confirmed natural methylation of mercury, the mechanism of this process is still unknown. It is generally accepted that, methylmercury can be formed in the aquatic environment by two possible pathways: microbial metabolism (biotic processes) and chemical methylation (abiotic processes). Although it is now a common cliché that biotic processes account for most if not all of environmental mercury methylation, a number of highly respected investigators have recently provided evidence of abiotic mercury methylation.[7-12] However, the relative importance of abiotic methylation of mercury is still ambiguous.

The site of mercury methylation in the aquatic environment is still unclear. Many of the studies have shown that the methylation of inorganic mercury occurs mostly in the sediments,[13-20] while others claim that the methylation reactions in the water column are another plausible way of methylmercury formation in the aquatic environment.[21-25]

The purpose of this study is to determine the contribution of abiotic mechanisms for mercury methylation in the water column and the conditions under which this contribution may become important. We have studied the aqueous phase reactions of mercury in different oxidation states, i.e. $Hg^{2+}_{(aq)}$, and $Hg^{0}_{(aq)}$ with some of the potential methyl-donors known to be present in the environment.

It is recognized that the formation of methylmercury in aquatic systems is influenced by a wide variety of environmental factors.[16,22,26-30] The efficiency of microbial mercury methylation generally depends on factors such as microbial activity and the concentration of bioavailable mercury (rather than the total mercury pool), which in turn are influenced by temperature, pH, redox potential and the presence of inorganic and organic complexing agents. Also the rate, mechanism and products of chemical

reactions of methyl transfer are considerably affected by the same parameters which influence the reactive species concentration, such as pH, chloride concentration and ionic strength.

In this study we investigate the kinetics of the methylation reactions and the yield of methylmercury in different experimental conditions, relevant to different environmental circumstances such as pH, temperature, ionic strength and chloride concentration. The objective is to determine the mechanisms of these reactions and to evaluate the conditions in which contribution of abiotic pathway to the mercury methylation in the aquatic environment becomes important.

1.1.1 Biological pathway of mercury methylation

Biotic methylation of mercury was first described in 1968, when it was shown that a methylcobalamine-utilizing methanogenic bacterium causes methylation of mercury in sediments.[31] Since then, sediments containing microorganisms from several taxonomic groups have been shown to methylate inorganic mercury under laboratory conditions.[17,21,32-35] A number of studies indicate that sulfate-reducing bacteria (SRB) are the primary mercury methylators in freshwater and estuarine anoxic sediments.[13,14,18-20] Studies utilizing molybdate to inhibit microbial sulfate reduction resulted in up to 95% reduction of mercury methylation in sediments.[13,36] Sterilization of sediments also decreased methylation rates significantly.[37]

Nevertheless, the mechanism of biotic mercury methylation is still unclear. Methylcobalamin has been suggested to facilitate methyl group transfer.[38,39] Some data

suggest that the methyl group is derived from the amino acid serine,[40] while others show that methylmercury synthesis by the sulfate-reducing bacteria *Desulfovibrio desulfuricans* and other closely related organisms, involves the acetylcoenzyme A pathway, with methyl group transfer from methyltetrahydrofolate in conjunction with methylcobalamin.[39,41] Recently, Siciliano and Lean demonstrated the biological methylation of mercury by a methyltransferase pathway, similar to the biological synthesis of methionine by homocysteine.[42]

The biotic process of mercury methylation requires that a significant amount of mercury exists uncomplexed as "free Hg^{2+}" inside the cell.[39] However, mercury is the heavy metal cation with the highest toxicity to bacteria,[43] and it is still unknown why the SRB population is resistant to mercury while other bacteria are highly vulnerable.

Two observations created the impression that mercury methylation under natural conditions is exclusively biological. First, higher concentrations of methylmercury are found in sediments with high microbial activity. Second, no methylation is observed in sediments when microbial activity was inhibited by sterilization or by treatment with molybdate. However, these experiments do not prove that biological methylation causes all methylmercury formation. Chemical and physical sterilization techniques (using HCl or γ-radiation, respectively) are known to alter the chemical structure of sediments, and consequently mercury speciation, which would alter the potential of sediments for abiotic methylation. Additionally, the mechanism of SRB inhibition by molybdate is not yet known, and the assumption that molybdate does not affect the mercury bioavailability or abiotic methylation of mercury, has not been established.

In situ studies have demonstrated the potential for methylation by SRBs in lakes with pH values 4 to 6,[14,44,45] while laboratory studies show that the methylation of mercury by *Desulfovibrio desulfuricans* LS bacteria is highly pH dependent: the methylation rates reach a maximum at pH 7 and decrease significantly with decreasing pH. Nevertheless, other studies of mercury methylation in lake water have shown that decreasing the pH significantly increases the methylation rates and the methylmercury yield, although the respiration rates (which indicate the microbial activity) do not change significantly.[22,26] These conflicting findings show that biological methylation can not be the only pathway of mercury methylation, especially in acidic lakes.

Furthermore, microbial methylation of mercury is highly dependent on sulfate concentration. The optimum sulfate concentration for sulfate reducing bacteria to produce methylmercury is ca. 0.3 mM[14] and methylation completely stops when sulfate ions concentration is 5 mM.[8] The concentration of sulfates in seawater is relatively high (ca. 28 mM)[8] and so, the occurrence of methylmercury in the marine environment is not consistent with the biotic methylation hypothesis.

Methylmercury is also found in environments where biological activity is hardly expected, such as the atmosphere and Polar Regions. In the northern hemisphere, the amount of methylmercury entering the aquatic environment through wet deposition ranges from 0.39 to 2.9 mg ha^{-1} yr^{-1}.[5] Although the mechanism of methylmercury formation in the atmosphere is not yet clear,[1,2,46] it demonstrates that chemical methylation of mercury in natural conditions is possible.[47] Recent studies in the Arctic also show that methylmercury can be produced in Arctic wetlands at 4°C or less through

processes that implicate mechanisms other than SRBs activity and other microbial reactions.[48]

These observations suggest that methylation of mercury in the environment is not entirely a biological process. Therefore, it is reasonable to presume that the role of chemical reactions of mercury methylation is underestimated and that this role should be re-evaluated.

1.1.2 Abiotic contribution to mercury methylation

Purely chemical methylation of mercury is possible if suitable methyl donors are present. The methyl donors available in aqueous, particulate or sediment environments are mostly products of biological processes. However, methylation of mercury by these compounds is considered to be abiotic.[7,10,49]

The methyl-transfer reactions can proceed in three different ways: transfer of carbocation Me^+, carbanion Me^- or radical $Me^\bullet$,[49] depending on the chemical properties of methylation agents. Chemical reagents thought to lead to abiotic methylmercury formation include small organic molecules such as methyl iodide and dimethylsulfide, and larger organic components of dissolved organic matter such as fulvic and humic acids. Transmethylation reactions involving organometallic compounds such as methylcobalamin, methyllead, or methyltin compounds have also been considered as possible pathways for chemical methylation of mercury in the aquatic environment.

Methyl iodide is one of the most abundant potential methylators in the marine environment.[8] Although it may not directly transfer Me^+ to Hg(II), methylation by

oxidative addition to Hg^0 is possible.[7] In this study (Chapter 3), we examined the mechanism of the reaction of $Hg^{2+}_{(aq)}$ and $Hg^0_{(aq)}$ with methyl iodide and suggest the potential role of these reactions in methylmercury formation in environmental conditions.

Another plausible methyl donor is methylcobalamin, which can methylate Hg(II) abiotically, by transfer of the carbanion, Me^-.[50-54] The concentration of this compound in the aquatic environment is vanishingly low, ca. 0.9 μg/g sediment (dry weight)[8]. Previous studies have shown, the reaction is quite fast and methylmercury yield is high. The mechanism is most probably an electrophilic attack of Hg^{2+} to Me-Co bond.[55] In Chapter 4, we studied the mechanism of the reaction of aqueous mercuric solutions with methyl-(aqua)-bis (dimethylglyoximato)cobalt(III), a compound used to mimic the methylcobalamine chemistry, and showed the effect of pH, ionic strength, temperature and chloride in the rate of the reaction and the yield of methylmercury.

Methyl transfer from more abundant methyl tin compounds is considered more plausible. It was previously shown that the rates of these reactions are highly dependent on conditions such as pH, ionic strength, and temperature and chloride concentration.[56-59] However the mechanism of these reactions is not known yet and the information in the literature is inconsistent. Our study, presented in Chapter 5, showed that mono, di and trimethyltin compounds react with mercuric ions in aqueous solutions with rates and methylmercury yields, highly dependent on experimental conditions. When these conditions are optimal, the reactions are fast and the transformation of mercury to methylmercury is almost quantitative.

1.2 Chemistry of mercury

1.2.1 Discovery and occurrence

Mercury occurs naturally in the environment and exists in a large number of forms. The average proportion of mercury in the Earth's crust is about 5 x 10^{-5} %; it is 62nd in order of abundance.[60] It is rarely found in nature as the pure, liquid metal, but rather as inorganic salts in minerals. Although its average concentration is quite low, mercury often occurs in concentrated deposits, and almost always as the sulfide HgS (cinnabar). The world's largest deposit of cinnabar is at Almaden, in Spain. This deposit has been worked since Roman times. The content of mercury in minerals of this area is about 6% on average, which is exceptionally high. Other large mines are found in Tuscany (Italy), Idria (Slovenia), California (USA) and also in Russia, Mexico and Canada. Usually, the mercury content of the ore does not exceed 1%.[60]

Throughout history, deposits of cinnabar have been the source ores for commercial mining of metallic mercury. The metallic form is refined from mercuric sulfide ore by heating to temperatures above 540°C, in the presence of oxygen, iron metal or calcium oxide. This reduces and vaporizes the mercury in the ore, eq. 1-3; the vapors are then captured and cooled to yield liquid mercury.[60,61]

$$HgS_{(s)} + O_2 \rightarrow Hg_{(g)} + SO_{2(g)} \quad (1)$$

$$HgS_{(s)} + Fe_{(s)} \rightarrow Hg_{(g)} + FeS \quad (2)$$

$$4\ HgS_{(s)} + 4\ CaO \rightarrow Hg_{(g)} + 3\ CaS_{(s)} + CaSO_{4(s)} \quad (3)$$

The first three ionization potentials of Hg(0) are 10.43, 18.65 and 34.4 eV,[62] therefore chemical reactions will result in the removal of a maximum of two electrons from the mercury atom. Mercury exhibits a surprisingly different chemistry from its congeners, zinc and cadmium, a feature that is probably a consequence of the poor shielding of electrons in the completely filled $4f$ and $5d$ sublevels.[61]

1.2.2 Elemental mercury

Hg(0) has the electronic configuration (Xe) $4f^{14}\ 5d^{10}\ 6s^2$. Solid mercury has a distorted hexagonal crystal structure in which each mercury atom is surrounded by six nearest neighbors in adjacent close-packed planes and six more distant neighbors in the same plane. Mercury has an unusual low melting point (-39°C), which makes it the only metal which is liquid at room temperature. It has a high vapor pressure (1.9×10^{-3} mm/ 25°C),[60] indicative of very low interatomic forces, a high density (13.5 g cm^{-3} at 20°C),[61] a relatively low viscosity and an unusually high electrical resistivity (95.8 Ω cm),[61] which is higher than that of any other metal except bismuth. Mercury vapor, even at room temperature, is almost completely monatomic. Besides the noble gases, mercury is the only element that shows this behavior at such low temperatures.[60]

Mercury has long been known to readily dissolve many other metals to form alloys, termed amalgams. These may be simple solutions, compounds or mixtures of both, exactly as with the other alloy systems: they differ in often being liquid or pasty at room temperature. The solubility of mercury in air-free water is 3.3×10^{-7} mol L^{-1} at 25°C.[63,64]

1.2.3 Compounds of mercury(I)

Mercury is the only member of Group 12 to have a substantial chemistry in the +1 oxidation state. Hg(I) compounds can be prepared by the reduction of Hg(II) in aqueous acidic media. Hg(I) forms a polymetal cation, Hg_2^{2+} which exhibits metal-metal bonding.[60-62,65] Hg_2^{2+} disproportionate to Hg^{2+} and Hg^0, eq. 4:

$$Hg_2^{2+} \leftrightarrows Hg^0_{(l)} + Hg^{2+} \qquad K = [Hg^{2+}] / [Hg_2^{2+}] = 1.14 \times 10^{-2} \text{ at } 25^\circ C^{61} \quad (4)$$

The disproportionation is especially favored in the presence of ligands which coordinate strongly to Hg(II). The most important compounds of Hg(I) are the halides, which have a linear X-Hg-Hg-X structure. All are somewhat light-sensitive, and have very low solubility in water. They are also readily oxidized to mercury(II) oxyhalides.[60,61]

Several salts containing oxoanions, including the water-soluble nitrate, chlorate, perchlorate and water-insoluble bromate, iodate and sulfate, are also known. Hg_2^{2+} forms stable compounds with sulfur donor ligands such as $(Hg)_2(SCN)_2$ and nitrogen donor ligands such as ammonia. The chemical and physical properties of these compounds have been studied extensively.[60-62,65]

1.2.4 Compounds of mercury(II)

The mercuric ion, which has a d^{10} electronic configuration, exhibits neither paramagnetism nor 'd-d' transition spectra. Its radius is about the same as that of Ca^{2+}, but it is much more strongly polarizing as a result of the relatively inefficient shielding of the nucleus by the completed *4f* and *5d* shells. In acidified aqueous solutions of Hg^{2+}, in the presence of non-coordinating anions, mercury exists as $Hg(H_2O)_6^{2+}$ with a regular octahedral structure.[62]

The formation of hydroxo complexes was first studied by Hietanen and Sillen,[66] who found the two hydroxo species $HgOH^+$ and $Hg(OH)_2$ in aqueous solutions of $Hg(ClO_4)_2$ at concentrations up to 0.015 M. Several investigators have measured hydrolysis constants for aqueous solutions of Hg^{2+}, eq. 5-6:[62,67]

$$Hg^{2+} + H_2O \leftrightarrows HgOH^+ + H^+ \qquad \log K_1 = -3.48 \pm 0.033 \qquad (5)$$

$$Hg^{2+} + H_2O \leftrightarrows Hg(OH)_2 + 2\,H^+ \qquad \log(K_1K_2) = -6.18 \pm 0.02 \qquad (6)$$

Arnek and Kakolowicz suggested that the second acidity constant of Hg(II) is larger than the first one because two different processes are happening during hydrolysis of aqua mercuric ion $Hg(H_2O)_2^{2+}$: firstly the proton is split from the water molecule bound to mercury and then, from the OH bound to mercury.[67]

Compounds of Hg(II) with halides, oxide and sulfide ligands are all highly covalent. When dissolved in water, they remain largely undissociated, existing for example as discrete $HgCl_2$ or HgS molecules in solution. The oxide and hydroxide

(which has not been isolated) are very weak bases. The most common coordination arrangements are linear and tetrahedral, although five- and six-coordination are also known. [61]

1.2.5 Organomercury(II) compounds

In 1852, Edward Franklin synthesized the first organomercury compound, MeHgI, which was among the first organometallics reported. Some organomercurials are readily synthesized by direct reaction of mercuric salts with an aliphatic or aromatic compound.[68] The principal methods of making Hg-C bonds are based on the electrophilic behavior of mercuric salts in substitution and addition reactions.[69] They include transmetallation, mercury-for-hydrogen substitution, elimination of CO_2, SO_2 or SO_3 and oxidative addition.[70] The literature contains many reports on the preparation of organomercury compounds and their use in organic synthesis.[60,61,65,68,70]

Compared to organic compounds of zinc and cadmium, Hg-C bond is much less reactive towards water and oxygen.[70] Theoretical studies demonstrate that this bond is very stable in a large variety of chemical environments.[71-73] R-Hg-X compounds have normally linear structure which is thought to arise from *sp* hybridization at mercury.[72]

1.3 Mercury in the environment

Mercury enters the biosphere from both natural and anthropogenic sources. Natural sources include the release of naturally-occurring mercury from the Earth's crust, volcanic activity, evaporation from soil and water surfaces, weathering of rocks and forest fires. One of the most important anthropogenic sources is the emission of mercury impurities from fossil carbon fuels (i.e. coal, petroleum and natural gas) used in power, heat and other energy generation (the largest single source of atmospheric emissions). Also, mining and other metallurgic activities involving the extraction and processing minerals are essential in mercury release in the environment. Other sources involve incineration of products in municipal, medical and hazardous wastes, small-scale gold and silver mining (amalgamation), chlor-alkali production, dental amalgam fillings, manufacturing of products containing mercury, (fluorescent lamps, thermometers, manometers, electrical and electronic switches).

Although attempts to directly measure natural emissions are ongoing, investigations of glacial ice-cores over the past 270 years reveal that anthropogenic inputs contributed 52%, volcanic events 6% and background sources 42% of total mercury emissions in the environment.[74] The decline in mercury emissions that has been recorded during the last 10 years, is thought to be mostly due to the emission controls implemented in Europe and North America.[74]

Mercury is inherently a persistent pollutant, i.e., it cannot be broken down in the environment. Once released into the atmosphere, mercury returns to the Earth's surface via wet and dry deposition. Its residence time in the atmosphere is ca. one year[75] which

is sufficient for a redistribution of mercury over the entire planet before returning to the land, lakes, sea and ice. Consequently, mercury pollution is truly global, affecting the most remote areas of the planet. Historical records from lake sediments provide evidence that remote areas receive significant inputs of anthropogenic mercury by long-range atmospheric transport. [76]

As the only long-term sinks for removal of mercury from the biosphere are deep-sea sediments where mercury is either precipitated as HgS or adsorbed on sediments the process of mercury depletion from surface soils and water is very slow, despite recent measures taken to significantly decrease anthropogenic inputs.

1.4 Mercury in the aquatic environment

The most important sources of mercury in the aquatic environment are atmospheric input[77-79] and the land runoff.[80,81] The most abundant forms of mercury are soluble Hg(II) compounds. Some Hg(II) persists in this form, while some is trapped in particulate matter, and some is methylated by chemical and/or biological processes. Contaminated sediments at the bottom of surface waters can serve as an important mercury reservoir, with sediment-bound mercury recycling back into the aquatic ecosystem for decades or longer. Chemical and/or biological processes reduce some of the Hg(II) to Hg(0),[82] which is returned to the atmosphere through volatilization, scavenged by particles and transported deeper in oceanic waters or retained in the watersheds. The flux of mercury from water to air and *vice versa* is a very complex process which depends on physical factors (Henry's Law, solubility of Hg(0)) and environmental conditions (salinity, wind

speed, temperature) and plays a very important role in understanding the cycle of mercury in the aquatic environment.[83]

Sediments are the ultimate sink for mercury in the aquatic environment. However, they also play an important role in mercury cycling due to a whole series of chemical and biological transformations which account for reduction, complexation and methylation of mercury.

Mercury in the water column is either dissolved or absorbed (chemically or physically) to the particulate matter. Concentrations of dissolved mercury in the ocean waters are very low, usually below 1 ng L^{-1}, Table 1.1, of which a portion is present as soluble chloro complexes and the remainder is bound to particles. Mercury concentrations in coastal areas are higher than in the open sea, due to the greater abundance and deposition of particulate mercury. Concentrations of dissolved mercury in coastal areas range from 0.3 to 1.6 ng L^{-1}, while particulate mercury ranges from 0.05 to 1 μg g^{-1} in uncontaminated areas to several μg g^{-1} in contaminated areas.[84]

The nature of particulate mercury is uncertain. Babiarz et al. studied the partitioning of mercury and methyl mercury to the particulate phase in freshwater and calculated the distribution coefficients 5 x 10^3 and 2.5 x 10^6, respectively, using 0.4 μm as the boundary between the particulate phase and the dissolved phase.[85] Although the distribution coefficients depend on pH, ionic strength and dissolved organic matter concentration, their high values account for the high percentage of mercury and methylmercury found in the particulate phase.

Dissolved mercury is distributed among hydroxide complexes ($Hg(OH)^+$, $Hg(OH)_2$ and $Hg(OH)_3^-$) and chloride complexes ($HgCl^+$, HgOHCl, $HgCl_2$, $HgCl_3^-$,

$HgCl_4^{2-}$), depending on pH and salinity. Nearly 95% of oxidized inorganic mercury in lakes forms stable complexes with dissolved organic matter. [86-88] In deep, anoxic waters and in sediments, mercuric ion exhibits an extremely high affinity for sulfide, so that the main species are sulfide and bisulfide complexes ($Hg(SH)_2$, $HgS(SH)^-$ and HgS_2^{2-}) even at total sulfide concentrations as low as 1 nM.[89-92]

The oxidation of Hg(0) to Hg(II) in natural waters by oxygen occurs in natural fresh and sea water. It is enhanced by the presence of chloride, photoactive compounds such as fulvic acids, light and the appropriate particulate surfaces.[82,93,94] In coastal areas, where the particulate matter loading is higher, the oxidation rate can be as high as 10% per hour.[95]

Complexation reactions play a significant role in the biogeochemistry of aquatic mercury. Natural organic matter (NOM), especially humic substances, are the most important complexing compounds of mercury in the aquatic environment.[86,88,96,97] Both mercuric and methylmercury ions have a high affinity for the reduced sulfur sites of NOM,[98,99] forming very strong complexes with conditional stability complexes ranging from 1.1×10^{13} to 1×10^{14} for strong binding sites and 1.4×10^{12} to 1.2×10^{13} for weak binding sites on freshwater humic substances.[87]

Hg(II) in surface and deep waters is reduced to Hg^0 by biological and chemical processes such as microbial reduction,[35,100] photoreduction[101,102] and reduction by humic substances.[103] The mechanisms of these processes are still uncertain. It is believed that the microbial reduction is induced by mer-operon bacteria in highly contaminated waters,

Table 1.1 Mercury concentrations in ocean and coastal waters[77]

	Dissolved Hg ng L^{-1}	Particulate Hg $\mu g\ g^{-1}$	Other forms of Hg
Rivers			
non-contaminated	0.3 – 1.0	0.044 – 1.40	MeHgX: 1-10% of particulate
contaminated	2 – 4	1.2 – 30	Hg; <1% of dissolved Hg
			Hg^0: < 0.2 ng L^{-1}
			Me_2Hg: not detectable
Lakes[105]	0.16 – 3.6	0.09 – 1.7	MMHg in ng L^{-1}:
			0.1 – 2.8 (total)
			0.02 – 0.87 (dissolved)
Coastal areas			
near shore	0.5 – 2.0	0.04 – 1.88	MeHgX: 3% of particulate Hg
offshore	0.2 – 0.4		5-50 pg L^{-1} in contaminated
contaminated area	0.6 – 2.3	0.1 – 2.14	areas
			Me_2Hg: up to 58 pg L^{-1}
Ocean			
NW Atlantic	0.6 – 1.3	low abundance of	MeHgX: < 20 pg L^{-1}
NE Pacific	0.2 – 0.6	particulates	Hg^0: 40 – 80 pg L^{-1}
Mediterranean Sea	0.1 – 0.8		Me_2Hg: <10% of total Hg

while photoreduction is more important in clean waters, and may be enhanced by the presence of iron, manganese or humic acids.[103,104]

1.5 Ecotoxicology of mercury

Toxicological, ecological and environmental studies of mercury received special interest starting in the 1950s, as a result of the Minamata disaster. Methylmercury poisoning resulted from ingestion of fish and shellfish contaminated by mercury-containing industrial effluents discharged into Minamata Bay, Japan. A second incident occurred in Niigata, Japan, for the same reason. Between them, they accounted for several hundred deaths and a large number of non-fatal victims. In the late 1950s and again in 1972, methyl- and ethylmercury poisonings occurred in Iraq following consumption of seed grain that had been treated with fungicides containing organomercury compounds. Thousands were admitted to the hospitals with symptoms of mercury poisoning and about 600 people died.

The toxicity of mercury and its compounds is believed to be determined by the amount of mercury binding to the receptors of target molecules,[106] although the exact binding sites of mercury inside the cell are not known yet. The mechanism of toxicity is highly dependent on mercury speciation. Acute exposure to high levels of elemental mercury (> 1 mg m^{-3}) can cause pneumonitis and lung damage, while inorganic compounds of mercury primarily target the kidneys.[106] Methylmercury, which is by far the most toxic compound of mercury in environment, selectively damages the adult central nervous system and developing brain. A particularly disturbing observation made

following the Minamata outbreak was that an unborn child could experience brain damage from parental exposure even if the mother was little affected.

Methylmercury is also the only form of mercury which is biomagnified in food chains. Levels of methylmercury in biota are much higher than the environment (water or sediments) where they live. In 1992 Bloom showed that most of the mercury in edible fish tissue and mussels is as methylmercury.[107] Since most of the methylmercury in fish tissue is covalently bound to sulfhydryl groups of proteins, it has a long half-life for elimination (about two years).[108] This accounts for a high biomagnification of methylmercury in the food chain. Exceptionally high biomagnification is observed in older fish at higher trophic levels. Consequently, fish consumption is considered a major route for human exposure to methylmercury. Several countries have issued consumption advisories for fish, and sometimes marine mammals. People, especially those in sensitive subgroups (such as pregnant women and young children) are warned to limit or avoid consumption of certain types of fish.

In 1991, the WHO concluded that the lowest observed adverse effects level (LOAEL) associated with the risk of prenatal poising is 10 to 20 $\mu g\ g^{-1}$ in maternal hair and 40 to 80 $\mu g\ L^{-1}$ in blood, while the no adverse effect level (NOAEL) or safe level is 6 $\mu g\ g^{-1}$ in hair and 20 $\mu g\ L^{-1}$ in whole blood.[109] The US National Research Council estimates the NOAEL to be 44 $\mu g\ L^{-1}$ total mercury in blood or 11 $\mu g\ g^{-1}$ total mercury in maternal hair.[110]

Mercury also has a significant impact on wildlife. Abnormal behaviors among animals and birds were the first signs of the disaster in Minamata Bay. Hatching success

for loons in Canadian lakes is inversely correlated with elevated levels of methylmercury in their blood.

As mentioned above, the formation of methylmercury and its accumulation in the food chain is a current international crisis that demands attention to the details of mechanisms of mercury transformation and methylation.

References

(1) Hall, B.; Bloom, N. S.; Munthe, J. *Water Air Soil Poll.* **1995,** *80*, 337-341.

(2) Munthe, J.; Hultberg, H.; Iverfeldt, A. *Water Air Soil Poll.* **1995,** *80*, 363-371.

(3) Louis, V. L. S.; Rudd, J. W. M.; Kelly, C. A.; Beaty, K. G.; Flett, R. J.; Roulet, N. T. *Environ. Sci. Technol.* **1996,** *30*, 2719-2729.

(4) Driscoll, C. T.; Holsapple, J.; Schofield, C. L.; Munson, R. *Biogeochemistry* **1998,** *40*, 137-146.

(5) Rudd, J. W. M. *Water Air Soil Poll.* **1995,** *80*, 697-713.

(6) Jensen, S.; Jernelov, A. *Nature* **1969,** *223*, 753-754.

(7) Craig, P. J. Organometallic compounds in the environment; Longman: London, 1986.

(8) Weber, J. H. *Chemosphere* **1993,** *26*, 2063-2077.

(9) Ebinghaus, R.; Wilken, R. D. *Appl. Organomet. Chem.* **1993,** *7*, 127-135.

(10) Falter, R.; Wilken, R.-D. *Vom Wasser* **1998,** *90*, 217-231.

(11) Falter, R. *Chemosphere* **1999,** *39*, 1075-1091.

(12) Falter, R. *Chemosphere* **1999,** *39*, 1051-1073.

(13) Compeau, G. C.; Bartha, R. *Appl. Environ. Microbiol.* **1985,** *50*, 498-502.

(14) Gilmour, C. C.; Henry, E. A.; Mitchell, R. *Environ. Sci. Technol.* **1992,** *26*, 2281-2287.

(15) Zhang, L.; Planas, D. *Bull. Environ. Contam. Toxicol.* **1994,** *52*, 691-698.

(16) Choi, S.-C.; Bartha, R. *Bull. Environ. Contam. Toxicol.* **1994,** *53*, 805-812.

(17) Farrell, R. E.; Huang, P. M.; Germida, J. J. *Appl. Organomet. Chem.* **1998,** *12*, 613-620.

(18) King, J. K.; Saunders, F. M.; Lee, R. F.; Jahnke, R. A. *Environ. Toxicol. Chem.* **1999,** *18*, 1362-1369.

(19) King, J. K.; Kostka, J. E.; Frischer, M. E.; Saunders, F. M. *Appl. Environ. Microbiol.* **2000,** *66*, 2430-2437.

(20) King, K. J.; Kostka, J. E.; Frischer, M. E.; Saunders, F. M.; Jahnke, R. A. *Environ. Sci. Technol.* **2001,** *35*, 2491-2496.

(21) Furutani, A.; Rudd, J. W. M. *Appl. Environ. Microbiol.* **1980,** *40*, 770-776.

(22) Miskimmin, B. M.; Rudd, J. W. M.; Kelly, C. A. *Can. J. Fish. Aquat. Sci.* **1992,** *49*, 17-22.

(23) Regnell, O. *Environ. Pollut.* **1994,** *84*, 7-13.

(24) Matilainen, T.; Verta, M. *Can. J. Fish. Aquat. Sci.* **1995,** *52*, 1597-1608.

(25) Mauro, J. B. N.; Guimaraes, J. R. D.; Hintelman, H.; Watras, C. J.; Haack, E. A.; Ceolho-Souza, S. A. *Anal. Bioanal. Chem.* **2002,** *374*, 983-989.

(26) Xun, L.; Campbell, N. E. R.; Rudd, J. W. M. *Can. J. Fish. Aquat. Sci.* **1987,** *44*, 750-757.

(27) Miskimmin, B. M. *Bull. Environ. Contam. Toxicol.* **1991,** *47*, 743-750.

(28) Watras, C. J.; Morrison, K. A.; Bloom, N. S. *Water Air Soil Poll.* **1995,** *84*, 253-267.

(29) Mauro, J. B. N.; Guimaraes, J. R. D.; Melamed, R. *Appl. Organomet. Chem.* **1999,** *13*, 631-636.

(30) Matilainen, T.; Verta, M.; Korhonen, H.; Rauva, A. U. ; Niemi, M. *Water Air Soil Poll.* **2001,** *125*, 105-119.

(31) Wood, J. M.; Kennedy, F. S.; Rossen, C. G. *Nature* **1968,** *220*, 173-174.

(32) Fischer, R. G.; Rapsomanikis, S.; Andreae, M. O. *Environ. Sci. Technol.* **1995,** *29*, 993-999.

(33) Vaithiyanathan, P.; Richardson, C. J.; Kavanaugh, R. G.; Craft, C. B.; Barkay, T. *Environ. Sci. Technol.* **1996,** *30*, 2591-2597.

(34) Pak, K. R.; Bartha, R. *Appl. Environ. Microbiol.* **1998,** *64*, 1987-1990.

(35) Siciliano, S. D.; O'Driscoll, N.; Lean, D. *Environ. Sci. Technol.* **2002,** *36*, 3064-3068.

(36) Chen, Y.; Bonzongo, J.-C. J.; Lyons, W. B.; Miller, G. C. *Environ. Toxicol. Chem.* **1997,** *16*, 1568-1574.

(37) Berman, M.; Bartha, R. *Bull. Environ. Contam. Toxicol.* **1986,** *36*, 401-404.

(38) Choi, S.-C.; Bartha, R. *Appl. Environ. Microbiol.* **1993,** *59*, 290-295.

(39) Choi, S.-C.; Chase, T.; Bartha, R. *Appl. Environ. Microbiol.* **1994,** *60*, 1342-1344.

(40) Berman, M.; Chase, T.; Bartha, R. *Appl. Environ. Microbiol.* **1990,** *56*, 298-300.

(41) Choi, S.-C.; Chase, T.; Bartha, R. *Appl. Environ. Microbiol.* **1994,** *60*, 4072-4077.

(42) Siciliano, S. D.; Lean, D. *Environ. Toxicol. Chem.* **2002,** *21*, 1184-1190.

(43) Nies, D. H. *App. Microbiol. Biotechnol.* **1999,** *51*, 730-750.

(44) Pak, K. R.; Bartha, R. *Appl. Environ. Microbiol.* **1998,** *64*, 1013-1017.

(45) Macalady, J. L.; Mack, E. E.; Nelson, D. C.; Scow, K. M. *Appl. Environ. Microbiol.* **2000,** *66*, 1476-1488.

(46) Tokos, J. J. S.; Hall, B.; Calhoun, J. A.; Prestbo, E. M. *Atmos. Environ.* **1998,** *32*, 823 -827.

(47) Gardfeldt, K.; Munthe, J.; Stromberg, D.; Lindqvist, O. *The Science of the Total Environment* **2003,** *304*, 127-136.

(48) Loseto, L., Methyl mercury formation in the arctic;M.Sc.Thesis University of Ottawa: Ottawa, 2001;

(49) Krishnamurthy, S. *Chem. Environ.* **1992,** *69*, 347-350.

(50) Nobumasa, I.; Eiji, S.; Shoe-Kung, P.; Kiyoshi, N.; Jong-Yoon, K.; Kwan, T.; Tyunosin, U. *Science* **1971,** *172*, 1248-1249.

(51) Bertilsson, L.; Neujahr, H. Y. *Biochemistry* **1971,** *10*, 2805-2808.

(52) DeSimone, R. E.; Penley, M. W.; Charboneau, L.; Smith, S. J.; Wood, J. M.; Jill, H. A. O.; Pratt, J. M.; Ridsdale, S.; Williams, R. J. P. *Biochim. Biophys. Acta* **1973,** *304*, 851-863.

(53) Chu, V. C. W.; Gruenwedel, D. W. *Bioinorg. Chem.* **1977,** *7*, 169-186.

(54) Filippelli, M.; Baldi, F. *Appl. Organomet. Chem.* **1993,** *7*, 487-493.

(55) Adin, A.; Espenson, J. H. *Chem. Commun.* **1971,** *13*, 653-654.

(56) Jewett, K. L.; Brinckman, F. E.; Bellama, J. M. In Organometals and organometalliods: Occurrence and fate in the environment; Brinckman, F. E., Bellama, J. M., Eds.; American Chemical Society: Washington, D.C., 1978; Vol. 82, pp 158 -185.

(57) Bellama, J. M.; Jewett, K. L.; Nies, J. D. In Environmental inorganic chemistry; Irgolic, K. J., Martell, A. E., Eds.; VCH: Deerfield Beach, Fla., 1985; pp 239- 247.

(58) Brinckman, F. E., Ed. Environmental inorganic chemistry of main group elements with special emphasis on their occurrence as methyl derivatives; VCH: Deerfield Beach, Fla., 1985.

(59) Cerrati, G.; Bernhard, M.; Weber, J. H. *Appl. Organomet. Chem.* **1992,** *6*, 587-595.

(60) Bailar, J. C., Jr.; Emeleus, H. J.; Nyholm, S. R.; Trotman-Dickenson, A. F. Comprehensive inorganic chemistry; Pergamon Press: Elmsford, N.Y., 1973; Vol. 3.

(61) Grant, G. J., Ed. Mercury: Inorganic and coordination chemistry; Wiley: Chichester, New York, 1994; Vol. 4.

(62) Brodersen, K.; Hummel, H.-U. In Comprehensive coordination chemistry. The synthesis, reaction, properties and applications of coordination compounds; Gillard, R. D., McCleverty, J. A., Eds.; Pergamon Press: Toronto, 1987; Vol. 5. Late Transition Elements, pp 1047-1097.

(63) Choi, S. S.; Tuck, D. G. *J. Chem. Soc.* **1962,** 4080.

(64) Clever, H. L.; Johnson, S. A.; Derrick, M. E. *J. Phys. Chem. Ref. Data* **1985,** *14*, 632-680.

(65) Constable, E. C. *Coord. Chem. Rev.* **1984,** *58*, 53-85.

(66) Hietanen, S.; Sillen, L. G. *Acta Chem. Scand.* **1952,** *6*, 747.

(67) Arnek, R.; Kakolowicz, W. *Acta Chem. Scand.* **1967,** *21*, 1449-1456.

(68) Larock, R. C. Organomercury compounds in organic synthesis; Springer- Verlag: New York, 1985.

(69) Jensen, F. R.; Rickborn, B. Electrophilic substitutions of organomercurials; McGraw Hill: New York, 1968.

(70) Aylett, B. J., Ed. Organometallic derivatives of the main group elements; Butterworths University Park: London, 1975; Vol. 4.

(71) Barone, V.; Bencini, A.; Totti, F.; Uytterhoeven, M. G. *J. Phys. Chem.* **1995,** *99*, 12743-12750.

(72) Adams, D. M.; Pogson, M. *J. Phys. Chem.* **1988,** *21*, 1065-1079.

(73) Hounslow, A. M.; Lincoln, S. F.; Tiekink, R. T. *J. Organomet. Chem.* **1988,** *354*, C9-C11.

(74) Schuster, P. F.; Krabbenhoft, D. B.; Naftz, D. L.; Dewayne, L. C.; Olson, M. L.; Dewild, J. F.; Susong, D. D.; Green, J. R.; Abbott, M. L. *Environ. Sci. Technol.* **2002,** *36*, 2303-2310.

(75) Loon, L. L. V.; Mader, E. A.; Scott, S. L. *J. Phys. Chem. A* **2001,** *105*, 3190-3195.

(76) Fitzgerald, W. F.; Engstrom, D. R.; Mason, R. P.; Nater, E. A. *Environ. Sci. Technol.* **1998,** *32*, 1-12.

(77) Horvat, M.; Covelli, S.; Faganeli, J.; Logar, M.; Mandic, V.; Rajar, R.; Sirca, A.; Zagar, D. *Sci. Total Environ,* **1999,** *237/238*, 43-56.

(78) Watras, C. J.; Morrison, K. A.; Hudson, R. J. M.; Frost, T. M.; Kratz, T. K. *Environ. Sci. Technol.* **2000,** *34*, 4051- 4057.

(79) Malcolm, E. G.; Keeler, G. J. *Environ. Sci. Technol.* **2002,** *36*, 2815-2821.

(80) Rencz, A. N.; O'Driscoll, N. J.; Hall, G. E. M.; Peron, T.; Telmer, K.; Burgess, N. M. *Water Air Soil Poll.* **2003,** *143*, 271-288.

(81) Page, K. D.; Murphy, B. J. *Environ. Geol.* **2003,** *43*, 882-891.

(82) Lalonde, J. D.; Amyot, M.; Kraeppiel, A. M. L.; Morel, F. M. M. *Environ. Sci. Technol.* **2001**, *35*, 1367-1372.

(83) Poissant, L.; Amyot, M.; Pilote, M.; Lean, D. *Environ. Sci. Technol.* **2000**, *34*, 3069-3078.

(84) Horvat, M. In Global and regional mercury cycles: Sources, fluxes and mass balances; Baeyens, W., Ebinghaus, R., Vasiliev, O., Eds.; Kluwer Academic: Netherlands, 1996.

(85) Babiarz, C. L.; Hurley, J. P.; Hoffmann, S. R.; Andren, A. W.; Shafer, M. M.; Armstrong, D. E. *Environ. Sci. Technol.* **2001**, *35*, 4773-4782.

(86) Hintelmann, H.; Welbourn, P. M.; Evans, R. D. *Water Air Soil Poll.* **1995**, *80*, 1031-1034.

(87) Hintelmann, H.; Welbourn, P. M.; Evans, R. D. *Environ. Sci. Technol.* **1997**, *31*, 489-495.

(88) O'Driscoll, N.; Evans, R. D. *Environ. Sci. Technol.* **2000**, *34*, 4039- 4043.

(89) Paquette, K. E.; Helz, G. R. *Environ. Sci. Technol.* **1997**, *31*, 2148-2153.

(90) Jay, J. A.; Morel, F. M. M.; Hemond, H. F. *Environ. Sci. Technol.* **2000**, *34*, 2196-2200.

(91) Benoit, J. M.; Gilmour, C. C.; Mason, R. P.; Heyes, A. *Environ. Sci. Technol.* **1999**, *33*, 951-957.

(92) Benoit, J. M.; Gilmour, C. C.; Mason, R. P. *Environ. Sci. Technol.* **2001**, *35*, 127-132.

(93) Yamamoto, M. *Chemosphere* **1996**, *32*, 1217-1224.

(94) Lalonde, J. D.; Poulain, A. J.; Amyot, M. *Environ. Sci. Technol.* **2002**, *36*, 174- 178.

(95) Amyot, M.; Gill, G. A.; Morel, F. M. M. *Environ. Sci. Technol.* **1997,** *31*, 3606-3611.

(96) Amirbahman, A.; Reid, A. L.; Haines, T. A.; Kahl, J. S.; Arnold, C. *Environ. Sci. Technol.* **2002,** *36*, 690-695.

(97) Haitzer, M.; Aiken, G. R.; Ryan, J. N. *Environ. Sci. Technol.* **2002,** *36*, 3564-3570.

(98) Khwaja, A. R.; Lin, C. J.; Brezonik, P.; Bloom, P. R. In *223rd ACS National Meeting*; American Chemical Society: Orlando, FL, 2002.

(99) Hesterberg, D.; Chou, J. W.; Hutchison, K. J.; Sayers, D. E. *Environ. Sci. Technol.* **2001,** *35*, 2741-2745.

(100) Mason, R. P.; Morel, F. M. M.; Hemond, H. F. *Water Air Soil Poll.* **1995,** *80*, 775-787.

(101) Amyot, M.; Lean, D.; Mierle, G. *Environ. Toxicol. Chem.* **1997,** *16*, 2054-2063.

(102) Amyot, M.; Mierle, G.; Lean, D.; McQueen, D. J. *Geochim. Cosmochim. Acta* **1997,** *61*, 975-988.

(103) Rocha, J. C.; Junior, E. S.; Zara, L. F.; Rosa, A. H.; Santos, A. d.; Burba, P. *Talanta* **2000,** *53*, 551-559.

(104) Morel, F. M. M.; L.Kraepiel, A. M.; Amyot, M. *Annu. Rev. Ecol. Syst.* **1998,** *29*, 543-566.

(105) Watras, C. J.; Morrison, K. A.; Bloom, N. S. *Water Air Soil Poll.* **1995,** *84*, 253-267.

(106) Clarkson, T. W. *Critical Reviews in the Clinical Laboratory Sciences* **1997,** *34*, 369-403.

(107) Bloom, N. S. *Can. J. Fish. Aquat. Sci.* **1992,** *49*, 1010-1140.

(108) UNEP "Global mercury assessment," United Nations Environmental Program., 2002.

(109) WHO "Environmantal health criteria 101: Methylmercury," World Health Organization, 1991.

(110) NRC "Toxicological effects of methylmercury," Committee on the toxicological effects of methylmercury, Board on Environmental Studies and Toxicology, Commission of Life Sciences, National Research Council, 2000.

Chapter 2

Experimental

2.1 Introduction

The experimental part of this thesis was designed to fulfill three main purposes: preparation of solutions of known concentration, evaluation of analytical methods used for different quantitative analyses and setting up reliable kinetic probes for the reactions studied herein.

All solutions were prepared in Milli-Q deionized water (18.2 MΩ resistivity) in glass bottles and handled with all-glass syringes and analytical micropipettes (Eppendorf). The glassware was cleaned with aqueous HNO_3 (1:1 v/v) and rinsed thoroughly with deionized water prior to use.

2.2 Preparation and standardization of stock and working solutions

2.2.1 Hg(II) solutions

Hg(II) solutions were prepared by dissolving a measured amount of red HgO (Aldrich, 99.999%) in concentrated $HClO_4$ (Analr, 70%) and diluted to produce stock solutions of approximately 20 mM Hg^{2+} in 0.2 M $HClO_4$. These solutions were standardized by

titration with 0.05 M KSCN (Baker ACS Reagent) to the ferric alum endpoint.[1] The indicator, $(NH_4)Fe(SO_4)_2 \cdot 12H_2O$ (Aldrich, 99%) was dissolved in 6 M HNO_3 (EM Science, ACS Reagent 98%). 20 mL of the mercury solution was titrated with the KSCN solution, in presence of 10 mL 6M HNO_3 until the appearance of a light red-brown colour. The titration proceeds as follows, eq 1-3:

$$Hg(SCN)^+ + SCN^- \leftrightarrows Hg(SCN)_2 \quad (1)$$

$$Hg(SCN)^+ + Hg^{2+} \leftrightarrows 2\ Hg(SCN) \quad (2)$$

$$Fe^{3+} + SCN^- \rightarrow Fe(SCN)^{2+} \quad (3)$$

Hg^{2+} solutions prepared in this way were stable for up to two months. Diluted solutions were prepared daily as needed.

Other mercuric compounds used occasionally were 20 mM $HgCl_2$ (Fisher Scientific, 99.5%) dissolved in 0.2 M HCl (EM Science, ACS Reagent 98%), 20 mM $Hg(NO_3)_2$ (Fisher Scientific, 99.9%) dissolved in 0.2 M HNO_3 and 20 mM $Hg(O_2CCH_3)_2$ dissolved in 0.2 M $HClO_4$. The same method was used for their standardization. Dilutions were made daily, prior to use.

2.2.2 Hg(I) solutions

Hg(I) solutions were normally prepared by dissolving a measured amount of mercurous acetate $Hg_2(O_2CCH_3)_2$ (Fisher Scientific, purified) in concentrated $HClO_4$ and diluted to prepare a stock solution of approximately 20 mM Hg_2^{2+} in 0.2 M $HClO_4$. The exact

concentration of the solution was calculated from the absorbance and the known extinction coefficient of Hg_2^{2+} aqueous solutions at 236 nm ($\varepsilon = 2.8 \times 10^4\ M^{-1}\ cm^{-1}$).[2,3]

The stock solution prepared in this way was stable for up to one month. Diluted solutions were prepared daily as needed.

2.2.3 Hg^0 solutions

Saturated solutions of Hg^0 (Aldrich, 99.9995%) were prepared by stirring a drop of liquid mercury in water for 2-3 days. The mercury drop was first placed in a glass bottle and washed five times with 2 mL 0.1 M $HClO_4$ and 10 times with 5 mL deionized water.[4] The bottle was then filled completely with deionized water, closed with a rubber septum and purged with oxygen-free argon for 2 hours. Finally, the solution was stirred for two days to ensure that saturation of Hg^0 in water was achieved.

The concentration of Hg^0 in this solution was determined by the dithizone method.[5] This method is based on the absorbance of the Hg^{2+} complex with dithizone in chloroform at 496 nm. First, 50 mL of a saturated Hg^0 solution was boiled for 30 min with 100 μL 5% $KMnO_4$ and 1 mL concentrated H_2SO_4 to ensure that all Hg^0 was oxidized to Hg^{2+}. Then 0.5 mL 5% $K_2S_2O_8$ was added and the solution was allowed to cool. A few drops of $NH_2OH \cdot HCl$ were added to discharge the pink color of the solution. The solution was transferred to a 250 mL separatory funnel where 2 mL buffer (10.7 g $Na_2HPO_4 \cdot 7H_2O$ (Fisher Scientific, ACS grade) and 3.8 g K_2CO_3 (Fisher Scientific, ACS grade) in 100 mL deionized water) and 2 mL 6 μg/mL dithizone in chloroform were added. The funnel was shaken and the organic phase was collected.

Extraction with dithizone was repeated three times and the extracts combined. The orange mercury-dithizone complex in chloroform was filtered into a quartz cuvette through a microcolumn filled with Na_2SO_4 crystals and the absorbance at 496 nm measured.

The concentration of total mercury ($Hg^{2+} + Hg^0$) in solution was calculated based on a calibration curve made with a stock solution of 100 μg/mL $HgCl_2$ in 0.02 M HNO_3, Figure 2.1. The same procedure was then repeated except for the oxidation step, in order to measure the concentration of Hg^{2+}. The difference in these two measurements represents the Hg^0 content of the sample. Using this method, we found that the concentration of a saturated solution of $Hg^0_{(l)}$ is (2.6 ± 0.5) x 10^{-7} M (three separate replicates of three different solutions), which is in reasonable agreement with previously reported values (1.8- 2.3 x 10^{-7} M)[4] and 3.30 x 10^{-7} M.[6]

Solutions prepared in this way are not stable, either due to evaporation of mercury vapor or its adsorption on the glass walls of its container. For this reason, solutions were freshly prepared as needed. The saturated solution of Hg^0 was normally used without further dilution. For calibration of the mercury analyzer, however, it was diluted in order to construct a calibration curve. Dilute solutions are even less stable and were prepared immediately prior to measurements.

2.2.4 Methylmercury solutions

Methylmercury chloride standard solutions were prepared by dissolving 20 mg MeHgCl (Aldrich, ACS Reagent 99%) in 20 mL methanol (EM Science, ACS Reagent 99.91%) to

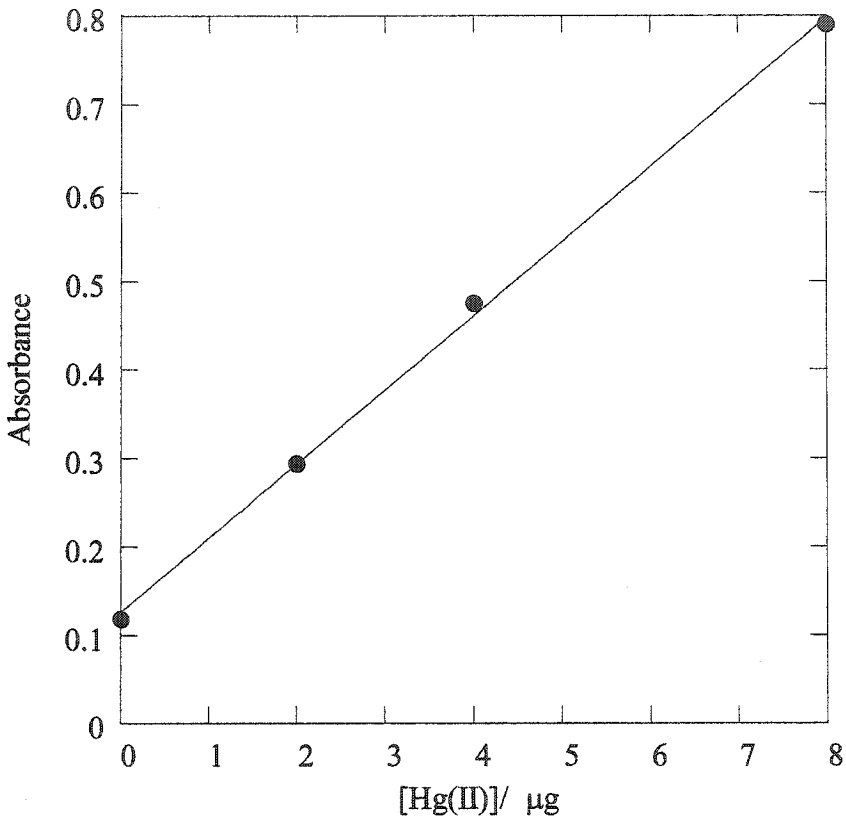

Abs = b + m × [Hg]	
Parameter	Value
b	0.125 ± 0.009
m	0.084 ± 0.002
R	0.9994

Figure 2. 1 Calibration curve for Hg^{2+} determination by dithizone method

yield a MeHgCl concentration of approx. 1000 ppm. Further dilutions with water were made as needed.

2.2.5 Methyl iodide solutions

Methyl iodide (99%, Aldrich) was distilled to a liquid nitrogen trap to remove traces of iodine. Aqueous solutions of methyl iodide show a strong absorption band at 250 nm, Figure 2.2. The absorbance of the solution at this wavelength increases linearly with methyl iodide concentration up to 80 mM, and stays constant for concentrations higher than that. In Figure 2.3, the absorbance at 250 nm is plotted versus MeI concentration for 5 to 100 mM stock solutions diluted 10 times in a 1 cm cuvette. The saturation behavior of the calibration curve is typical of a compound with limited solubility. Therefore concentrations of stock solutions were always less than 80 mM. The extinction coefficient of aqueous MeI at 250 nm is $\varepsilon = (176 \pm 1)\ M^{-1}\ cm^{-1}$, Figure 2.4.

Stock solutions of methyl iodide were unstable, even when they were kept in tightly-closed vials wrapped with aluminum foil, and stored in dry, dark, cool place. They were prepared daily by diluting 15 μL MeI in 3 mL deionized water. Further dilutions were made immediately prior to use.

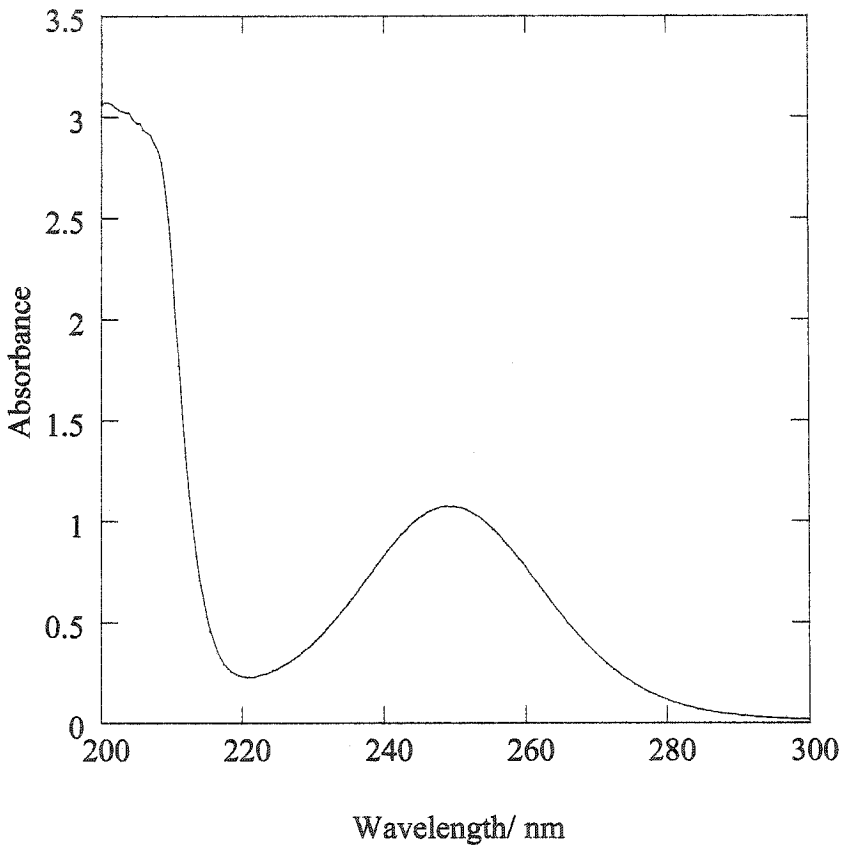

Figure 2. 2 UV spectrum of 6.8 mM aqueous MeI

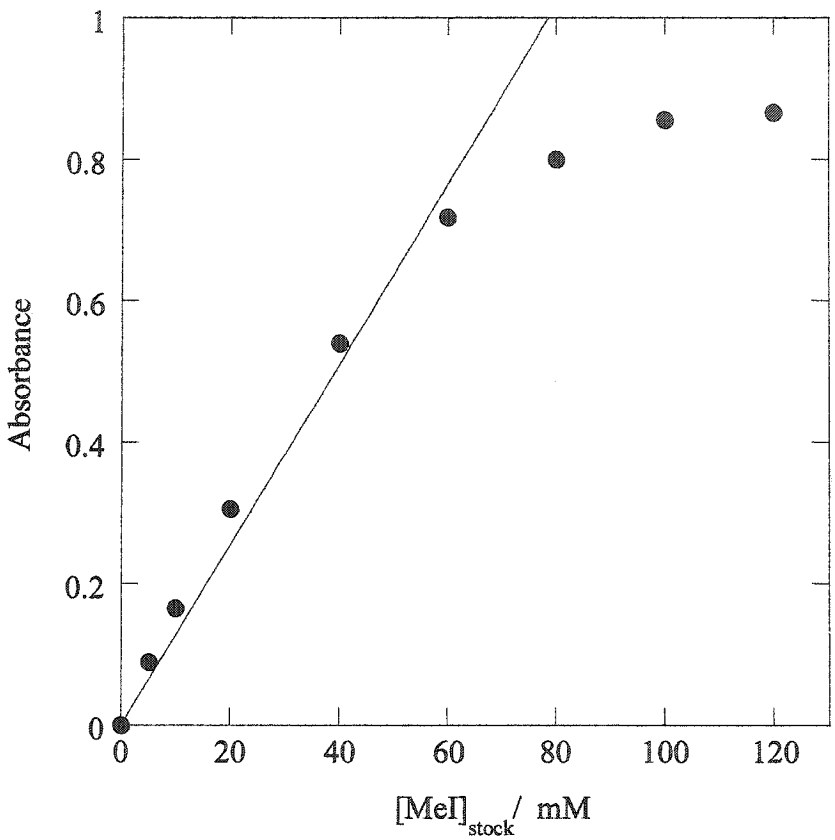

Figure 2. 3 Saturation behavior of MeI in aqueous solution

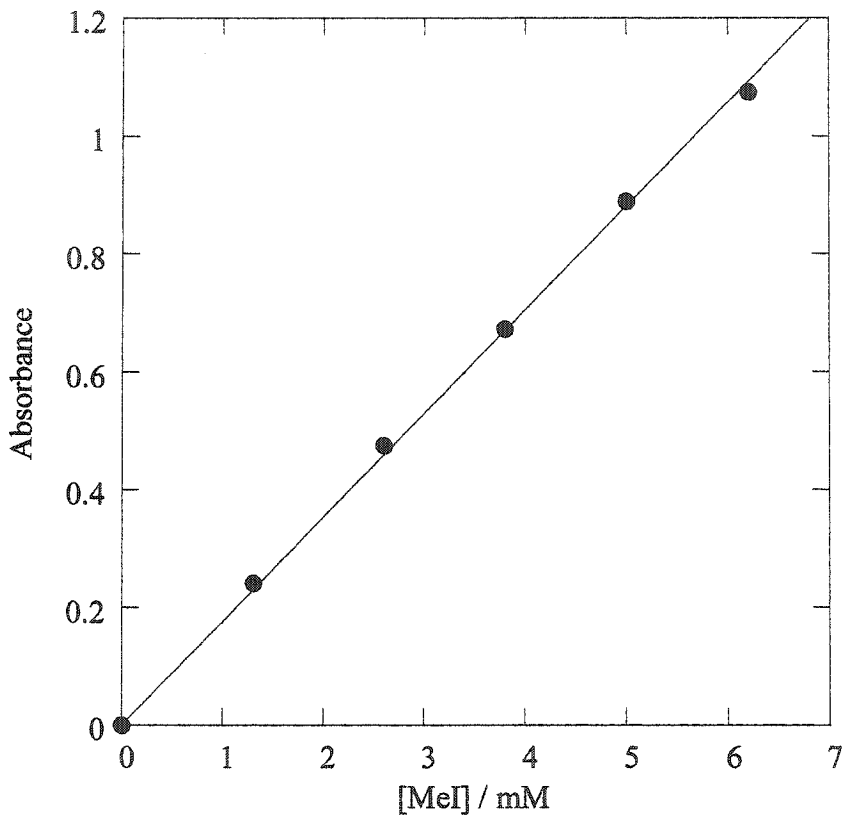

Abs = m × [Hg]	
Parameter	Value
m	0.176 ± 0.001
R	0.9995

Figure 2. 4 Calibration curve for aqueous solutions of methyl iodide

2.2.6 Methyltin solutions

Methyltin solutions were prepared by dissolving a measured amount of the reagent in deionized water. Monomethyltin trichloride (97%, Aldrich) was purchased in 250 mg sealed ampoules. The entire content of an ampoule was transferred to a 25 mL volumetric flask and then diluted with water to produce a 41.6 mM stock solution of monomethyltin.

Because dimethyltin dichloride (97%, Aldrich) and trimethyltin chloride (97%, Aldrich) are moisture- and air-sensitive, their containers were opened and the compounds weighed in the glove box under a N_2 atmosphere. The weighed amount was transferred to a volumetric flask, removed from the box and diluted with water to produce stock solutions of 10.9 mM dimethyltin and 77.3 mM trimethyltin. Stock solutions were stored in septum-closed glass bottles at room temperature, and diluted just prior to the kinetic runs as needed.

2.2.7 Synthesis of methylaquacobaloxime

The compound was synthesized following a literature procedure.[7] Under a nitrogen atmosphere, 300 mL methanol was stirred with a suspension of 29.0 g dimethylglyoxime, to which 29.7 g $CoCl_2 \cdot 6H_2O$ was then added. The mixture was cooled to 20°C. 25.4 g methyl iodide and 15.0 g NaOH in 50 mL water were added successively and the mixture was stirred for one hour. Finally, methanol was removed under reduced pressure and the

remaining solution was left to stand overnight in an ice bath, resulting in the precipitation of dark red crystals of the product.

The UV-vis spectrum of an aqueous solution of methylaquacobaloxime consists of two peaks at 440 and 380 nm, with extinction coefficients 1.39 x 10^3 and 1.61 x 10^3 M^{-1} cm^{-1}, respectively, Figure 2.5.

A 10 mM stock solution was prepared weekly. Further dilutions were made just prior to kinetics experiments.

2.2.8 Other solutions

KCl (Fisher Scientific, ACS grade) and $NaClO_4$ (Aldrich ACS Reagent, 99%) was used to prepare 1.0 M solutions used to maintain ionic strength. Perchloric acid, sodium hydroxide and hydrogen peroxide solutions were prepared by diluting concentrated $HClO_4$, NaOH (Aldrich, 99.999%) and H_2O_2 (EM Science, ACS 30% solution) to the desired concentration.

Solutions of potassium iodide and mercuric iodide were prepared by dissolving a measured amount of KI (Aldrich, ACS Reagent 99%,) or red HgI_2 (Aldrich, ACS Reagent 99%) respectively, in water. While KI dissolved readily, HgI_2 solutions required stirring for 2 hours at ca. 50°C. HgI_2 solutions were prepared at concentration much lower than its solubility (6 wt.% in water at 25°C).[8] HgI^+ solutions were prepared by mixing appropriate amounts of Hg^{2+} solutions and KI.

The pH 10.5 buffer was prepared by mixing 10.7 g $Na_2HPO_4 \cdot 7H_2O$ (Fisher Scientific, ACS grade) and 3.8 g K_2CO_3 (Fisher Scientific, ACS grade) in 100 mL deionized water.

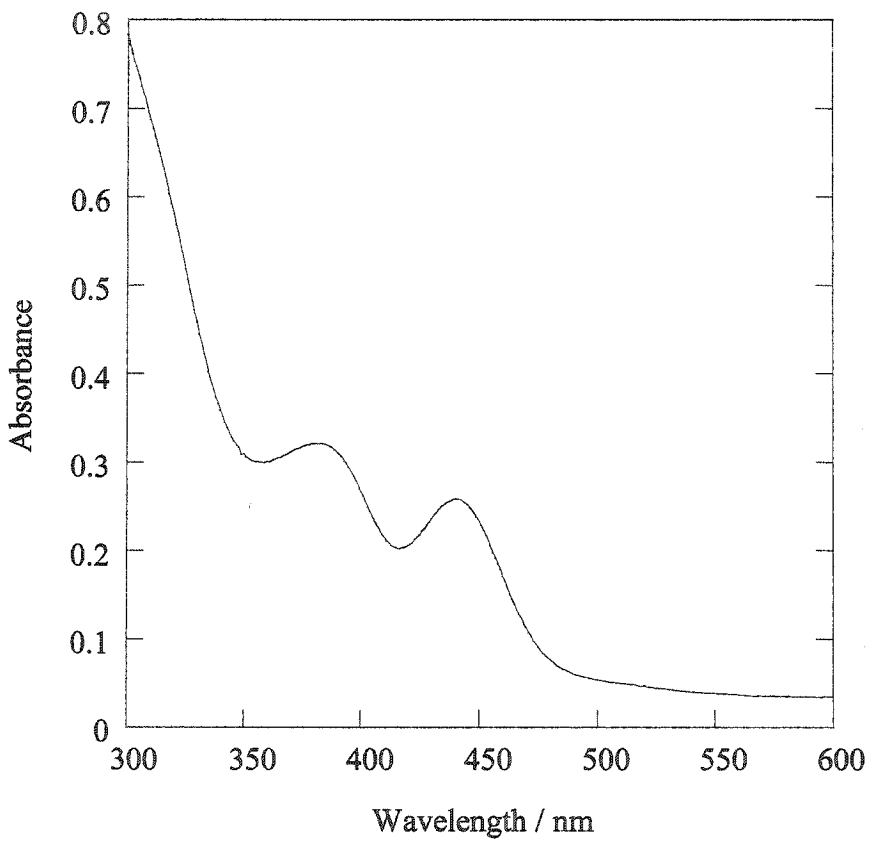

Figure 2. 5 UV-vis spectrum of a 2 mM aqueous solution of methylcobaloxime

For variable pH kinetics, pH was adjusted by addition of 0.1 M NaOH or $HClO_4$ to 0.1 M Na_2HPO_4.

2.3 Quantitative analyses

2.3.1 Mercury analysis

Quantitative determinations of low concentration of inorganic mercury were performed by Cold Vapor Atomic Absorption Spectroscopy, using a Varian M-6000A CETAC Technologies CV-AAS instrument. A 5% $SnCl_2$ solution (Fisher Scientific, ACS grade) in 7% HCl was used as the reducing agent. A schematic diagram of the measuring part of the instrument is presented in Figure 2.6.

Solutions of Hg^{2+} and $SnCl_2$ were mixed by a peristaltic pump. Hg^{2+} was reduced to Hg^0 and separated from the liquid in the gas-liquid separator. Hg^0 vapor was carried to the sample cell by a stream of N_2. Its absorbance was measured at 254 nm using a mercury lamp.

A calibration curve from 1 to 10 ppb mercury in 1% HNO_3 was run with each set of samples. A typical curve for determination of mercury with this instrument is presented in Figure 2.7. A 1000 ppm Hg(II) stock solution (VWR brand, mercuric oxide dissolved in HNO_3) was diluted as needed before each analysis. The detection limit of the method was 0.1 ppb.

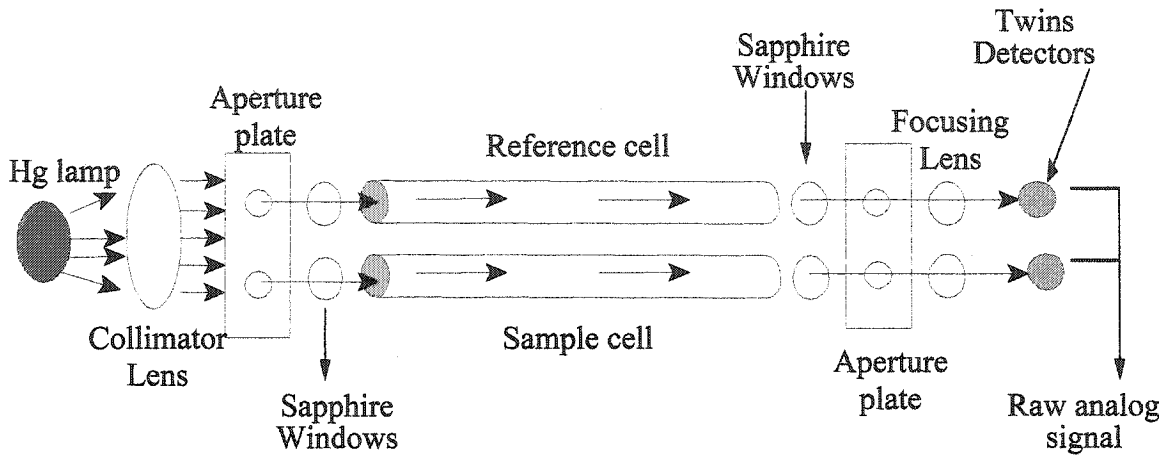

Figure 2. 6 A schematic diagram of the mercury analyzer

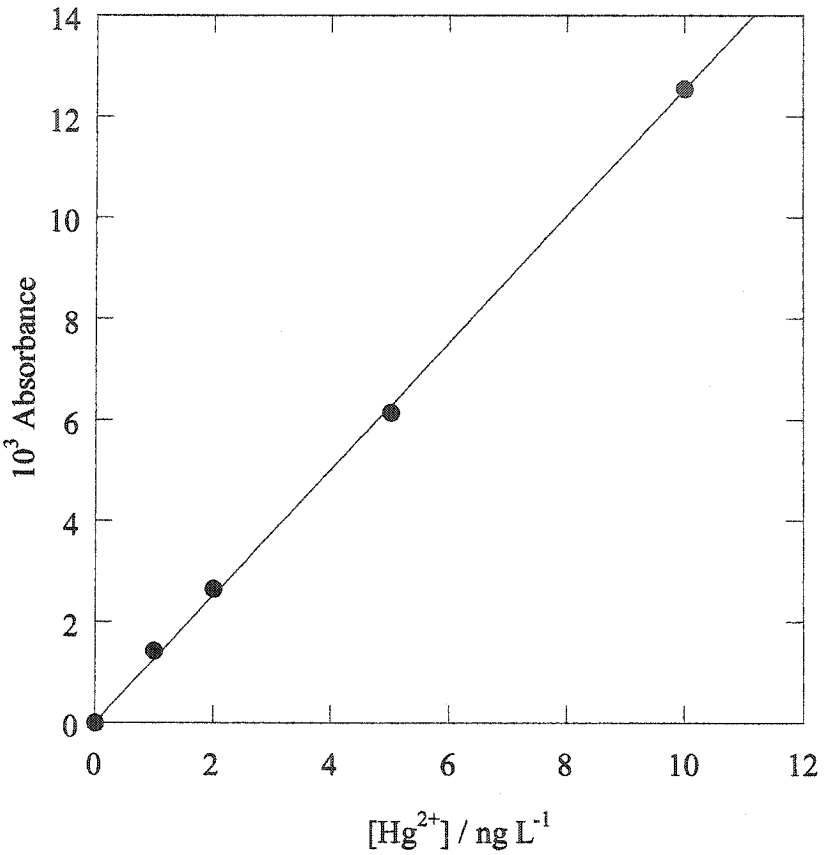

$$Abs = m \times [Hg^{2+}]$$

Parameter	Value
m	$(1.242 \pm 0.002) \times 10^3$
R	0.9998

Figure 2. 7 Mercury calibration curve on CV/AAS instrument

This method was modified for Hg^0 analysis by replacing the $SnCl_2$ solution with deionized water. To avoid cross-contamination, completely separate sets of tubing and gas-liquid separators were used for Hg^0 and Hg(II) analyses. The instrument was calibrated with a saturated Hg^0 analyzed with the dithizone method, as described above. The CV/AAS calibration curve for Hg^0 is presented in Figure 2.8.

2.3.2 Methylmercury analysis

2.3.2.1 Preparation of sulfydryl-cotton fiber (SCF) adsorbent

Sulfhydryl cotton fiber was prepared by the method of Lee and Mowrer[9] with a few modifications. 15.0 g of non-sterile, bleached cotton was shredded and weighed. In a round-bottom flask wrapped with aluminum foil, the following reagents were added in order: 100 mL mercaptoacetic acid (Research Chemicals Ltd., 98%), 60 mL acetic anhydride (BDH, ACS Reagent 98.0%), 40 mL 36% acetic acid (EM Science, ACS Reagent 99.7%) and 0.30 mL concentrated sulfuric acid (EM Science, ACS Reagent 98%). The mixture was swirled, then the flask was allowed to cool to room temperature and the cotton was added. After it was completely wetted, it was placed in an oven for three days at 45°C. It was then washed with 5 L deionized water, cut into small pieces (so that it would dry faster), and placed in a shallow bowl covered with aluminum foil for 24 hours at 40°C. The dried cotton was again shredded into small pieces and stored in the

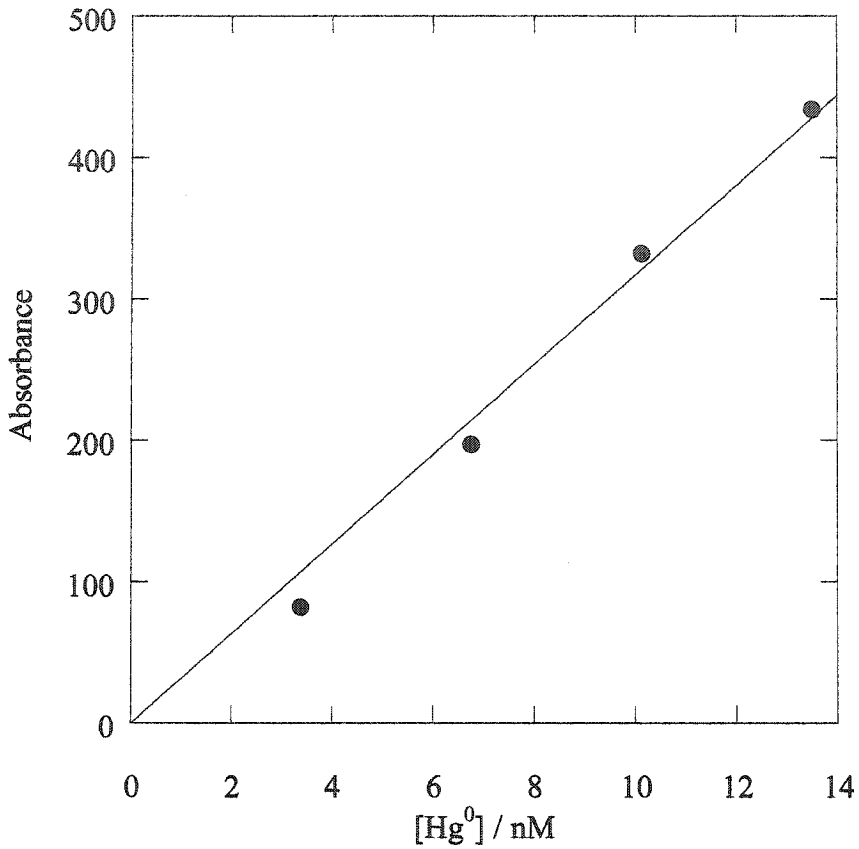

$Abs = m \times [Hg^0]$

Parameter	Value
m	32 ± 1
R	0.9924

Figure 2. 8 Calibration curve for CV AAS determination of Hg^0

refrigerator in a dark bottle wrapped with aluminum foil. SCF columns were prepared from 5 mL disposable screening columns (Fisher Scientific) containing 0.160 g absorbent packed to the 1 mL line.

2.3.2.2 Preconcentration and extraction of methylmercury

Solutions of either Hg^{2+} or MeHgCl were preconcentrated and extracted following the procedure of Cai et al.[10] Approximately 100 mL of each solution, with a known concentration of either inorganic mercury or methylmercury, was treated with 1 mL 0.1M pH 3.8 acetate buffer ($[CH_3COOH]/[CH_3COONa] = 9$) and passed through an SCF column, using a peristaltic pump (ISMATEC) to maintain a flow rate of 5 mL min^{-1}. The columns were then washed with 15 mL deionized water and placed over 7 mL borosilicate glass scintillation vials (Fisher Scientific). Methylmercury was eluted from the columns using 6 mL of a 2:1 mixture of 1.5 M KBr (EM Science, ACS Reagent 99.0%) in 1.0 M H_2SO_4 and 1.0 M $CuSO_4$ (EM Science, ACS Reagent 98%) in deionized water.

300 μL dichloromethane (EM Science, ACS Reagent 99.97%) was added to extract methylmercury bromide. The solutions were shaken for 15 min in an automatic shaker (Lab-Line Orbit Shaker) and centrifuged for another 15 min using a Beckman J2-MC Centrifuge, set at 20°C and 3500 rpm. The dichloromethane layer was then passed through a microcolumn filled with Na_2SO_4 crystals (EM Science, ACS Reagent 99.0%) into the insert of a gas chromatographic vial. Injections of volume 5 μL were analyzed by GC/AFS.

Calibration standards were prepared by adding known amounts of a 5 ppb methylmercury standard solution to 1 mL deionized water in 7 mL borosilicate glass vials. 5 mL of the acidic $KBr/CuSO_4$ mixture and 300 µL dichloromethane were added and the standards subjected to the same subsequent procedure as for the preconcentrated samples.

2.3.2.3 Measurements

Quantitation of methylmercury was achieved by gas chromatographic separation followed by atomic fluorescence detection. An HP 6890 Plus GC was coupled to a PSA Millenium Merlin Detector via a pyrolysis oven held at 800°C. The gas chromatograph was equipped with a DB-1 Megabore column (J&W Scientific) of dimensions 15 m x 0.53 µm i.d., coated with a 1.5 µm thick film of 100% dimethylpolysiloxane. It was held isothermal at 50°C for 1 min, then ramped at 60°C/min to 140°C, where it was held for 3.5 min keeping the carrier gas flow at 3.5 mL min^{-1}. A split/splitless injector was used in splitless mode at 250°C with a gas flow of 93.6 mL min^{-1} He. In these conditions the retention time of methylmercury was ca. 4 min, Figure 2.9 and the calibration curve was linear ($R^2 \sim 1$) in the range 0.25 to 2.5 ng Hg as $MeHg^+$, Figure 2.10. No methylmercury was detected in the calibration curve blanks. Recovery experiments were run with each set of samples. The reported results are corrected with the recovery coefficient.

Calibration standards, blanks and methylmercury spikes were analyzed with each batch of samples. The detection limit was deemed to be three times the standard

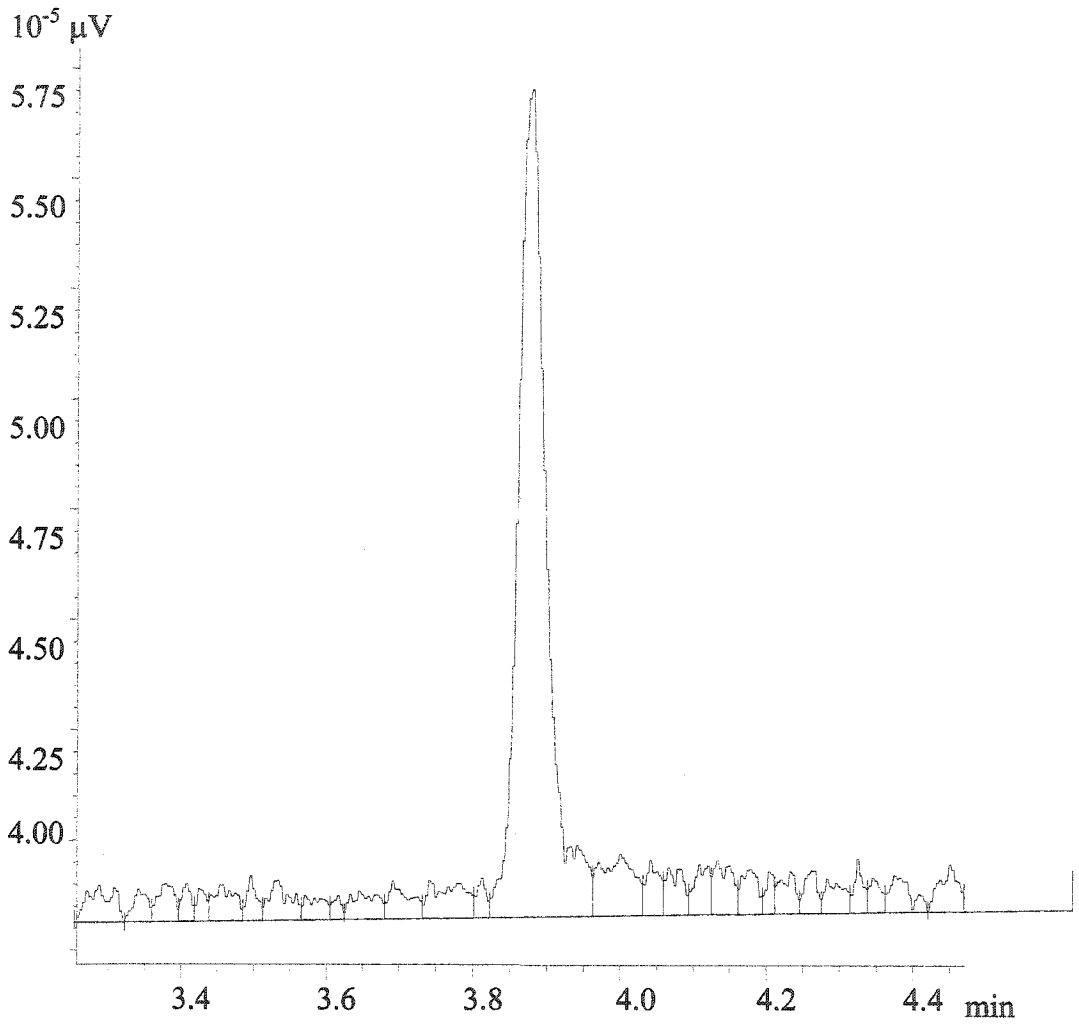

Figure 2. 9 GC/AFS chromatogram of 1 ng MeHg extracted into dichloromethane.

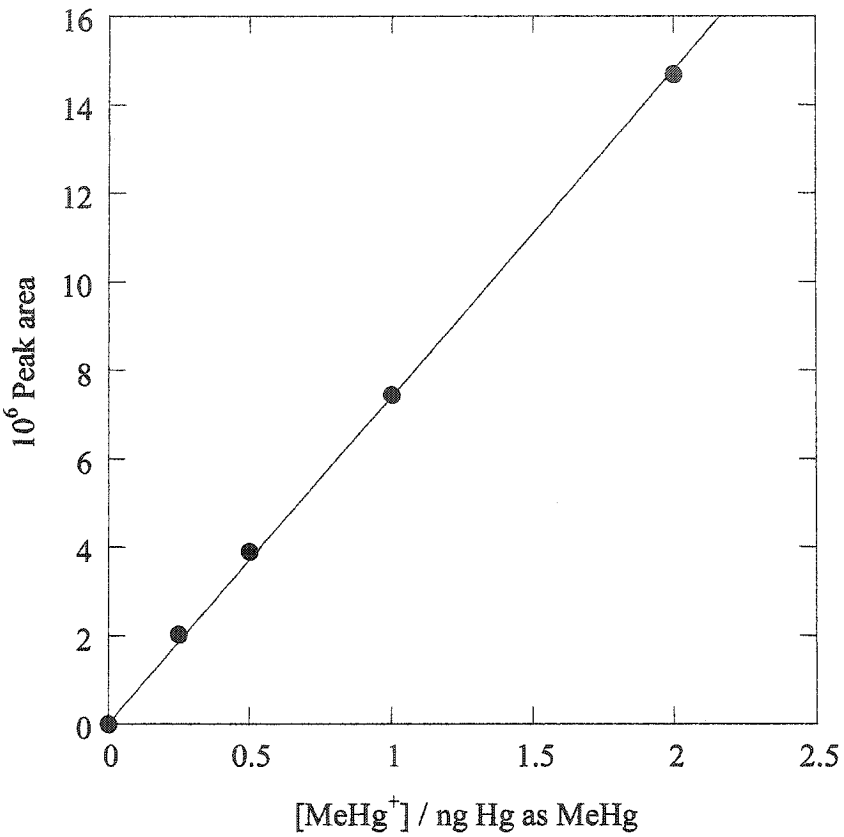

Abs = m × [MeHg$^+$]

Parameter	Value
m	(7.39 ± 0.06) x 10^5
R	0.9999

Figure 2. 10 GC/AFS calibration curve of methylmercury extracted in dichloromethane

deviation of 10 injections. For a 5 μL injection containing 0.2 ng Hg as $MeHg^+$, in 300 μL dichloromethane, this limit was 0.02 ng.

2.3.3. Other analyses

Methanol was quantified by GC/FID on an HP 6890. CH_3CN (Fisher Scientific, HPLC grade) was used as the internal standard. The calibration curve used for quantitation is shown in Figure 2.11.

2.4 Kinetics experiments

Solutions for kinetics experiments were prepared using all-glass syringes in quartz cuvettes capped with white rubber septa (Aldrich). The cuvettes were filled with all but one of the reagents and placed in the thermostated cell compartment of a Cary 300 spectrophotometer for at least 15 minutes in order to allow thermal equilibration (± 0.1°C) via a circulating water bath. To initiate the reaction, the last reagent was added by syringe and the solutions are mixed just before measurements. UV-vis spectra were monitored as a function of time. Kinetic curves were extracted as a plot of absorbance at a certain wavelength vs time. The absorbance readings were measured with four decimal places.

For variable pH experiments, the pH was measured using a Thermo-Orion, Model 525 A+ pH-meter. The instrument was calibrated using two standard buffers with pH 7

and pH 10 (Thermo-Orion Applications Solutions).All solutions were stirred continuously during the pH measurements. KCl (Fisher Scientific, ACS grade) was used to maintain the desired chloride concentration.

Kaleidagraph™ 3.5 (Synergic Software) was used for non-linear curve fitting of kinetic data.

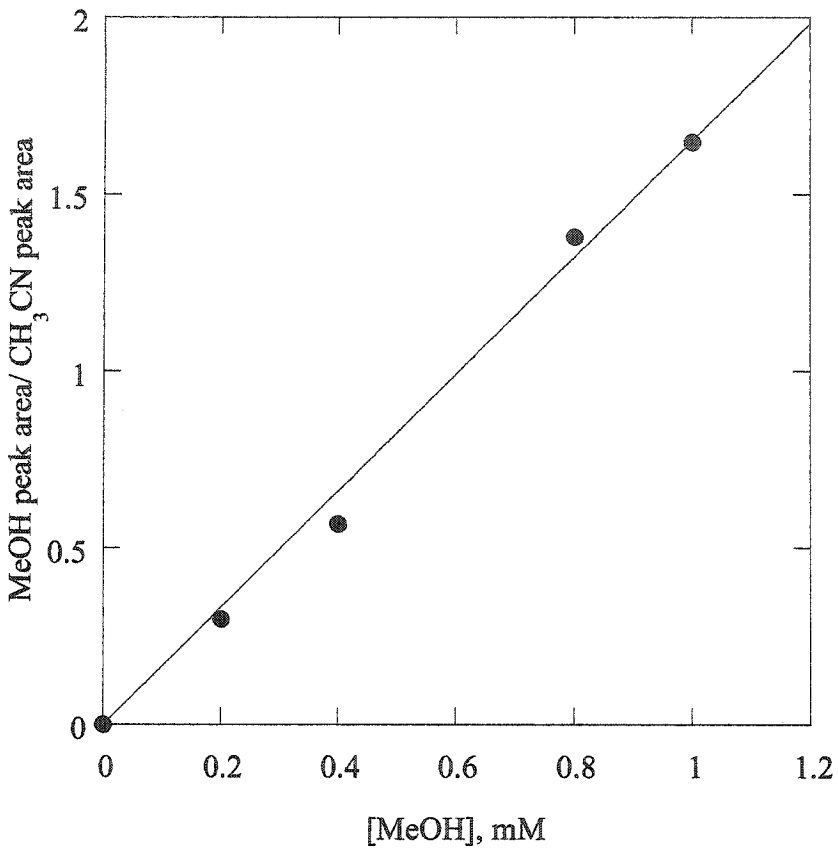

Abs = m × [MeOH]	
Parameter	Value
m	1.65 ± 0.04
R	0.9968

Figure 2.11 Calibration curve for the GC/FID determination of methanol

References

(1) Kolthoff, M.; Sandell, E. B. *Textbook of Quantitative Inorganic Analysis*; Macmillan: New York, 1952.

(2) Higginson, W. C. E. *J. Chem. Soc.* **1951**, 1438.

(3) Fujita, S.; Horii, H.; Taniguchi, S. *J. Phys. Chem.* **1973**, *77*, 2868-2871.

(4) Lin, C.-J.; Pehkonen, S. O. *J Geophys. Res.* **1998**, *103*, 28093-28102.

(5) Eaton, A. D.; Clesceri, L. S.; Greenberg, A. E. *Standard Methods for Examination of Water and Wastewater*; United Book Press: Baltimore, Md, 1996.

(6) Clever, H. L.; Johnson, S. A.; Derrick, M. E. *J. Phys. Chem. Ref. Data* **1985**, *14*, 632-680.

(7) Yamazaki, N.; Hohokabe, Y. *Bull. Chem. Soc. Jpn.* **1971**, *44*, 63-69.

(8) Choi, S. S.; Tuck, D. G. *J. Chem. Soc.* **1962**, 4080.

(9) Lee, Y. H.; Mowrer, J. *Anal. Chim. Acta* **1989**, *221*, 259-268.

(10) Cai, Y.; Jaffe, R.; Azaam, A.; Jones, R. D. *Anal. Chim. Acta* **1996**, *334*, 251- 259.

Chapter 3

Abiotic Methylation of Aqueous Mercury by Methyl Iodide

3.1 Introduction

Methyl iodide plays an important role in the biogeochemical cycle of iodide in seawater, and methyl iodide from the oceans is the principal source of iodide to the atmosphere.[1,2] The annual production of methyl iodide in seawater is estimated to be 4 x 10^{10} kg.[3] Concentrations of methyl iodide in open ocean waters range from 1.2 to 235 pg/g,[4] but levels can be thousands of times higher in coastal areas with intensive biomass production. In waters off southwest Ireland, concentrations between 3.4 ng/g and 0.12 mg/g have been detected.[4]

While methyl iodide has been used to recover metals from their naturally-occurring ores and scrap,[5-7] anthropogenic input to the aquatic environment is small compared to natural sources.[8,9] Marine organisms play a key role in the production of simple haloalkanes including $CHCl_3$, CCl_4, CBr_4, CH_3Cl and CH_3I.[10] Methyl iodide is a product of both exo- and endocellular biological processes.[11] Seaweed,[12] marine algae[3] and fungi[13] all produce methyl iodide as a defense compound or as a by-product of the production or breakdown of larger molecular weight defense compounds.

A growing body of evidence shows that methyl iodide can also be produced photochemically. Moore and Zafiriou[14] suggested that methyl iodide results from photolysis of dissolved organic matter (DOM) in seawater, eq 1-2:

$$DOM + h\nu \rightarrow {}^{\bullet}CH_3 \quad (1)$$

$$^{\bullet}CH_3 + I_2 \rightarrow CH_3I + I^{\bullet} \quad (2)$$

Methyl iodide interacts with reduced metals by oxidative addition, as in the following reactions with zinc, eq 3-4: [15]

$$Zn + MeI \rightarrow MeZnI \quad (3)$$

$$2\ MeZnI \rightarrow Me_2Zn + ZnI_2 \quad (4)$$

In contrast, the reaction of methyl iodide with oxidized metal compounds, such as ores containing metal chalcogenides and pnictides, results in methylation of the main group anion (sulfide, selenide, telluride, phosphide, arsenide, antimonide, etc.). This is typified by the following reaction with ferrous sulfide, eq 5: [6]

$$FeS + 2\ MeI \rightarrow FeI_2 + Me_2S \quad (5)$$

Such reactions may cause mobilization of toxic metals.[4-7,16-18] If both ligand metathesis and two-electron oxidation of the metal are possible, methylation of both components may be observed, as is the case for stannous sulfide, eq 6: [19]

$$SnS + 4\ MeI \rightarrow MeSnI_3 + Me_3S^+ + I^- \quad (6)$$

The role of methyl iodide in the biogeochemical cycle of mercury is a topical issue.[20-23] Methylation of the mercuric ion by methyl iodide has been reported,[24] but the mechanism of the reaction and its role in the aquatic environment is not yet clear.

The hydrolysis of alkyl halides to give alcohols, eq 7, has been extensively studied.[25]

$$RX + H_2O \rightarrow ROH + H^+ + X^- \qquad (7)$$

It is catalyzed by OH^-, except for activated substrates such as allylic and benzylic halides which undergo hydrolysis at neutral pH.[26] In particular, methyl iodide is stable in neutral and acidic aqueous solutions.

Catalysis of hydrolysis by specific metal ions has been observed. Zamashchikov et al.[27] reported acceleration of the rates of hydrolysis of primary alkyl iodides in the presence of Ag(I) and Hg(II) cations. Heterolytic C-X cleavage was suggested to be assisted by these electrophiles.[27] Two proposed transition states are associated with the M^+-S_N1 mechanism (A) and the M^+-S_N2 mechanism (B):

$CH_3{}^{\delta+}\cdots I^{\delta-}\cdots Hg^{2+}$ A

$H_2O\cdots CH_3{}^{\delta+}\cdots I^{\delta-}\cdots Hg^{2+}$ B

Mercuric ions have also been shown to promote the hydrolysis of benzaldehyde(O-ethyl,S-ethyl)acetal,[28,29] and were once used industrially to catalyze the hydrolysis of acetylene for the production of acetaldehyde.[30]

Maynard first observed that Hg^0 is methylated slowly by methyl iodide at room temperature, in 1932.[31] This reaction was the basis for the first synthesis of methylmercury.[32] Consequently, Fieser & Fieser recommended that methyl iodide not be stored near mercury because of the risk of inadvertent methylmercury iodide formation.[33] Several authors have studied the reaction of methyl iodide with Hg^0 to yield methylmercury.[21,32-34] In all cases, reported yields are low and rates are slow, although the reaction is accelerated by UV radiation.[22] The methylation mechanism is likely oxidative addition, eq 8, which is a common reaction for metals with two stable oxidation states separated by two units.

$$Hg^0 + MeI \rightarrow MeHgI \qquad (8)$$

Methylmercury is more efficiently synthesized by the reaction of methyl iodide with mercurous acetate and sulfate, eq 9:[35]

$$Hg_2X_2 + MeI \rightarrow MeHgX + HgIX \qquad (9)$$

The yield is ca. 80%, making this reaction useful on a preparative scale. The mechanism was suggested to be oxidative addition of MeI across the Hg-Hg bond.

In contrast, reaction of methyl iodide with Hg(II) cannot occur by oxidative addition, since mercury already in its maximum oxidation state.

Weber proposed that MeHgX could be formed abiotically in the environment by the reaction of methyl iodide with Hg^0.[20] Methyl iodide is known to methylate other

metal ions, such as lead[17] and tin[4,18] in the aquatic environment, usually by oxidative addition to reduced forms. Also, methyl iodide has been blamed for artifact formation of methylmercury during its analysis.[36] However, Tokos concluded that methyl iodide is not geochemically important in the cycling of gaseous mercury in the atmosphere,[23] and Hall observed no significant methylmercury formation from methyl iodide and Hg^0 in aqueous phase experiments and only small amounts in the gas phase.[22]

The mechanism of the reactions of mercury in different oxidation states with methyl iodide and the importance of these reactions in environment remains obscure. In this chapter we present the results of our work on the mechanism of the reaction of mercury (Hg^{2+} and Hg^0) with methyl iodide in aqueous solutions.

3.2 Kinetics of the reaction between $Hg^{2+}_{(aq)}$ and excess MeI

Acidic aqueous solutions of Hg^{2+} with concentrations up to 10 mM have no absorbance peaks in the UV region between 200 and 350 nm. The UV spectra of aqueous solutions of methyl iodide consist of a peak at 249 nm, $\varepsilon = 175\ M^{-1}\ cm^{-1}$, Figure 3.1. Upon mixing 0.40 mM $Hg^{2+}_{(aq)}$ with 4.0 mM MeI, two intense peaks are seen to grow in, Figure 3.2. The peak maxima are initially located at 215 and 275 nm. As the reaction proceeds, the position of the longer wavelength peak shifts from 275 to 265 nm.

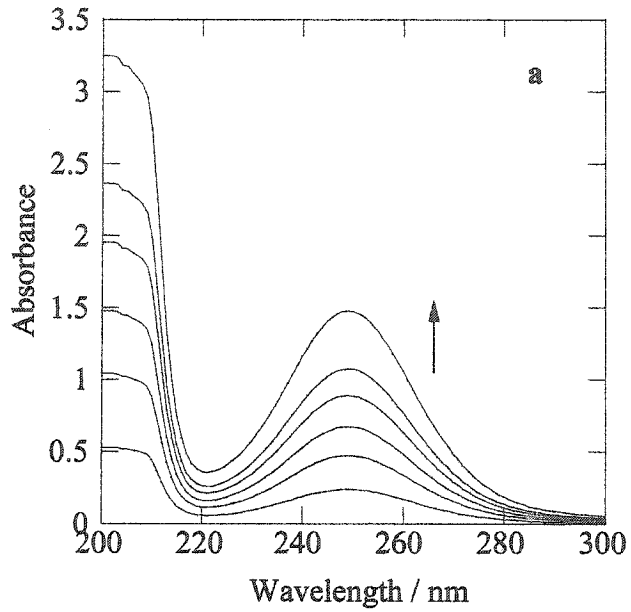

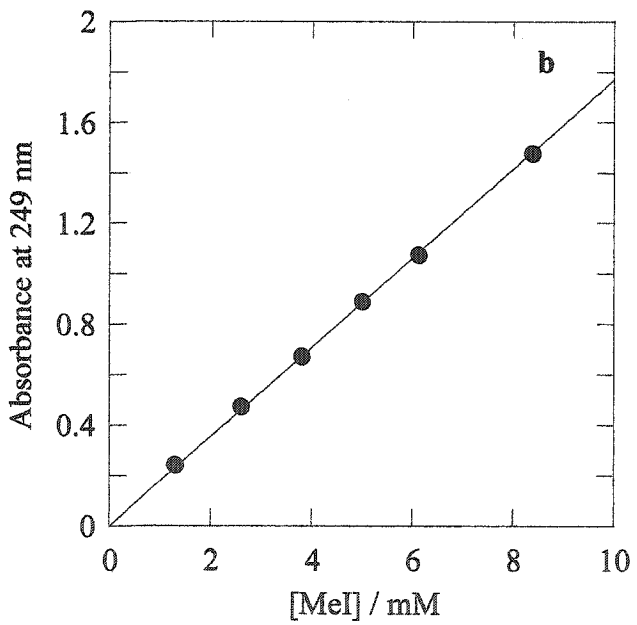

	Abs = ε * [MeI]
ε	0.177 ± 0.007
Chisq	0.0004245
R	0.9998

Figure 3.1 (a) UV spectra of millimolar aqueous solutions of methyl iodide; (b) Determination of the extinction coefficient for methyl iodide at 249 nm (pathlength 1 cm).

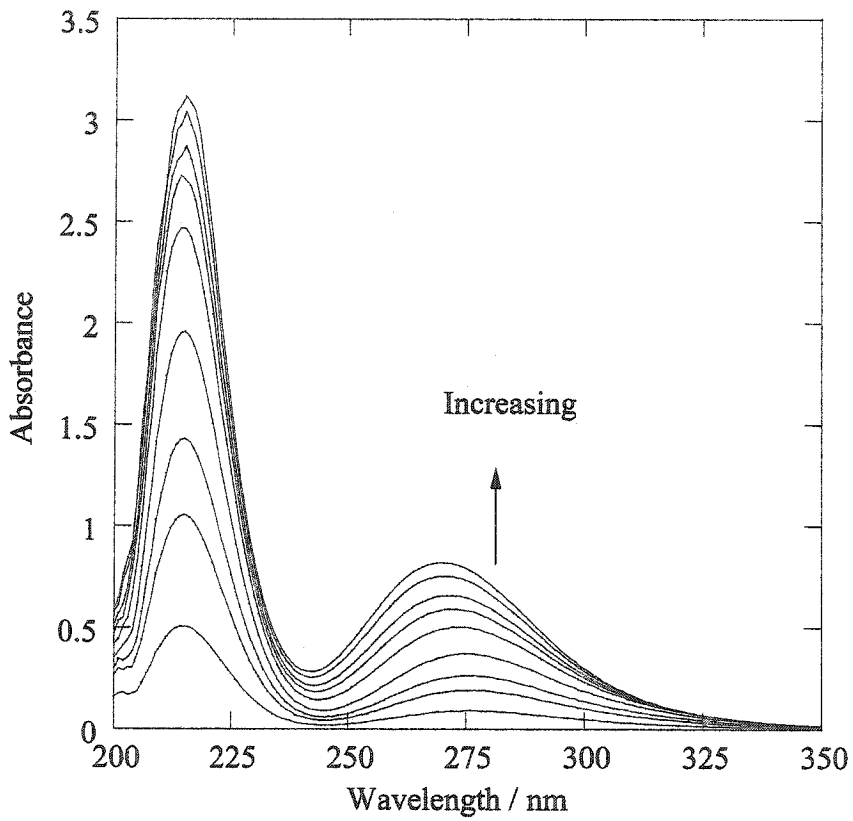

Figure 3.2 Evolution of the UV spectrum of 0.40 mM Hg^{2+} in the presence of 4.0 mM MeI at 38.8°C, pH 2.3 ($HClO_4$) and 0.010 M ionic strength ($HClO_4/NaClO_4$). Total time elapsed 1 hour.

At ca. 40°C, changes in the UV spectrum are sufficiently rapid to allow ready monitoring of the kinetics. The course of the reaction was monitored as the increase in absorbance at 275 nm, Figure 3.3. The time-evolution of the absorbance is poorly described by a single exponential function, eq 10, but is accurately described by a double exponential function, eq 11:

$$A_t = A_\infty + (A_0 - A_\infty) \exp(-k_{obs}\, t) \quad (10)$$

$$A_t = A_\infty + \alpha \exp(-k_{1obs}\, t) + \beta \exp(-k_{2obs}\, t) \quad (11)$$

where α and β are pre-exponential constants.[37] Two pseudo-first order rate constants, k_{1obs} and k_{2obs}, were obtained from the five-parameter (A_∞, α, β, k_{1obs}, k_{2obs}) nonlinear least-squares fit of the experimental data to eq 11.

Values of k_{1obs} and k_{2obs} measured at 38.8°C in the presence of varying excess concentrations of MeI are summarized in Table 3.1. Both observed rate constants depend linearly on the concentration of excess methyl iodide, Figure 3.4. From the slopes of these curves, two second-order rate constants were obtained: $k_{fast} = (1.31 \pm 0.06)\ M^{-1}\ s^{-1}$ and $k_{slow} = (0.176 \pm 0.003)\ M^{-1}\ s^{-1}$ at pH 2.3 ($HClO_4$) and 0.010 M ionic strength ($NaClO_4/HClO_4$).

Solutions bubbled with oxygen-free argon prior to kinetic measurements showed identical kinetic profiles to experiments without such treatment. The rate is therefore insensitive to the presence or absence of dissolved oxygen, Figure 3.5. The second-order

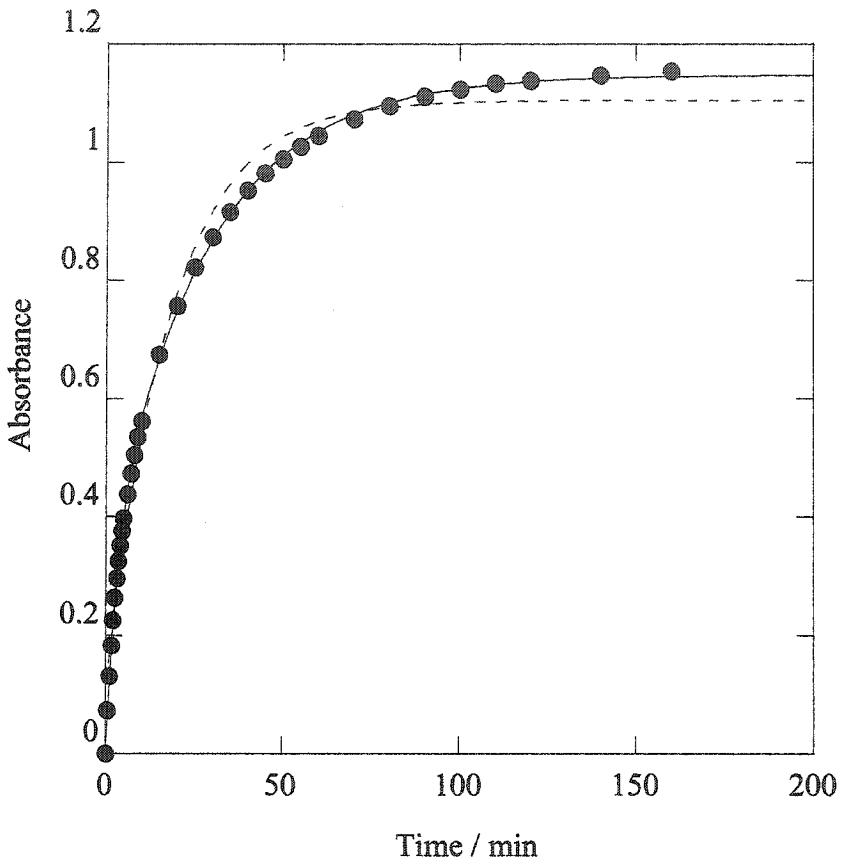

Figure 3.3 Kinetic profile (275 nm) for the reaction of 0.20 mM Hg^{2+} with 4.0 mM MeI at 38.8°C, pH 2.3 ($HClO_4$) and ionic strength 0.010 M ($HClO_4/NaClO_4$), showing single exponential (dashed line) and double exponential (solid line) curve fits.

Table 3.1 Pseudo-first-order rate constants[a] for the biphasic reaction of $Hg^{2+}_{(aq)}$ with excess MeI[b]

Temperature °C	[MeI] mM	10^3 k_{1obs} s^{-1}	10^3 k_{2obs} s^{-1}
11.5	6.50	0.98 ± 0.02	0.085 ± 0.003
20.6	9.20	3.23 ± 0.05	0.287 ± 0.006
29.5	8.10	6.17 ± 0.03	0.645 ± 0.004
38.8	0.90	1.28 ± 0.01	0.123 ± 0.003
38.8	1.45	2.02 ± 0.02	0.235 ± 0.003
38.8	1.73	2.57 ± 0.05	0.278 ± 0.005
38.8	2.51	3.03 ± 0.01	0.347 ± 0.008
38.8	3.02	3.39 ± 0.03	0.427 ± 0.007
38.8	3.04	3.19 ± 0.02	0.452 ± 0.005
38.8	4.34	5.41 ± 0.02	0.69 ± 0.01
38.8	6.73	8.93 ± 0.02	1.28 ± 0.01
38.8	7.49	10.21 ± 0.05	1.26 ± 0.02
38.8	10.2	15.32 ± 0.06	1.91 ± 0.02
48.1	4.80	10.20 ± 0.05	1.52 ± 0.04

[a] Errors are calculated from five-parameter nonlinear curve fits to eq 11.

[b] Conditions: 0.20 mM Hg^{2+}, pH 2.3, 0.010 M ionic strength ($HClO_4/NaClO_4$).

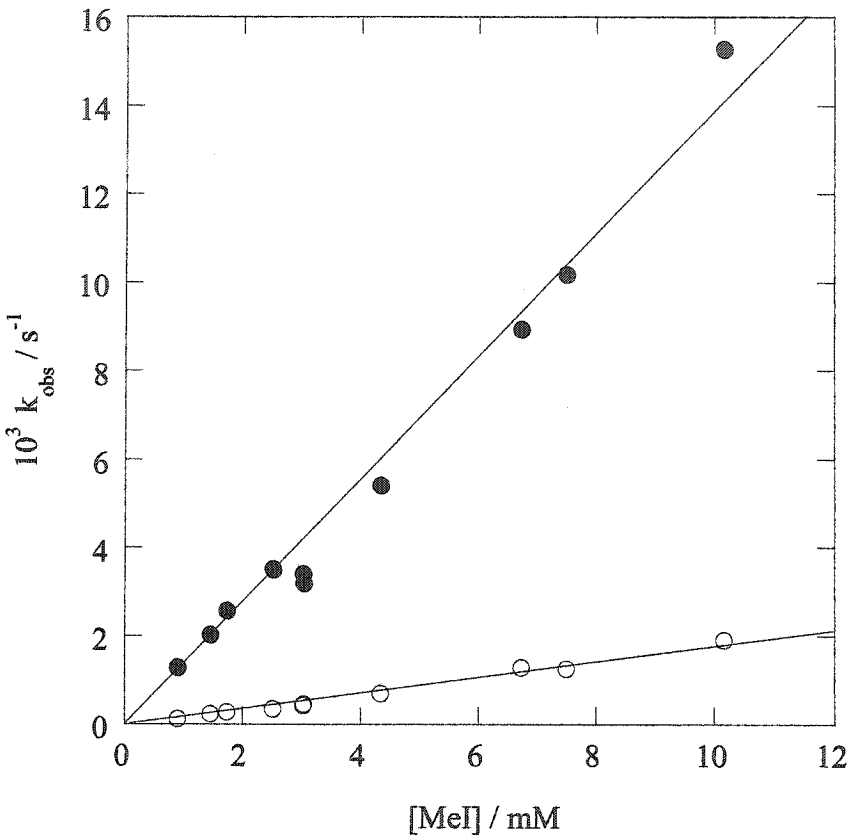

Figure 3.4 Dependence of pseudo-first-order rate constants k_{1obs} (filled circles) and k_{2obs} (open circles) for the reaction between Hg^{2+} and excess MeI, on the concentration of MeI at 38.8°C, pH 2.3 ($HClO_4$) and 0.010 M ionic strength ($HClO_4/NaClO_4$).

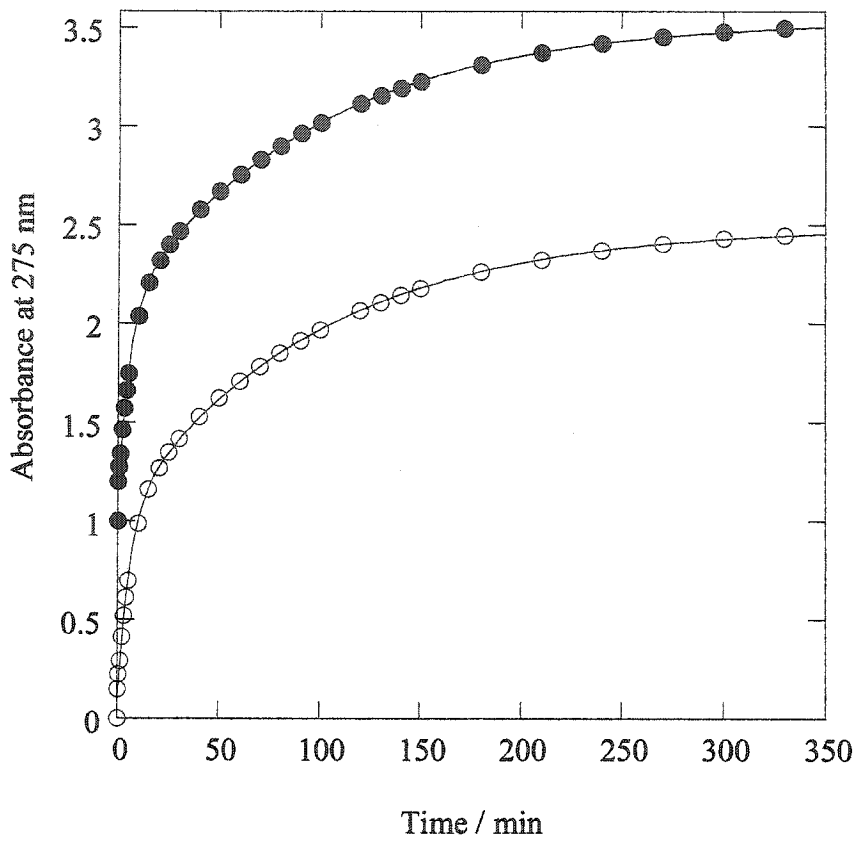

Figure 3.5 Kinetic profiles for the reaction of Hg^{2+} with excess methyl iodide at room temperature, pH 2.3, ionic strength 0.010 M ($HClO_4/NaClO_4$), in air-saturated (open circles) and in argon-saturated (filled circles) solutions. Solid lines are double exponential curve fits of the experimental data to equation 10 (see text); the upper curve is vertically offset to better display the data.

rate constants are further independent of the initial concentration of Hg^{2+} and the ionic strength, Figure 3.6.

3.3 Organic reaction products

Aqueous solutions of methyl iodide are stable in the dark at 38.8°C for 16 hrs. The absorbance of the peak at 249 nm remained constant and no other organic products were detected by GC/FID. However, in the presence of Hg(II), methanol was observed. Its concentration was determined by adding 10 μL acetonitrile diluted 1000X to each of 1 mL calibration standards and samples as an internal standard. The ratio of methanol peak area to acetonitrile peak area was used to construct the calibration curve shown in Figure 3.7. Yields of methanol are shown in Table 3.2.

With methyl iodide in excess, the final concentration of methanol is twice the initial concentration of mercuric ion. Based on these results, we infer that the observed reaction is the stoichiometric hydrolysis of MeI by Hg^{2+}, eq 12:

$$Hg^{2+} + 2\,MeI + 2\,H_2O \rightarrow HgI_2 + 2\,MeOH + 2\,H^+ \qquad (12)$$

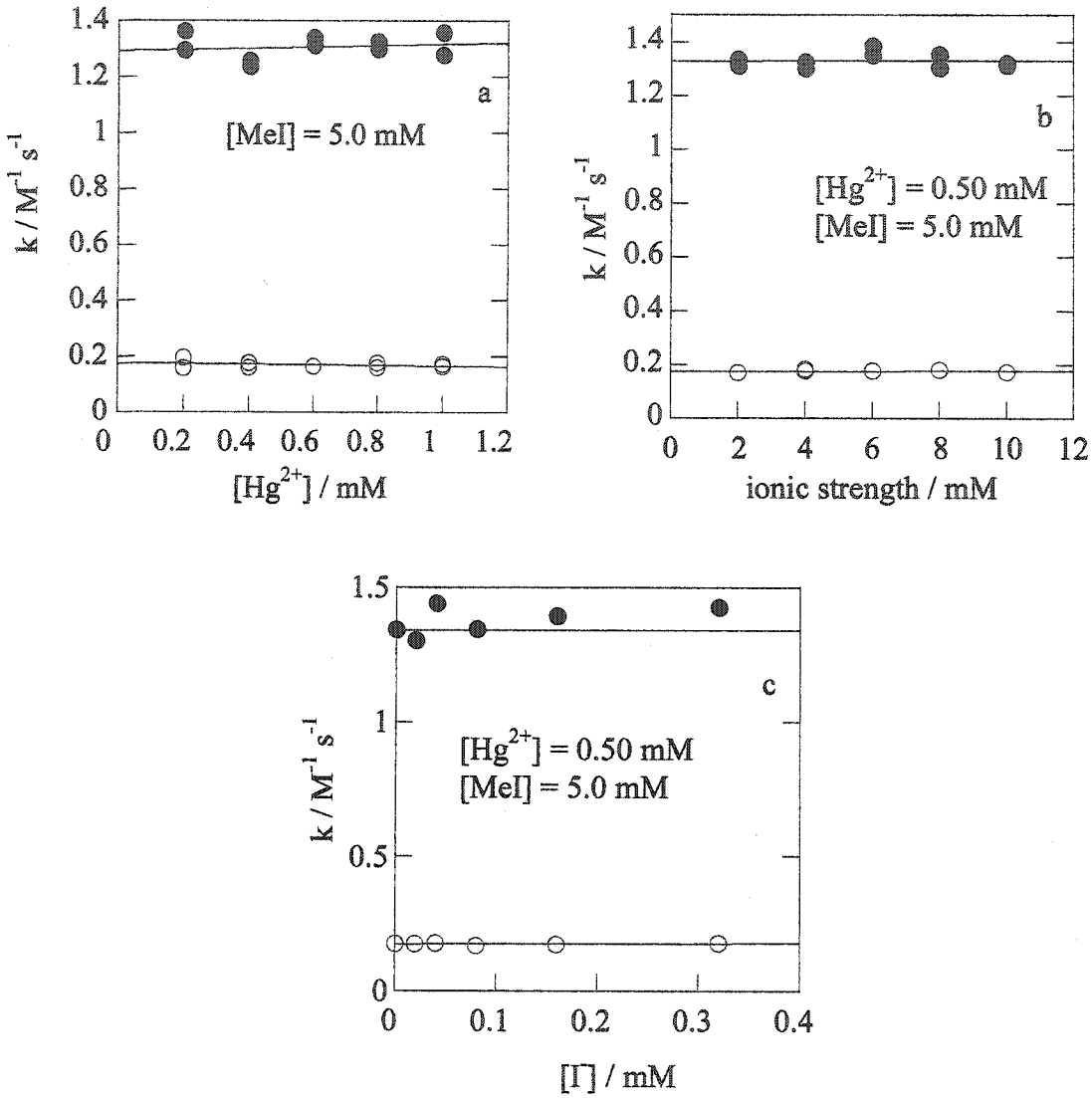

Figure 3.6 Dependence of the second-order rate constants k_1 (filled circles) and k_2 (open circles) for the reaction between Hg^{2+} and MeI at 38.8°C, pH 2.3 on (a) the concentration of Hg^{2+}; (b) the ionic strength ($HClO_4$, $NaClO_4$); (c) added iodide

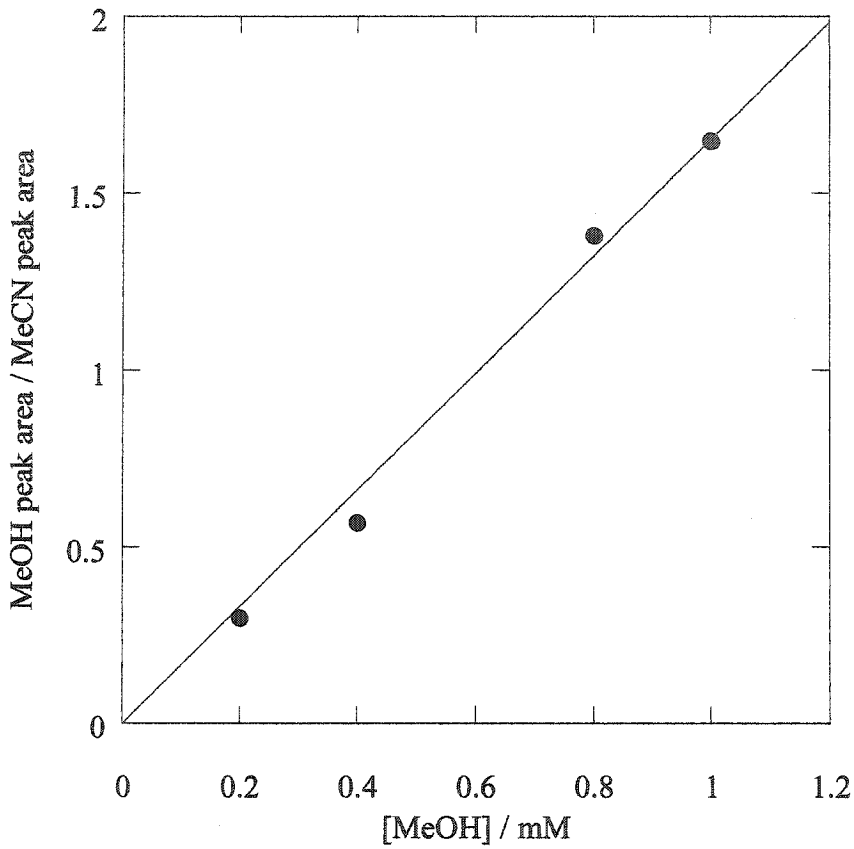

	Ratio = m * [MeOH]
m	1.65 ± 0.05
Chisq	0.010339
R^2	0.9974

Figure 3.7 GC/FID calibration curve for methanol

Table 3.2 Yields of methanol from the reaction of mercuric ion with 2.0 mM MeI[a]

$[Hg^{2+}]$ mM	[MeOH] mM
0.050	0.11
0.10	0.23
0.20	0.38

[a] Conditions: 2.0 mM MeI, 38.8°C, pH 2.3, ionic strength 0.0050 M ($HClO_4$).

3.4 Inorganic Reaction Products

The UV spectral changes observed upon mixing Hg^{2+} with MeI (Figure 3.1) are consistent with the formation of intensely absorbing mercury-iodide complexes. Authentic samples of HgI^+ and HgI_2 were prepared by mixing solutions of Hg^{2+} with KI such that $[Hg^{2+}] = [I^-]$ and $[Hg^{2+}] = 0.5\ [I^-]$, respectively, Chapter 2. The spectrum of HgI^+ exhibits peaks at 217 and 275 nm, while maxima for HgI_2 occur at 210 and 265 nm, Figure 3.8.[38,39] The shift of the peak maximum in Figure 3.1 from 275 to 265 nm as the reaction with methyl iodide proceeds is consistent with initial formation of HgI^+, followed by its subsequent conversion to HgI_2. Since the corresponding spectra of HgI_3^- and HgI_4^{2-} extend into the visible region,[39] their presence can be confidently ruled out Figure 3.9. Extinction coefficients for HgI^+ and HgI_2 at 265 and 275 nm were obtained from their spectra, Figure 3.10. The intermediacy of HgI^+ was confirmed by analysis of the preexponential parameters of the double exponential fit, eq 11.

The values of α and β depend on these extinction coefficients, eq.13 and 14.[37]

$$\alpha = (\varepsilon_1 k_1 - \varepsilon_2 k_2)\ [Hg^{2+}]_0 / (k_2 - k_1) \qquad (13)$$

$$\beta = (\varepsilon_2 - \varepsilon_1)\ k_1\ [Hg^{2+}]_0 / (k_2 - k_1) \qquad (14)$$

where ε_1 and ε_2 are the extinction coefficients for HgI^+ and HgI_2 at wavelength λ. The pre-exponential parameters calculated from double exponential fit of the absorbance-time

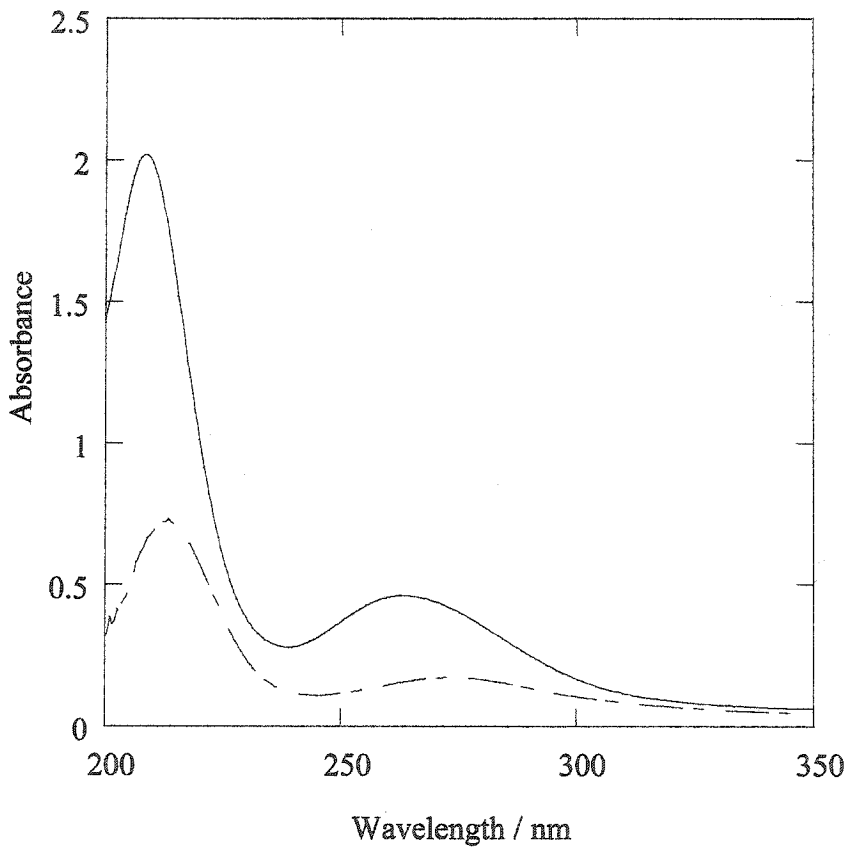

Figure 3.8 UV spectra of 0.07 mM aqueous solutions of HgI_2 (solid line) and HgI^+ (dashed line).

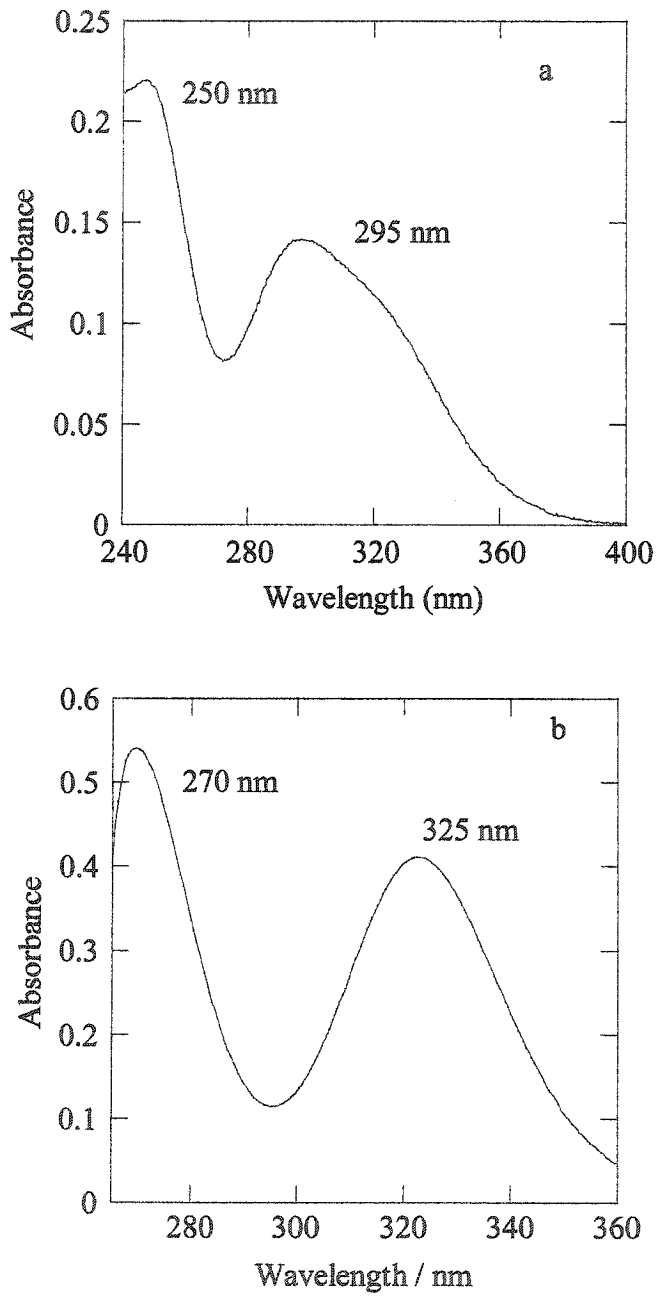

Figure 3.9 UV-Vis spectra for 1 mM aqueous solutions of (a) HgI_3^-; (b) HgI_4^{2-}.

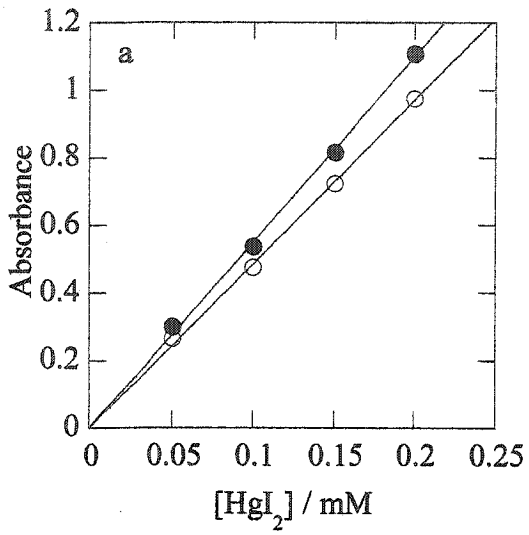

	Absorbance = ε * [HgI_2]	
λ	265 nm	275 nm
ε	5.5 ± 0.1	4.82 ± 0.09
R^2	0.9987	0.9990

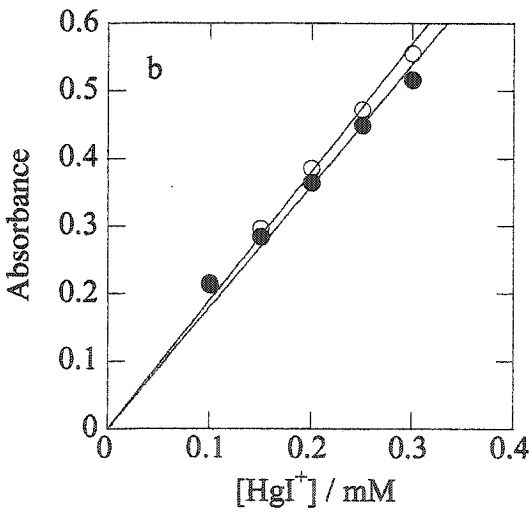

	Absorbance = ε * [HgI^+]	
λ	265 nm	275 nm
ε	1.70 ± 0.07	1.83 ± 0.05
R^2	0.9927	0.9965

Figure 3. 10 UV calibration curves for aqueous solutions of (a) HgI_2; and (b) HgI^+ at 265 nm (filled circles) and 275 nm (open circles)

profile at $\lambda = 275$ nm using $A_\infty = \varepsilon_2 [Hg^{2+}]_0$ are in reasonable agreement with the values calculated from nonlinear curve fits, Table 3.3.

Upon completion of the reaction of Hg^{2+} with methyl iodide, the yield of each complex was determined from the final UV spectrum of the reaction mixture, Table 3.4. Both HgI_2 and HgI^+ are present in appreciable quantities at the end of the reaction, signifying partial dissociation of HgI_2.

3.5 Mechanistic analysis

The absence of a significant ionic strength effect on either rate constant is consistent with a mechanism involving at least one uncharged reactant, *i.e.*, MeI. Furthermore, the absence of an effect of dissolved oxygen implies that methyl radicals are not involved. The double exponential kinetic form of the reaction between mercuric ion and methyl iodide indicates a mechanism involving two consecutive reactions. Furthermore, the shift in peak maximum from 275 nm (characteristic of HgI^+) to 265 nm (characteristic of HgI_2) as the reaction proceeds suggests that these two complexes are formed sequentially, eq 15-16:

$$Hg^{2+} + MeI + H_2O \rightarrow HgI^+ + MeOH + H^+ \quad (15)$$

$$HgI^+ + MeI + H_2O \rightarrow HgI_2 + MeOH + H^+ \quad (16)$$

Table 3.3 Non-linear curve fit parameters for biphasic kinetic data and calculated preexponential parameters (in parentheses) based on known extinction coefficients at 275 nm

$[Hg^{2+}]$ mM	A_∞	α	β
0.20	1.0 (0.95)	0.36 (0.30)	1.1 (0.96)
0.40	1.6 (1.9)	0.42 (0.58)	1.14 (1.33)
0.60	2.5 (2.9)	0.72 (0.87)	1.73 (1.99)
0.80	2.8 (3.2)	0.87 (1.07)	1.93 (2.04)
1.00	3.9 (4.3)	1.12 (1.24)	2.04 (2.33)

Table 3.4 Yields of mercuric iodide complexes upon reaction of Hg^{2+} with MeI

Reactants		Products[a,b]		
$[Hg^{2+}]$	$[CH_3I]$	$[HgI^+]$	$[HgI_2]$	$[HgI^+] + [HgI_2]$
mM	mM	mM	mM	mM
0.050	1.99	0.03 ± 0.01	0.04 ± 0.01	0.07 ± 0.02
0.10	1.83	0.04 ± 0.02	0.08 ± 0.02	0.12 ± 0.03
0.20	1.77	0.07 ± 0.04	0.19 ± 0.02	0.25 ± 0.04
0.23	3.04	0.04 ± 0.02	0.23 ± 0.02	0.26 ± 0.03
0.23	4.43	0.03 ± 0.02	0.23 ± 0.02	0.26 ± 0.03
0.23	7.65	0.05 ± 0.02	0.22 ± 0.04	0.27 ± 0.04

[a] Calculated from experimental UV spectra using measured extinction coefficients (see text).

[b] Uncertainties are calculated using the errors on extinction coefficients and the distribution of error formula

The concentrations of each mercury complex were calculated from the absorbances at 275 and 265 nm recorded during the course of the reaction with methyl iodide, using the measured extinction coefficients for HgI^+ and HgI_2. These concentrations are plotted in Figure 3.11, clearly showing initial formation of HgI^+. Its concentration passes through a maximum then decreases as it is converted to HgI_2. The latter begins to appear after an induction period corresponding to the time at which $[HgI^+]$ passes through its maximum. Double exponential curve fits of these concentration profiles yield the same values for k_{1obs} and k_{2obs} as do the double exponential fits to the absorbance-time profile. Therefore k_{fast} can be assigned as the rate constant for the reaction of Hg^{2+} with methyl iodide whilst k_{slow} is the rate constant for the reaction of HgI^+ with methyl iodide.

3.6 Effect of pH

Both second–order rate constants k_{fast} and k_{slow} depend on the concentration of hydrogen ion, Table 3.5. Both show saturation behavior at high $[H^+]$, Figure 3.12. The acid-dependence of the second–order rate constants is described by eq 17-18

$$k_{fast} = k_1 [H^+]^2 / (K_{a1}K_{a2} + K_{a1} [H^+] + [H^+]^2) \quad (17)$$

$$k_{slow} = k_2 [H^+] / (K_{a3} + [H^+]) \quad (18)$$

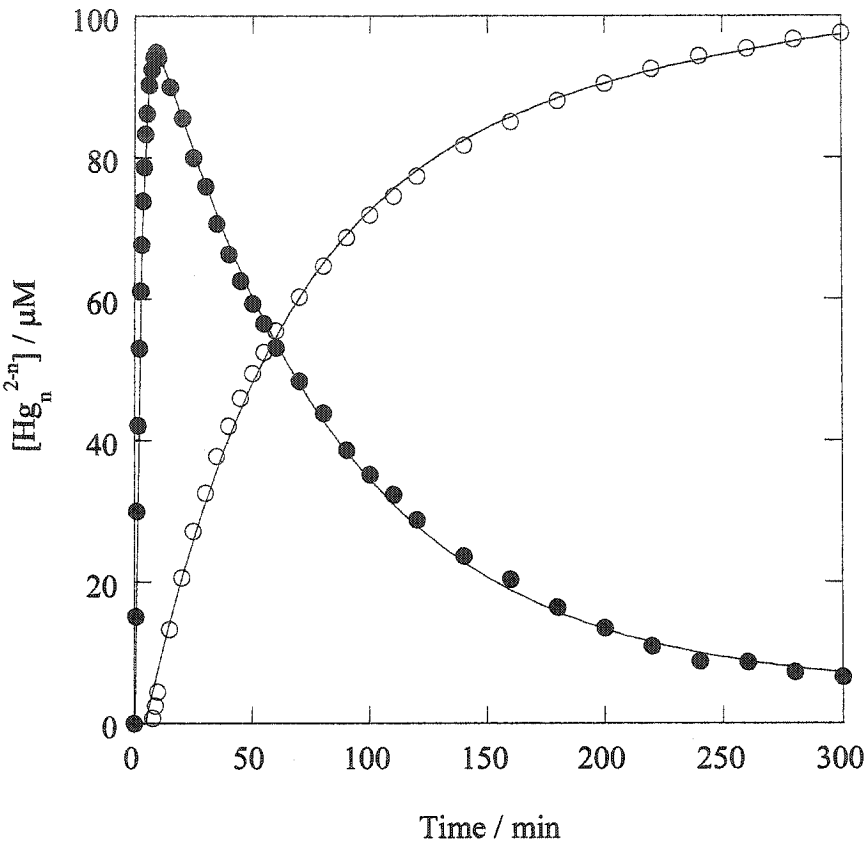

Figure 3. 11 Calculated kinetic profiles for the formation of HgI^+ (filled circles) and HgI_2 (open circles) in the reaction of 0.10 mM Hg^{2+} with 2.0 mM MeI at 38.8°C, pH 2.3 ($HClO_4$) and 0.010 M ionic strength ($HClO_4/NaClO_4$). Solid lines are 5-parameter fits to equation 11 (see text).

Table 3. 5 Dependence of the second-order rate constants k_{fast} and k_{slow} for the reaction of Hg^{2+} with MeI on the concentration of hydrogen ion, at 38.8°C and 0.050 M ionic strength ($HClO_4/NaClO_4$).

$[H^+]$ mM	pH	k_{fast}[a] $M^{-1} s^{-1}$	k_{slow}[a] $M^{-1} s^{-1}$
0.21	3.68	0.0772 ± 0.0003	0.00772 ± 0.00009
0.95	3.02	0.256 ± 0.005	0.0331 ± 0.0006
1.58	2.80	0.584 ± 0.006	0.0761 ± 0.0002
2.24	2.65	0.768 ± 0.003	0.0844 ± 0.0008
3.24	2.49	0.929 ± 0.002	0.0888 ± 0.0006
4.47	2.35	1.07 ± 0.03	0.115 ± 0.008
5.37	2.27	1.11 ± 0.04	0.113 ± 0.003
7.24	2.14	1.23 ± 0.02	0.116 ± 0.008
8.51	2.07	1.22 ± 0.03	0.123 ± 0.005
9.77	2.01	1.23	0.133 ± 0.005
13.2	1.88	1.24	0.134 ± 0.008

[a] Errors calculated from the non-linear regression fit to experimental data

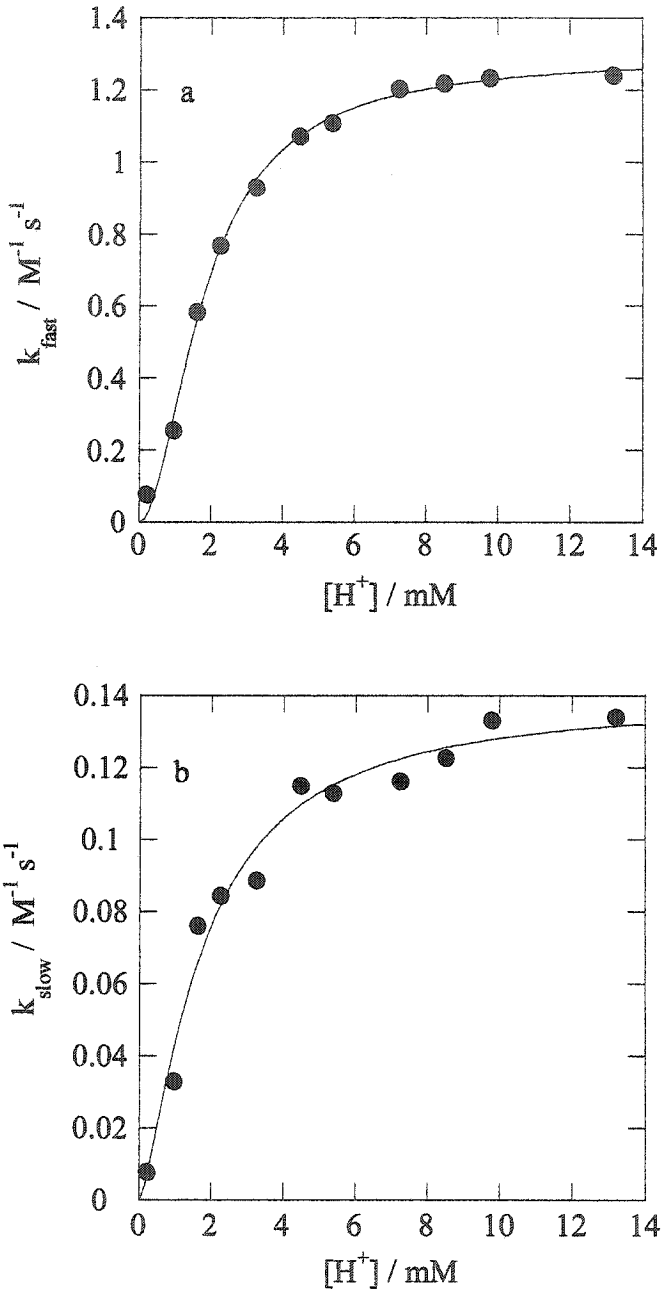

Figure 3.12 Dependence of the second-order rate constants k_{fast} and k_{slow} for the reaction of Hg^{2+} with MeI on the concentration of hydrogen ion, at 38.8°C and 0.050 M ionic strength ($HClO_4/NaClO_4$). The solid lines are non-linear curve fits to eq.17-18, respectively (see text).

The form of the pH dependence of k_{fast} implies that the mercury reagent is subject to pre-equilibrium hydrolysis, eq 19-20:

$$Hg^{2+} + H_2O \leftrightarrows HgOH^+ + H^+ \qquad K_{a1} \qquad (19)$$

$$HgOH^+ + H_2O \leftrightarrows Hg(OH)_2 + H^+ \qquad K_{a2} \qquad (20)$$

The three-parameter fit of the data in Figure 3.12a to eq 16 yields the intrinsic rate constant $k_1 = (1.34 \pm 0.02)\ M^{-1}\ s^{-1}$ and the acid dissociation constants $K_{a1} = (3 \pm 2) \times 10^{-4}$ and $K_{a2} = (2.3 \pm 0.4) \times 10^{-3}$ at 38.8°C and 0.010 M ionic strength. The fitted acid dissociation constants are comparable to literature values for the sequential hydrolysis of $Hg(H_2O)_6^{2+}$, 3.3×10^{-4} and $2.0 \times 10^{-3}\ M^{-1}$. The observed pH dependence of the rate constant k_{fast} as the pH decreases demonstrates that Hg^{2+} is reactive towards methyl iodide while $HgOH^+$ and $Hg(OH)_2$ are not.

Similarly, the two-parameter fit of the data in Figure 3.12b to eq 17 yields $k_2 = (0.16 \pm 0.01)\ M^{-1}\ s^{-1}$ and $K_{a3} = (2.2 \pm 0.4) \times 10^{-3}$, where K_{a3} corresponds to the hydrolysis of HgI^+, eq 21:

$$HgI^+ + H_2O \leftrightarrows Hg(I)(OH) + H^+ \qquad (21)$$

Thus HgI^+ is reactive towards methyl iodide while Hg(I)(OH) is not. These findings are consistent with the greater electrophilicity of the fully protonated forms of the mercuric complexes.

3.7 Effect of added iodide

The kinetic profiles remain distinctly biphasic and the magnitudes of the second–order rate constants are unchanged by the addition of small amounts of iodide ion, up to 0.32 mM in a 0.50 mM Hg^{2+} solution, Figure 3.6c. However, when 0.50 mM iodide was added to a 0.50 mM Hg^{2+} solution, the kinetics of the reaction with 5.0 mM methyl iodide are those of a single exponential growth, Figure 3.13a. Under these conditions, the mercuric ion is initially present as HgI^+, which is responsible for the high value of A_0 at 275 nm (see below). From the fitted value of $k_{obs} = (0.091 \pm 0.001)\ s^{-1}$, the second–order rate constant is calculated to be $(0.181 \pm 0.003)\ M^{-1}\ s^{-1}$, identical to k_{slow}, $(0.176 \pm 0.003)\ M^{-1}\ s^{-1}$ at pH 2.3 ($HClO_4$) and 0.010 M ionic strength ($NaClO_4/HClO_4$). Thus we have independent confirmation of the assignment of k_{slow} to the reaction of HgI^+ with MeI.

At higher concentrations, iodide inhibits the reaction completely. Thus no reaction was detected when a solution containing 0.20 mM Hg^{2+} and 0.40 mM I^- was mixed with 2.0 mM MeI, Figure 3.13b. Under these conditions, mercury is initially converted to HgI_2. The reactivity order $Hg^{2+} > HgI^+ > HgI_2$ towards methyl iodide is consistent with decreasing electrophilicity in this series.

3.8 Effect of temperature

Values of k_1 and k_2 between 10 and 50°C, obtained by correcting k_{fast} and k_{slow} for their H^+ dependence using eq.17-18, are collected in Table 3.6. Both rate constants show a

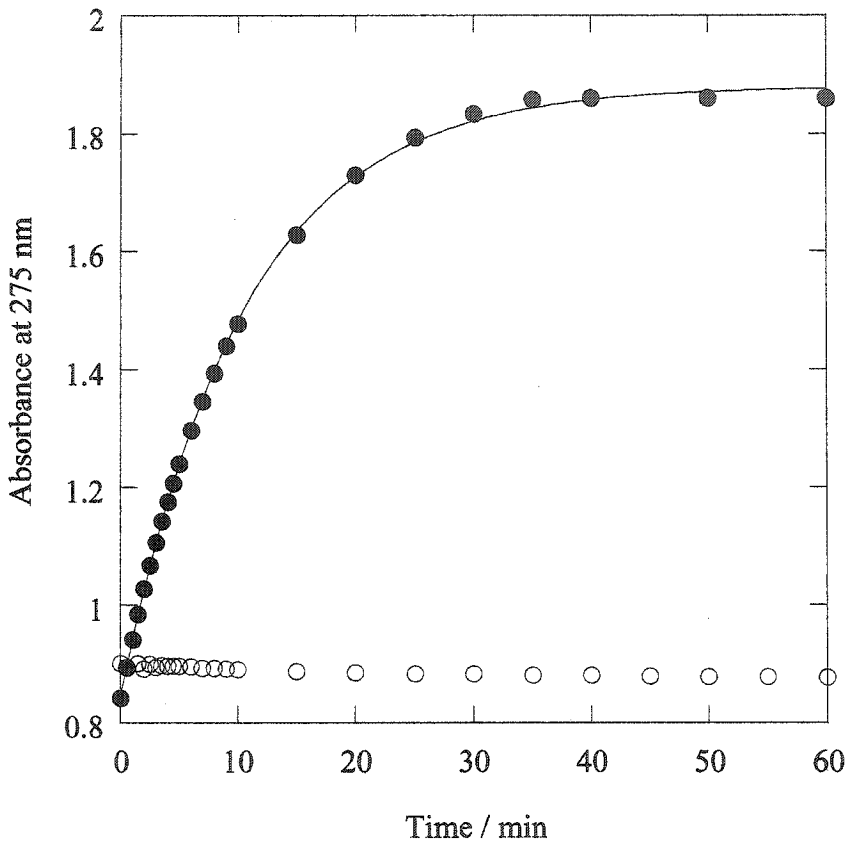

Figure 3.13 Kinetic profiles for the reactions of (a) 0.50 mM HgI^+ with 5.0 mM MeI (filled circles), and (b) 0.2 mM HgI_2 with 2 mM MeI (open circles) at 38.8°C, pH 2.3 ($HClO_4$) and 0.010 M ionic strength ($NaClO_4/HClO_4$). The solid line is the single-exponential fit to the experimental data.

Table 3.6 Temperature dependence of intrinsic second-order rate constants[a] for the reaction of Hg^{2+} with excess MeI [b]

Temperature °C	k_1 $M^{-1} s^{-1}$	k_2 $M^{-1} s^{-1}$
11.5	0.165 ± 0.003	0.019 ± 0.001
20.6	0.382 ± 0.004	0.045 ± 0.002
29.5	0.83 ± 0.02	0.115 ± 0.001
38.8	1.43 ± 0.06	0.234 ± 0.003
48.1	2.31 ± 0.03	0.456 ± 0.004

[a] Errors are calculated from distribution of errors formula.

[b] Conditions: 0.20 mM Hg^{2+}, pH 2.3, 0.010 M ionic strength ($HClO_4/NaClO_4$).

similar temperature dependence, in which their magnitude approximately doubles for each 10° increase in temperature. The Eyring plots, equation 22, are linear, Figure 3.14 and the activation parameters were obtained from their slopes and intercepts.[37]

$$\ln(k/T) = \ln(k_B/h) + \Delta S^{\ddagger}/R - \Delta H^{\ddagger}/(RT) \qquad (22)$$

where k_B is the Boltzmann constant, h is Planck's constant and R is the gas constant.

The values of $\Delta H_1^{\ddagger}$ and $\Delta S_1^{\ddagger}$ are (52 ± 3) kJ mol^{-1} and -(75 ± 5) J mol^{-1} K^{-1}, respectively. For $\Delta H_2^{\ddagger}$ and $\Delta S_2^{\ddagger}$, values are (64 ± 2) kJ mol^{-1} and -(52 ± 2) J mol^{-1} K^{-1}, respectively. Large negative values of $\Delta S_1^{\ddagger}$ and $\Delta S_2^{\ddagger}$ are consistent with bimolecular reactions in each step.

3.9 Kinetics of the reaction of MeI with excess Hg^{2+}(aq)

When the pseudo-first-order condition is reversed, such that Hg^{2+} is in large excess over methyl iodide, the spectral changes are those shown in Figure 3.15. In contrast to the results described above, the peak maximum at 275 nm does not shift over the course of the reaction and the kinetic profile is not biexponential. The inset to Figure 3.15 shows the fit of the absorbance-time profile to a single exponential function. Under these reaction conditions, we expect to observe only the formation of HgI^{+}.

Values of the pseudo-first-order rate constants k_{3obs} measured at pH 1.0, 0.10 M ionic strength and 30.0°C are shown in Table 3.7. They depend linearly on the concentration of the mercuric ion, Figure 3.16. The second-order rate constant for this

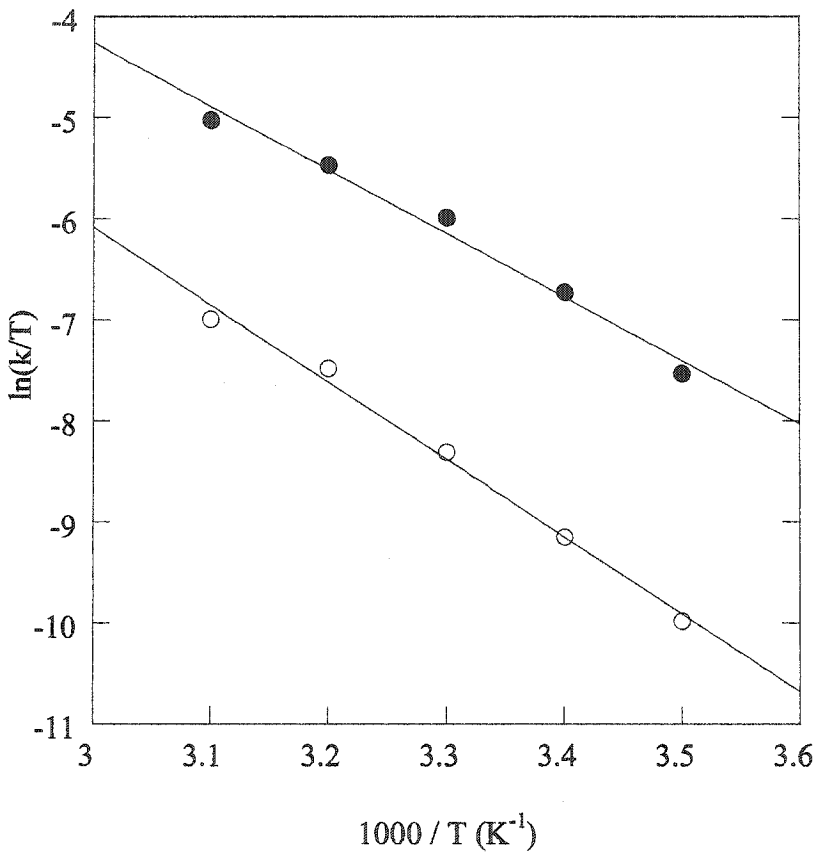

Figure 3. 14 Eyring plots for the intrinsic second-order rate constants k_1 (filled circles) and k_2 (open circles).

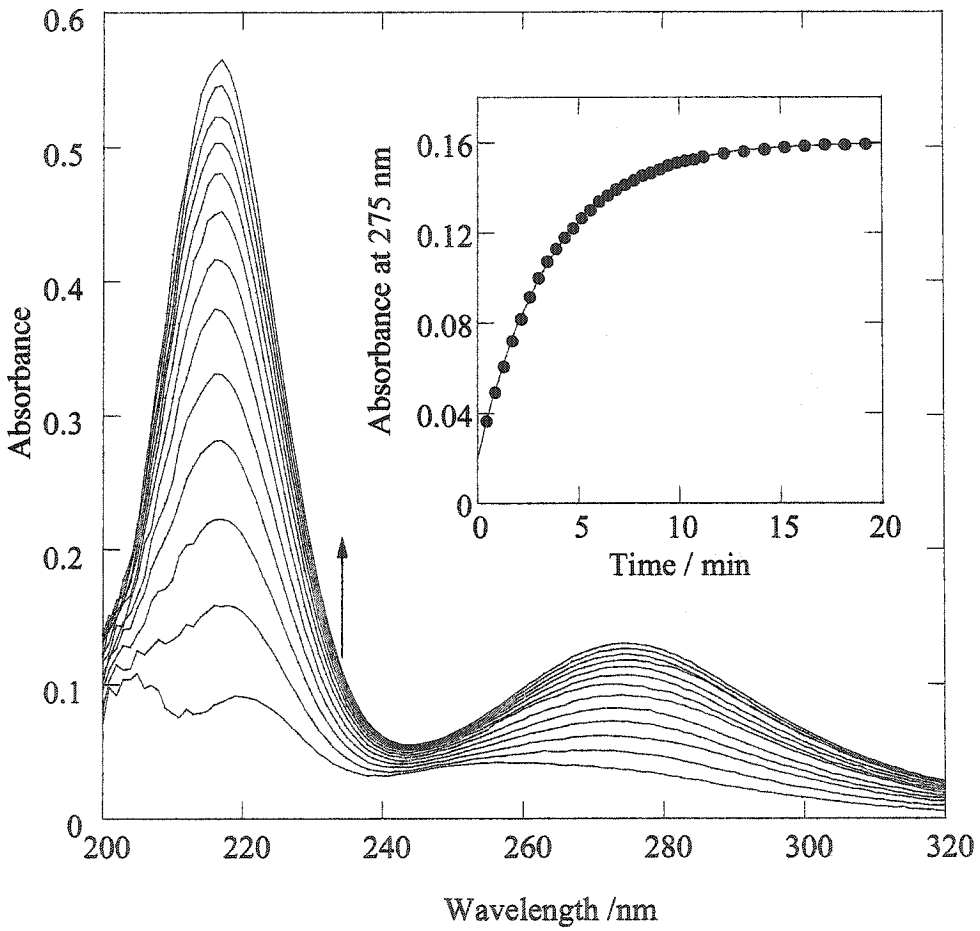

Figure 3.15 Evolution of the UV spectrum of a mixture of 2.0 mM Hg^{2+} and 0.20 mM MeI at 30.0°C, pH 2.3 ($HClO_4$) and 0.010 M ionic strength ($HClO_4/NaClO_4$). Total time elapsed 30 min. The inset shows the kinetic profile at 275 nm. The solid line is the single exponential fit to the experimental data.

Table 3.7 Pseudo-first-order rate constants[a] for the reaction of excess $Hg^{2+}_{(aq)}$ with MeI[b]

$[Hg^{2+}]$ mM	k_{3obs} x 1000 s^{-1}
2.0	3.07 ± 0.02
4.0	6.33 ± 0.03
6.0	9.47 ± 0.02
8.0	11.6 ± 0.1
10.0	14.0 ± 0.2

[a] Errors are calculated from three-parameter nonlinear curve fits to the integrated first-order rate equation, eq 10

[b] Conditions: 0.20 mM MeI, pH 1.0, 0.10 M ionic strength ($HClO_4/NaClO_4$), 30.0°C.

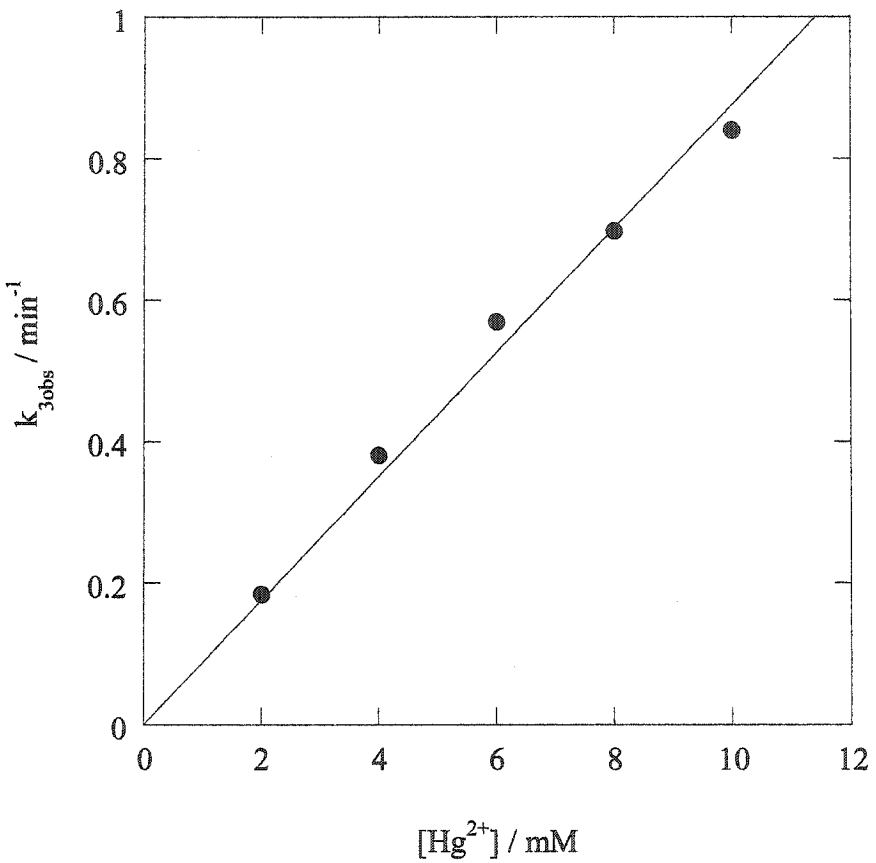

Figure 3.16 Dependence of the pseudo-first-order rate constants k_{3obs} for the reaction between excess Hg^{2+} and MeI, on the concentration of Hg^{2+} at 30.0°C, pH 1.0 ($HClO_4$) and 0.10 M ionic strength ($HClO_4$).

reaction is therefore (1.46 ± 0.03) M^{-1} s^{-1}, compared to (1.35 ± 0.02) M^{-1} s^{-1} M^{-1} s^{-1} for k_1 measured at the same pH and temperature. Hence we have independent confirmation of the assignment of k_{fast} to the reaction of Hg^{2+} with MeI.

3.10 Reaction of Hg^0 with methyl iodide

3.10.1 Yield of methylmercury

A saturated aqueous solution of Hg^0 (2.6 ± 0.5) x 10^{-7} M) was shaken overnight with 2.0 mM MeI in a dark bottle wrapped with aluminum foil (neutral pH, room temperature). The solution was found to contain methylmercury, (2.4 ± 0.9) nM (ten replicates). Its yield based on [Hg^0] is 1.1%. For comparison, Hall reported a methylmercury yield of 0.06 % after 5 hours reaction time. [22]

3.10.2 Kinetics of methylmercury formation

The rate constant k_{obs} for the formation of methylmercury was measured by withdrawing and analyzing aliquots from reaction mixtures saturated with Hg^0 and spiked with methyl iodide. Solutions were prepared in brown bottles wrapped with aluminum foil and shaken at room temperature (22.5 °C). The kinetic profiles are shown in Figure 3.17. The reaction is pseudo-first-order, such that the formation of methylmercury can be described by a single exponential function, eq 23:

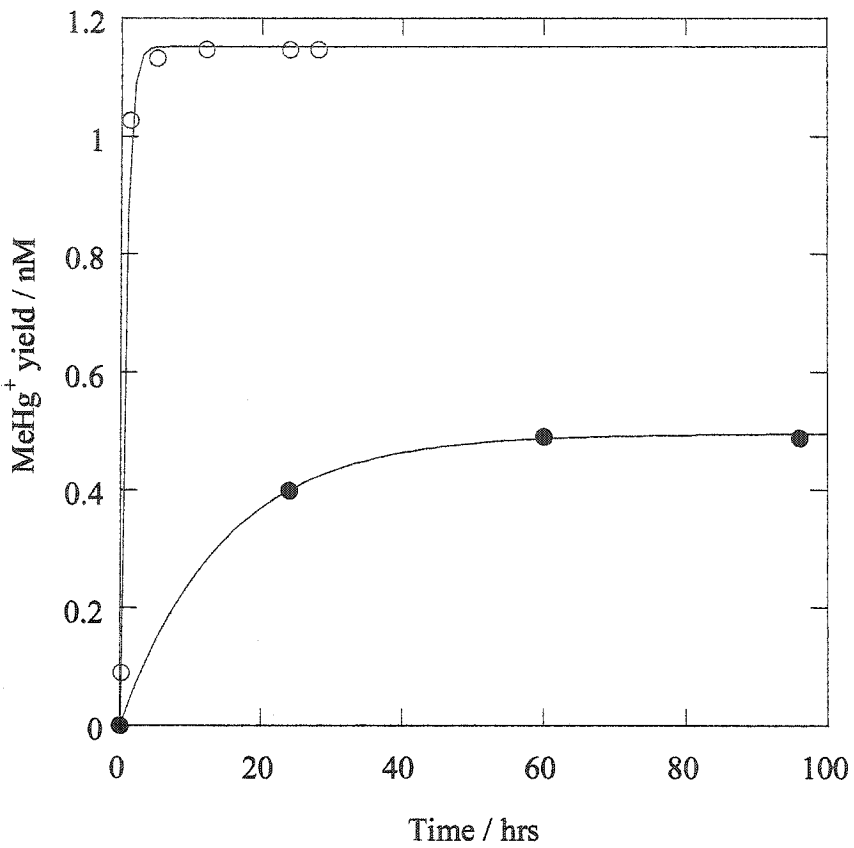

Figure 3.17 Kinetic profiles for the reaction of $Hg^0_{(aq)}$ with 1 mM MeI (filled circles) and 20 mM MeI (open circles) at neutral pH, and room temperature. The solid lines are the non-linear least squares curve fits to eq 23 (see text).

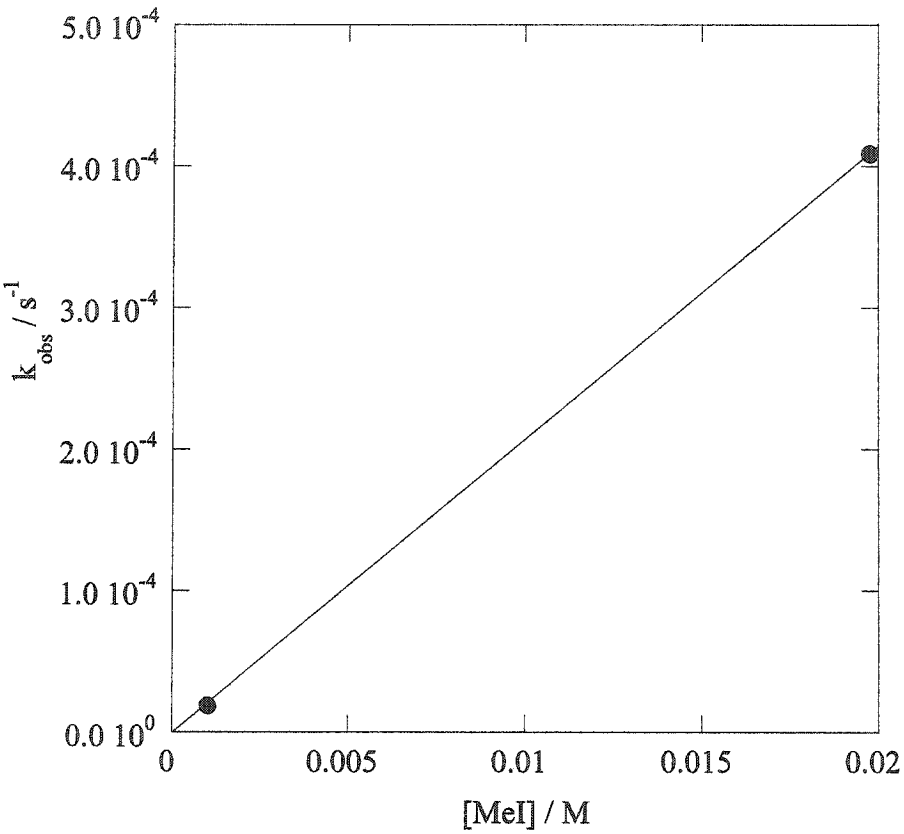

Figure 3.18 Dependence of the pseudo-first-order rate constants k_{obs} for the reaction between $Hg^0_{(aq)}$ and excess MeI, on the concentration of MeI.

$$[MeHg^{+}]_t = [MeHg]_\infty (1 - e^{-kobs\ t}) \quad (23)$$

The values of the observed rate constants are (1.90 ± 0.09) x 10^{-5} s^{-1} for 1.0 mM MeI and (4.2 ± 0.8) x 10^{-4} s^{-1} for 19.75 mM MeI. Thus k_{obs} depends linearly on the concentration of methyl iodide concentration, Figure 3.18, with k = 0.020 M^{-1} s^{-1}. This value corresponds to 3.3 x 10^{-23} cm^3 $molecules^{-1}$ s^{-1}, and is smaller than a value reported previously, 8.0 x 10^{-21} cm^3 $molecules^{-1}$ s^{-1}.[22] However, the latter was measured in the presence of a 700 W/m^2 solar flux and the rate of the reaction is known to be accelerated by radiation. [21,34]

3.12 Conclusions

The hydrolysis of methyl iodide in presence of the mercuric ions has been shown to be kinetically biphasic, consistent with the consecutive formation of HgI^+ and HgI_2. Since Hg^{2+} is a better electrophile than HgI^+ the first step of the reaction is ca. ten times faster than the second. The major products are methanol, HgI^+ and HgI_2.

The interaction of methyl iodide with mercuric ions may affect the geochemical cycle of mercury in the aquatic environment in two different ways. It promotes the formation of compounds such as HgI^+ and HgI_2 which are less reactive towards chemical and biological methylation and methylate Hg^0 which present when Hg^{2+} is reduced by reducing agents present in the aquatic environment.

As Thayer has pointed out, methyl iodide can play an important role in the solubilization and mobilization of metals in the sediments and in the aquatic

environment.[6] The amount of methyl mercury produced from the reaction of methyl iodide with mercury in aqueous solutions is relatively small (about 1% yield). However, in natural conditions, the consumption of methylmercury due to biological and chemical processes, will push the equilibrium forward and promote further production and biological consumption of methylmercury.

References

(1) Yokouchi, Y.; Nojiri, Y.; Barrie, L. A.; Toom-Sauntry, D.; Fujinuma, Y. *J. Geophys. Res., [Atmos.]* **2001,** *106*, 12661-12668.

(2) Moore, R. M.; Groszko, W. *J. Geophys. Res., [Oceans.]* **1999,** *104*, 11163-11171.

(3) Lovelock, J. E. *Nature* **1975,** *256*, 193-194.

(4) Craig, P. J.; Rapsomanikis, S. *Environ. Sci. Technol.* **1985,** *19*, 726-730.

(5) Thayer, J. S.; Olson, G. J.; Brinckman, F. E. *Appl. Organomet. Chem.* **1987,** *1*, 73-79.

(6) Thayer, J. S.; Olson, G. J.; Brinckman, F. E. *Environ. Sci. Technol.* **1984,** *18*, 726-729.

(7) Craig, P. J.; Laurie, S. H.; McDonagh, R. *Appl. Organomet. Chem.* **1998,** *12*, 237-241.

(8) Nightingale, P. D.; Malin, G.; Liss, P. S. *Limnol. Oceanogr.* **1995,** *40*, 680-689.

(9) Scarrat, M. G.; Moore, R. M. *Limnol. Oceanogr.* **1999,** *44*, 703-707.

(10) McMurry, J. Organic chemistry; Brooks/ Cole: Pacific Grove, California, 1988.

(11) Ehrich, H. L. Geomicrobiology; Marcel Dekker: New York, 1981.

(12) Lobban, C. S.; Wynne, M. J. The biology of seaweeds; University of California Press: Berkeley, 1981.

(13) Harper, D. B. *Nature* **1985,** *315*, 55.

(14) Moore, R. M.; Zafiriou, O. C. *J. Geophys. Res., [Atmos]* **1994,** *99*, 16415-16420.

(15) Thayer, J. S. *Adv. Organomet. Chem.* **1975,** *13*, 1-5.

(16) Krishnamurthy, S. *Chem. Environ.* **1992,** *69*, 347-350.

(17) Jarvie, A. W. P.; Whitmore, A. P. *Environ. Technol. Lett.* **1981,** *2*, 197-204.

(18) Lee, D. S.; Weber, J. H. *Appl. Organomet. Chem.* **1988,** *2*, 435-440.

(19) Manders, W. F.; Olson, G. J.; Brinckman, F. E.; Bellama, J. M. *J. Chem. Soc. Chem. Comm.* **1984**, 538.

(20) Weber, J. H. *Chemosphere* **1993,** *26*, 2063-2077.

(21) Craig, P. J. Organometallic compounds in the environment; Longman: London, 1986.

(22) Hall, B.; Bloom, N. S.; Munthe, J. *Water Air Soil Poll.* **1995,** *80*, 337-341.

(23) Tokos, J. J. S.; Hall, B.; Calhoun, J. A.; Prestbo, E. M. *Atmos. Environ.* **1998,** *32*, 823 -827.

(24) Ebinghaus, R.; Wilken, R. D. *Appl. Organomet. Chem.* **1993,** *7*, 127-135.

(25) Vollhard, K. P. C. Organic chemistry; Freeman: New York, 1987.

(26) March, J. Advanced organic chemistry. Reactions, mechanisms and structure; 3rd ed.; John Willey and Sons: Toronto, 1985.

(27) Zamashchikov, V. V.; Rudakov, E. S.; Bezbozhnaya, T. V. *React. Kinet. Catal. Lett.* **1984,** *24*, 65-69.

(28) Jensen, J. L.; Maynard, D. F. *J. Organomet. Chem.* **1990,** *55*, 4828- 4831.

(29) Jensen, J. L.; Maynard, D. F.; Shaw, G. R.; Tyrrell W. Smith, J. *J. Organomet. Chem.* **1992,** *57*, 1982-1986.

(30) Bunce, N. Environmental chemistry; 2nd ed.; Wuerz: Winnipeg, 1994.

(31) Maynard, J. L. *J. Am. Chem. Soc.* **1932,** *54*, 2108-2112.

(32) Larock, R. C. Organomercury compounds in organic synthesis; Springer- Verlag: New York, 1985.

(33) Fieser, L. F.; Fieser, M. Reagents for organic synthesis; John Wiley and Sons, Inc.: New York, 1967.

(34) Xinquan, R.; Jun, Z.; Wang, H. *Zhongguo Huanjing Kexue* **1998,** *18*, 524-526.

(35) Latyaeva V.N., M. A. V., Razuvaev G.A. *Zhurnal Vseso I Uznogo Khimicheskogo Obshchest Im D.I. Mendeleeva* **1962,** *7*, 594.

(36) Falter, R. *Chemosphere* **1999,** *39*, 1051-1073.

(37) Espenson, J. H. Chemical kinetics and reaction mechanisms; 2nd ed.; McGraw-Hill, Inc.: New York, 1981.

(38) Templet, P.; McDonald, J. R.; McGlynn, S. P. *J. Chem. Phys.* **1973,** *56*, 5746.

(39) Griffiths, R.; Anderson, R. A. *J. Chem. Soc. Farad.Trans.1* **1984,** *80*, 2361-2374.

Chapter 4

Reaction of Mercuric Ions with Methylcobaloxime

4.1 Introduction

The alkylation of mercuric ions by organocobalt complexes was first described by Halpern and Maher in 1964.[1] The environmental relevance of this reaction was soon realized when, in 1968, Wood, Kennedy and Rosen reported methylation of inorganic mercury by methanogenic bacteria in sediments.[2] These authors proposed methyl transfer from methylcobalamin to mercury as a result of both enzymatic and non-enzymatic processes. Soon after, it was demonstrated that methylcobalamin in aqueous abiotic systems is capable of transferring a methyl carbanion group to mercuric ions.[3-6] The reaction of mercuric ions with methylcobalamine is often used for the synthesis of various mercury-isotopes of methylmercury.[7]

The holoenzyme responsible for methylation consists of an enzyme-coenzyme complex. The enzyme is a peptide whose composition depends on its biological source, while the coenzyme is a cobalt complex which can be isolated by denaturation of the peptide.[9] The structures of Coenzyme B_{12} and its derivatives have been the subject of many studies.[10-15] Often called adenosylcobalamin and represented as $AdoB_{12}$,[9] its structure is shown in Figure 4.1, where R stands for 5′-deoxyadenosyl. The first derivative of this coenzyme to be characterized had the 5-deoxyadenosyl ligand replaced by cyanide. This compound is the so-called vitamin B_{12}, or cyanocobalamin. When 5′-deoxyadenosyl is replaced by water, the compound is called aquocobalamin or B_{12a},

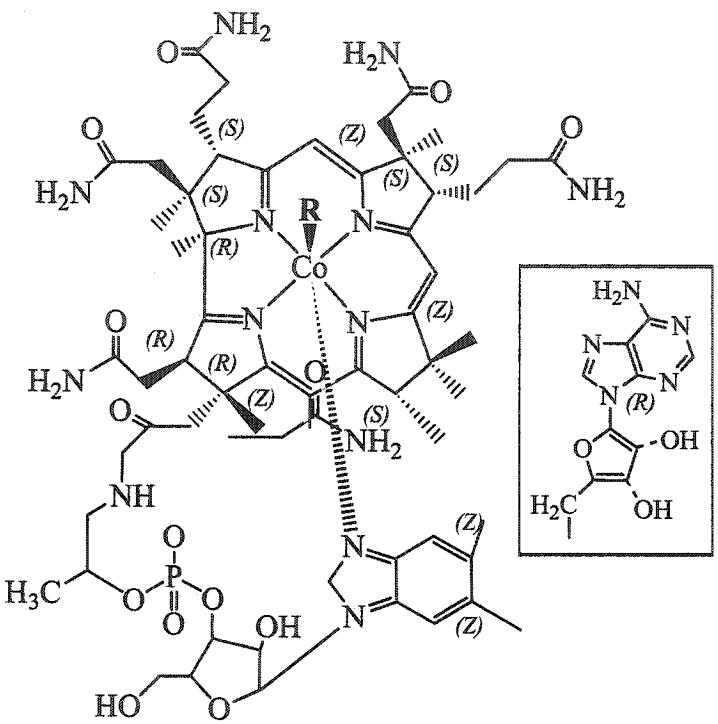

Figure 4.1 The structure of coenzyme B_{12} (R = 5′-deoxyadenosyl, shown in the inset) and its derivatives: cyanocobalamin or Vitamin B_{12} when R = CN; methylcobalamin when R=CH_3; aquocobalamin when R = H_2O.

while the methyl derivative is called methylcobalamin. In all of these compounds, cobalt is in oxidation state III with coordination number 6. The Co(III) ion in $AdoB_{12}$ and its derivatives can be reduced, to yield five-coordinate Co(II) and four-coordinate Co(I) derivatives called B_{12r} and B_{12s}, respectively.[9,16] In coenzyme B_{12}, the benzoimidazole ligand may be protonated and displaced by solvent to give the "base-off" form.

Vitamin B_{12} and related compounds are widely produced in the aquatic environment by both aerobic and anaerobic microbes such as *Pseudomonas denitrificans, Rhodospirillum rubrum, Salmonella typhimurium, Escherichia coli,* methanogens, acetogenic bacteria, clostridia and sulfate-reducing bacteria.[17] These compounds provide the coenzymes for two main groups of enzymatic reactions: isomerizations and methyl transfers, such as the reaction of 5N-methyl-tetrahydrofolic acid with homocysteine to give methionine.[16]

Methylcobalamin is also known to be biologically active and is essential for human metabolism.[12] Its chemistry has been the subject of many studies focused on biological methylation of heavy elements in the aquatic environment. As Pratt describes in his review of methyl transfer reactions of cobalt corrinoids,[16] the cobalt ion in B_{12} and its derivatives is readily interconverted between valences I, II and III. Thus the Co-Me bond can be made or broken by reactions with electrophiles such as Hg^{2+},[5,18] in which the transition state corresponds to (Co^{III}, Me^-), by photolytic homolysis, with transition state (Co^{II}, $Me\bullet$), or by reaction with nucleophiles such as MeI, corresponding to (Co^{I}, Me^+).[19] In his review of the mechanisms of B_{12}-dependent methyl transfer to heavy elements, Wood identifies four mechanisms of methyl transfer from methylcobalamin to metals:[20]

1. Electrophilic attack on the Co-C bond (S_E2 mechanism), as in the reaction with Hg^{2+},[5] Scheme 4.1;

Scheme 4.1 Bimolecular electrophilic substitution mechanism (S_E2) for methyl transfer from Co at methylcobalamin to Hg^{2+}

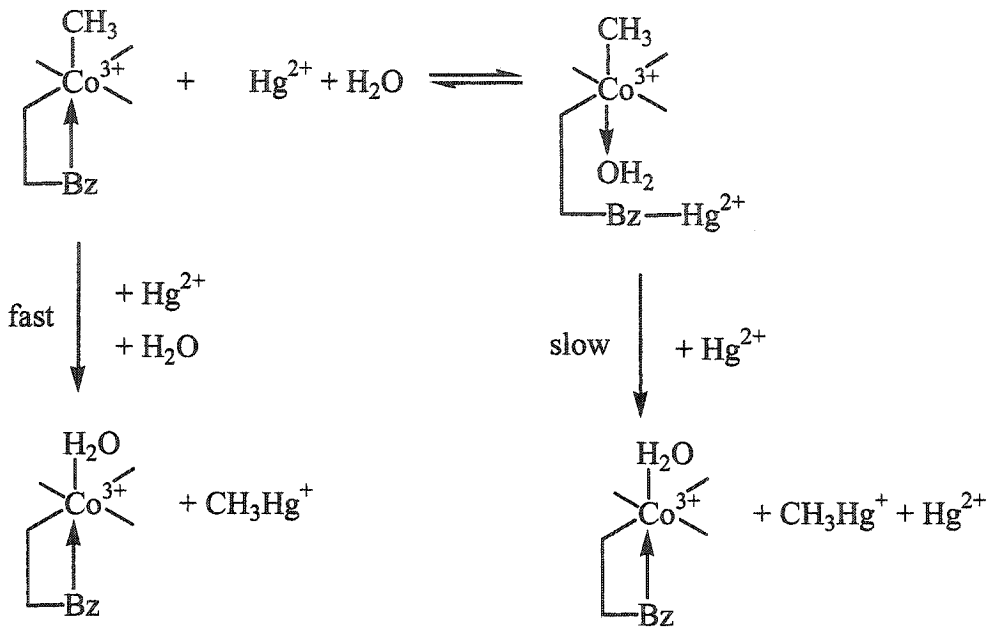

2. One equivalent "outer-sphere" oxidative cleavage of the Co-C bond, as in the reaction with $IrCl_6^{2-}$ [20], Scheme 4.2;

Scheme 4.2 Oxidation of alkylcobaloximes by hexachloroiridate followed by the nucleophilic attack on the Co(IV) intermediate by Cl^-.

$$R\text{-}Co^{III}(DH)_2H_2O \underset{e^-}{\overset{e^-}{\rightleftharpoons}} R\text{-}Co^{IV}(DH)_2H_2O \overset{Cl^-}{\rightleftharpoons} Co^{II}(DH)_2H_2O + RCl$$

3. Redox switch, as in the reaction with platinum salts where the transfer of methyl group to form the CH_3Pt^{IV} requires the presence of both $PtCl_4^{2-}$ and $PtCl_6^{2-}$ since this complex is formed by the oxidation of Pt^{II} through a two electron "redox-switch" with Pt^{IV} ; [21,22]

4. One equivalent reductive cleavage of the Co-C bond, as in the reaction with Sn^{2+}, [23] Scheme 4.3:

Scheme 4.3 Reductive cleavage of the Co-C bond by Sn^{III}•

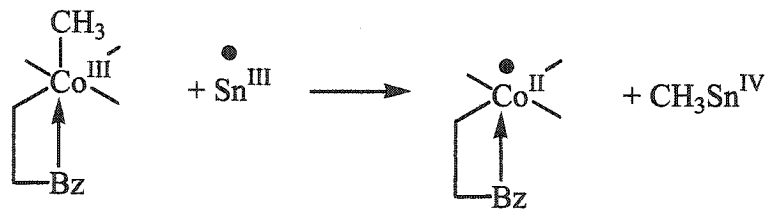

In order to study the biochemical functions of alkylcobalamins, which because of their alkylating properties can be considered to be "biological Grignard reagents" [24] it is useful to have recourse to simple model compounds, which may serve to test mechanistic postulates derived from the biological experiments. One class of simple model compounds which mimic various aspects of the chemistry of vitamin B_{12} are the alkylcobaloximes. Schrauzer was the first to show that bis(dimethylglyoximato) complexes of cobalt can be used as model compounds for vitamin B_{12} and other cobalamins.[15,24,25] Since then, the chemistry and structural properties of cobaloximes have been studied extensively, demonstrating the similarities and differences between

these compounds and B_{12} as well as the mechanisms of reactions of chemical, biological and environmental interest.[14,26-39] Although it is commonly accepted that methylcobalamin is responsible for some mercury methylation in the aquatic environment, the mechanism of this process is not yet clear. The early work of Bartha and co-authors seemed to show that mercury methylation by methylcobalamin is an enzymatic process requiring the presence of specific, strictly anaerobic bacteria, such as the sulfate-reducing *Desulfovibrio desulfuricans* LS.[40-42] Others have shown that this reaction proceeds rapidly even in the absence of biological activity.[3-5,43] The mechanism of chemical methylation was studied using methylcobaloximes as model compounds.[29,33-36] However, the significance of these reactions in the aquatic environment, where the presence of other components such as Cl^-, high ionic strength, etc, may play a considerable role, has not been established.

In this chapter, we report our studies of the kinetics of the reaction of methyl(aqua)bis(dimethylglyoximato)cobalt(III), $MeCo(dmg)_2H_2O$, with mercuric ions in aqueous acidic solution, including the effect of different environmental parameters (pH, ionic strength, presence of chloride ion) on the reaction rate.

4.2 Spectroscopic characterization of methyl (aqua) bis (dimethylglyoximato)Co(III)

The synthesis of $MeCo(dmg)_2H_2O$ was described in detail in Chapter 2. Aqueous solutions of $MeCo(dmg)_2H_2O$ at natural pH are yellow, and have strong absorption bands in the visible region, at 440 and 380 nm, Figure 4.2.[33,34,36] Extinction coefficients at 440 and 380 nm were determined from the spectra of a series of solutions of different

concentrations, Figure 4.3. Values of $\varepsilon_{440\ nm} = (1.39 \pm 0.01) \times 10^3\ M^{-1}\ cm^{-1}$ and $\varepsilon_{380\ nm} = (1.61 \pm 0.01) \times 10^3\ M^{-1}\ cm^{-1}$ agree well with previously reported values.[33,36]

The UV-visible spectrum of $MeCo(dmg)_2H_2O$ is unaffected by the presence of either 1.0 M $NaClO_4$, 0.1 M $NaNO_3$ or 1.0 M KCl, Figure 4.4. The spectrum does change significantly with pH. When an aqueous solution of 0.25 mM $MeCo(dmg)_2H_2O$ in 1.0 M $NaClO_4$ was made progressively more acidic by addition of HNO_3, the absorbance decreased while the peak maxima were red-shifted, Figure 4.5a. Adin and Espenson attributed the changes to protonation of the planar, hydrogen-bonded dimethylglyoxime framework, eq 1:[33,36]

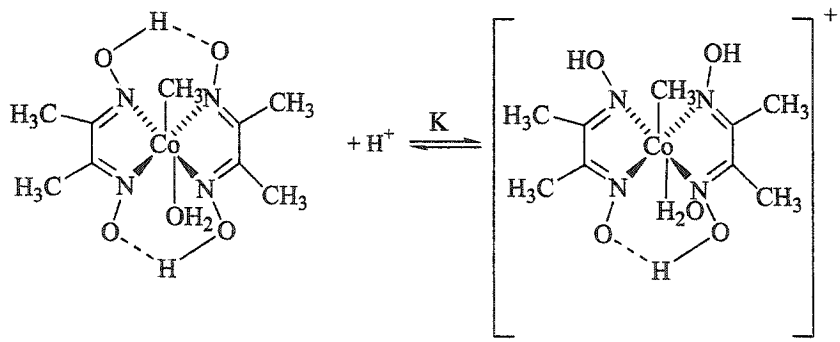

(1)

Figure 4.5b shows the spectrophotometric titration at 440 nm. The absorbance at each point in the titration curve can be expressed by eq 2:

$$Abs = \varepsilon_1 [MeCo(dmg)_2H_2O] + \varepsilon_2 [MeCo(dmg)(dmgH)H_2O^+] = \varepsilon_{app} [MeCo]_{total} \quad (2)$$

where ε_1 and ε_2 are the molar extinction coefficients of $MeCo(dmg)_2H_2O$ and $MeCo(dmg)(dmgH)(H_2O)^+$, respectively, at 440 nm. If $K = MeCo(dmg)(dmgH)(H_2O)^+] / [MeCo(dmg)_2H_2O][H^+]$, we have eq. 3-5:

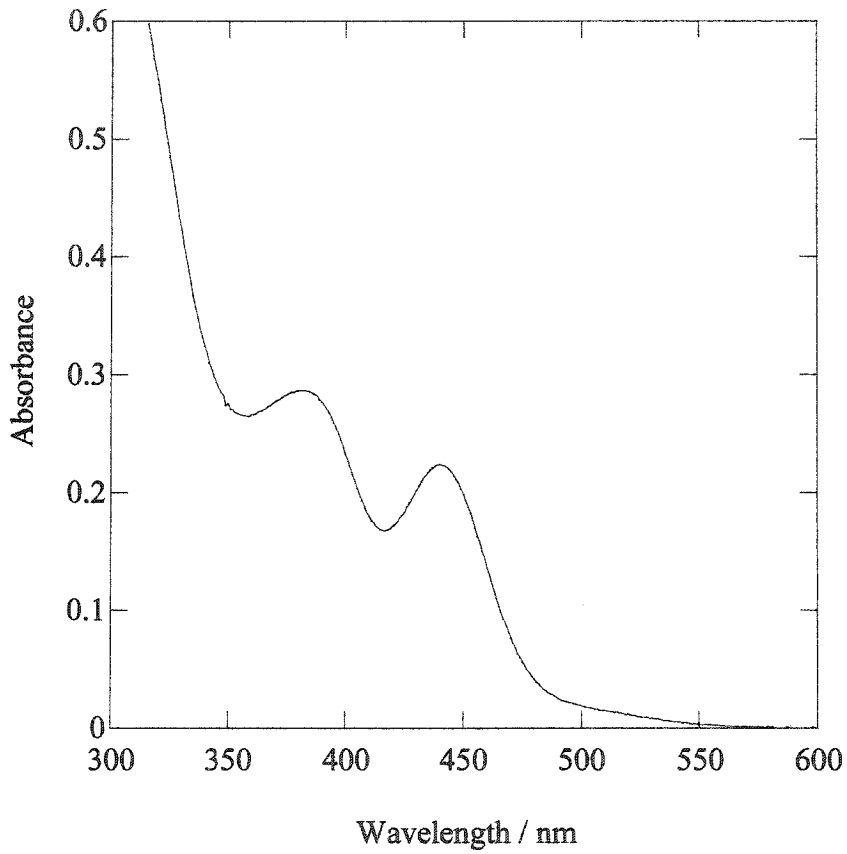

Figure 4.2 UV-visible spectrum of a 0.20 mM aqueous solution of $MeCo(dmg)_2H_2O$.

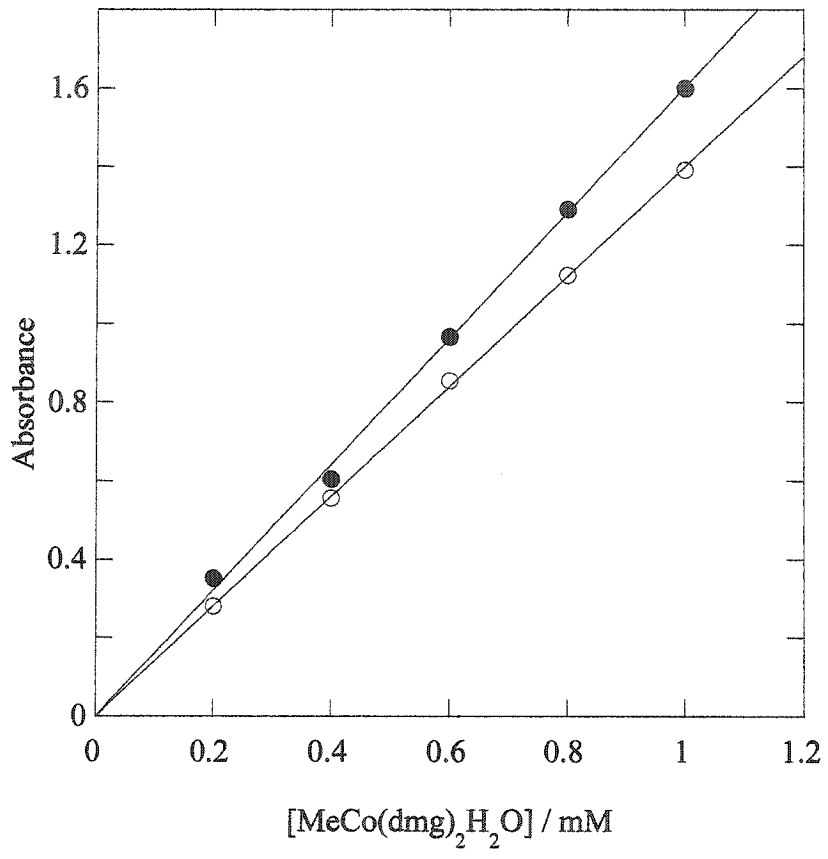

$Abs_{380\ nm} = \varepsilon_{380} * [MeCo(dmg)_2H_2O]$	
ε	(1600 ± 10) M^{-1} cm^{-1}
Chisq	0.002445
R	0.9998

$Abs_{440\ nm} = \varepsilon_{440} * [MeCo(dmg)_2H_2O]$	
ε	(1390 ± 10) M^{-1} cm^{-1}
Chisq	0.0003165
R	0.9998

Figure 4.3 Extinction coefficients for $MeCo(dmg)_2H_2O$ at 440 nm (open circles) and 380 nm (filled circles).

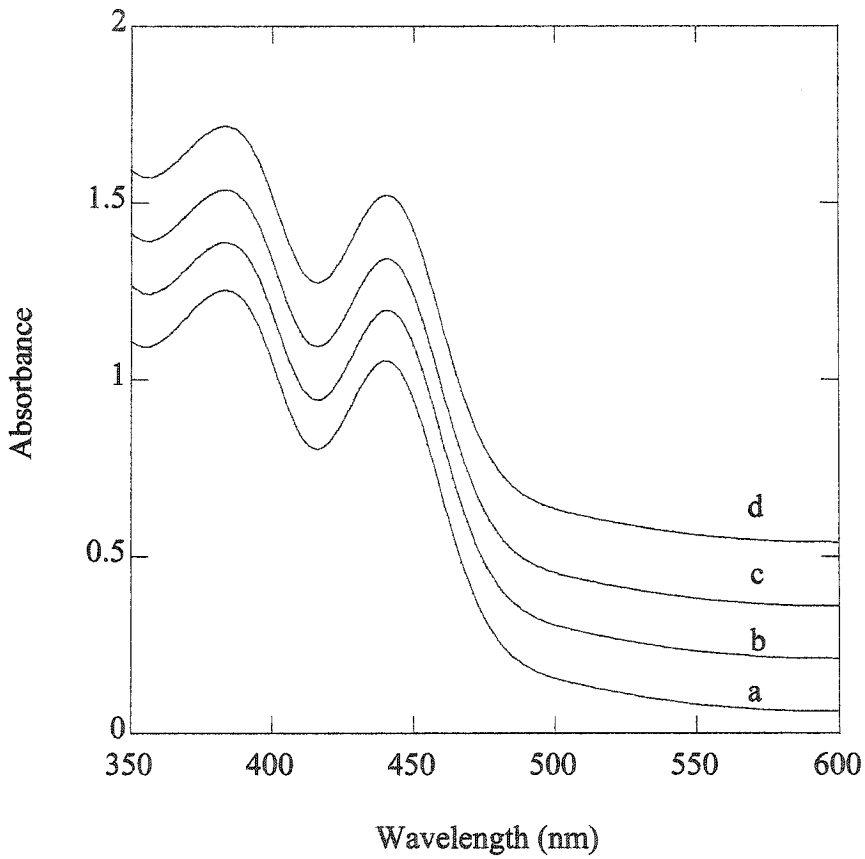

Figure 4.4 Visible spectra of a 0.95 mM $MeCo(dmg)_2H_2O$ solution in (a) deionized water; (b) 1.0 M $NaClO_4$; (c) 1.0 M KCl; and (d) 0.1 M $NaNO_3$. The spectra have been vertically offset for display purposes.

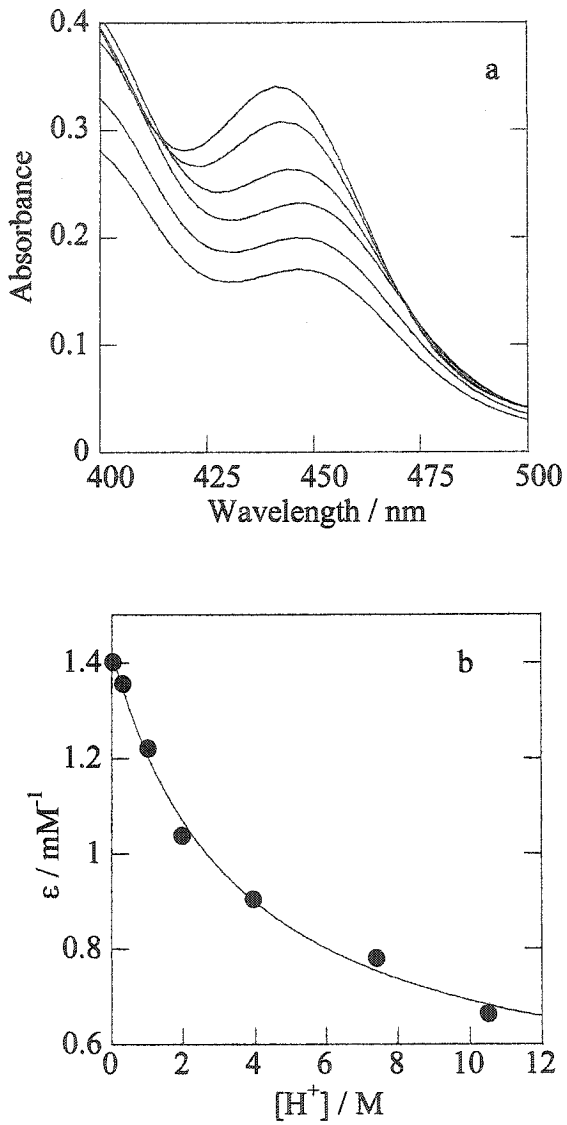

Figure 4. 5 (a) Evolution of the spectrum of 0.25 mM $MeCo(dmg)_2H_2O$ as the solution is made progressively more acidic by the addition of HNO_3; (b) Dependence of the absorbance at 440 nm on pH. The solid line is the curve fit of the experimental data to eq 5 (see text). Ionic strength is kept constant at 1 M ($NaClO_4$).

$$[MeCo(dmg)_2H_2O] = [MeCo]_{total} / (1 + K [H^+]) \quad (3)$$

$$[MeCo(dmg)(dmgH)H_2O^+] = [MeCo]_{total} K / (1 + K [H^+]) \quad (4)$$

$$\varepsilon_{app} = (\varepsilon_1 + \varepsilon_2 K [H^+]) / (1 + K [H^+]) \quad (5)$$

The experimental data were fitted to eq 5, yielding $\varepsilon_1 = (1.42 \pm 0.02) \times 10^3\ M^{-1}\ cm^{-1}$, $\varepsilon_2 = (0.43 \pm 0.07) \times 10^3\ M^{-1}\ cm^{-1}$ and $K = 3.6 \pm 0.7$. The equilibrium constant agrees well with the value reported by Adin and Espenson, [36] $3.23 \pm 0.15\ M^{-1}$, and Abley and coauthors, [33] $3.5\ M^{-1}$, both at 1.0 M ionic strength ($NaClO_4$).

Finally, the absorbance at 440 nm of a 1.5 mM solution of $MeCo(dmg)_2H_2O$ in 1.0 M $NaClO_4$ at neutral pH decreases gradually over the course of 1200 min at 21.1°C, Figure 4.6. The rate of the decomposition of $MeCo(dmg)_2H_2O$ under these conditions is $k_{dec} = (6.7 \pm 0.1) \times 10^{-5}\ s^{-1}$.

4.3 Yield of methylmercury

A solution containing 0.12 mM $MeCo(dmg)_2H_2O$ and 2.0 mM $Hg^{2+}_{(aq)}$ at pH 1.5 was allowed to react at 21.1°C for 30 min, then analyzed for methylmercury. The yield was (0.107 ± 0.005) mM $MeHg^+$ (average of 3 independent experiments), or (89 ± 4)% based on $MeCo(dmg)_2H_2O$. Methyl transfer from cobalt to mercury is therefore deemed to be essentially quantitative, eq 6:

$$Hg^{2+} + MeCo(dmg)_2H_2O + H_2O \rightarrow MeHg^+ + Co(dmg)_2(H_2O)_2^+ \quad (6)$$

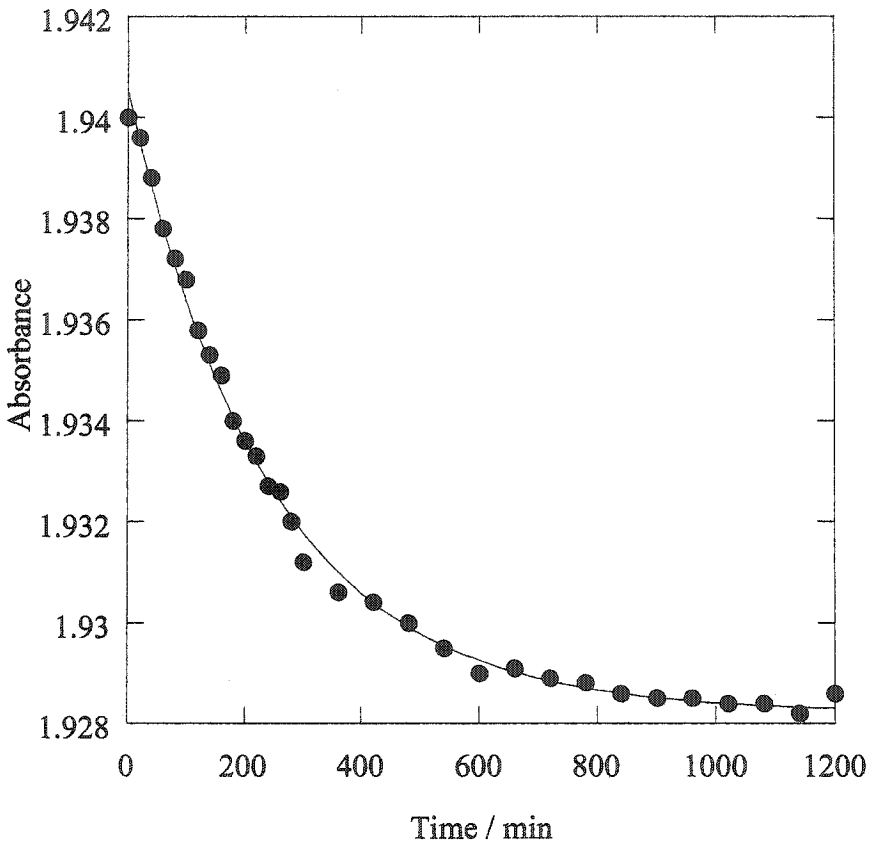

Figure 4.6 Kinetic profile for decomposition of $MeCo(dmg)_2H_2O$ in presence of 1.0 M $NaClO_4$ at neutral pH and 21.1°C.

In previous studies of this reaction, $Co(dmg)_2(H_2O)_2^+$ has been shown to be the second product of the reaction. [18,33,35,36] Dilute aqueous solutions of this compound are transparent in the visible region. [31,33]

The same experiment was conducted in the presence of 1.0 M KCl. Under the same reaction conditions (pH 1.5, 21.1°C, 30 min), when mercury is present as $HgCl_4^{2-}$, the amount of methylmercury formed was undetectable.

4.4 Kinetics of mercury methylation

When an aqueous solution of $MeCo(dmg)_2H_2O$ was mixed with excess $Hg^{2+}_{(aq)}$, the yellow color disappeared. The kinetics of the reaction were monitored as the decrease in absorbance at 440 nm, Figure 4.7. As the curve fit shows, the time-evolution of the absorbance change is pseudo-first-order, eq 7:

$$- d[MeCo(dmg)_2(H_2O)]/dt = k_{obs} [MeCo(dmg)_2(H_2O)] \quad (7)$$

The observed rate constants were calculated by fitting the experimental data to a single-exponential function, eq. 8:

$$Abs_t = Abs_\infty + (Abs_0 - Abs_\infty) \exp(-k_{obs} t) \quad (8)$$

Values of k_{obs} measured for the reactions of 0.15 mM $MeCo(dmg)_2H_2O$ with various concentrations of $Hg^{2+}_{(aq)}$ in 0.030 M HNO_3 are summarized in Table 4.1.

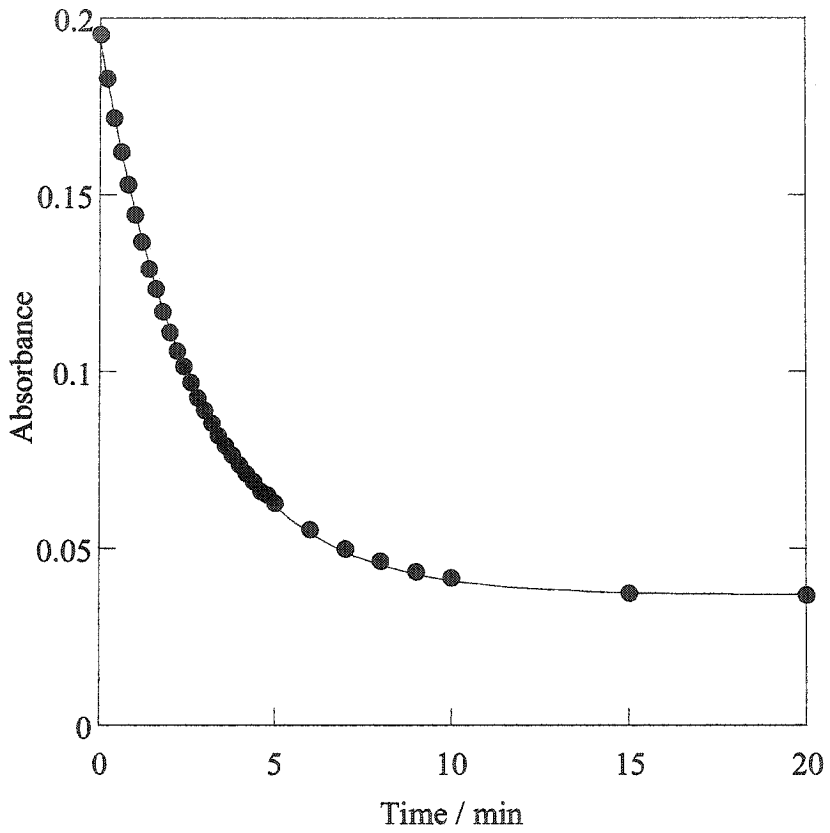

Figure 4.7 Kinetic profile for the reaction of 0.15 mM $MeCo(dmg)_2H_2O$ with 1.0 mM $Hg^{2+}_{(aq)}$ in 0.030 M HNO_3 at 21.1°C. The solid line is the curve fit to the integrated first-order rate equation.

The observed rate constants depend linearly on the concentration of excess $Hg^{2+}_{(aq)}$, Figure 4.8. From the slope of this curve, the value of the second-order rate constant is k = (6.8 ± 0.2) M^{-1} s^{-1} at 21.1°C, pH 1.5 and ionic strength 0.030 M (HNO_3).

4.5 Effect of pH

The observed rate constants for the reaction of $MeCo(dmg)_2H_2O$ with $Hg^{2+}_{(aq)}$ are highly pH-dependent. Increasing the acid concentration decreases the rate of the reaction, Table 4.2. This result agrees with the finding of Adin and Espenson that only $MeCo(dmg)_2(H_2O)$, and not $MeCo(dmg)(dmgH)(H_2O)^+$, reacts with Hg^{2+}. [36] Under these conditions, the rate law is shown in eq 9:

$$- d[MeCo]_{total}/dt = k\,[MeCo(dmg)_2(H_2O)][Hg^{2+}] = k'\,[MeCo]_{total}\,[Hg^{2+}]/(1 + K\,[H^+]) \quad (9)$$

where k′ is the intrinsic (pH-independent) rate constant. Since the kinetic measurements were run with $[Hg^{2+}]$ in excess over $[MeCo]_{total}$ the pH-dependent observed rate constant can be expressed as in eq 10:

$$k_{obs} = k'\,[Hg^{2+}] / (1 + K\,[H^+]) \quad (10)$$

Table 4.1 Pseudo-first-order rate constants [a] for the reaction of 0.15 mM $MeCo(dmg)_2H_2O$ with excess $Hg^{2+}_{(aq)}$ in 0.030 M HNO_3 at 21.1°C

$[Hg^{2+}]$ mM	k_{obs} s^{-1}
0.5	0.0028 ± 0.0005
1.0	0.006 ± 0.0003
2.0	0.013 ± 0.003
4.0	0.025 ± 0.001
5.0	0.036 ± 0.003

[a] Errors obtained from nonlinear curve fits to the integrated first-order rate equation.

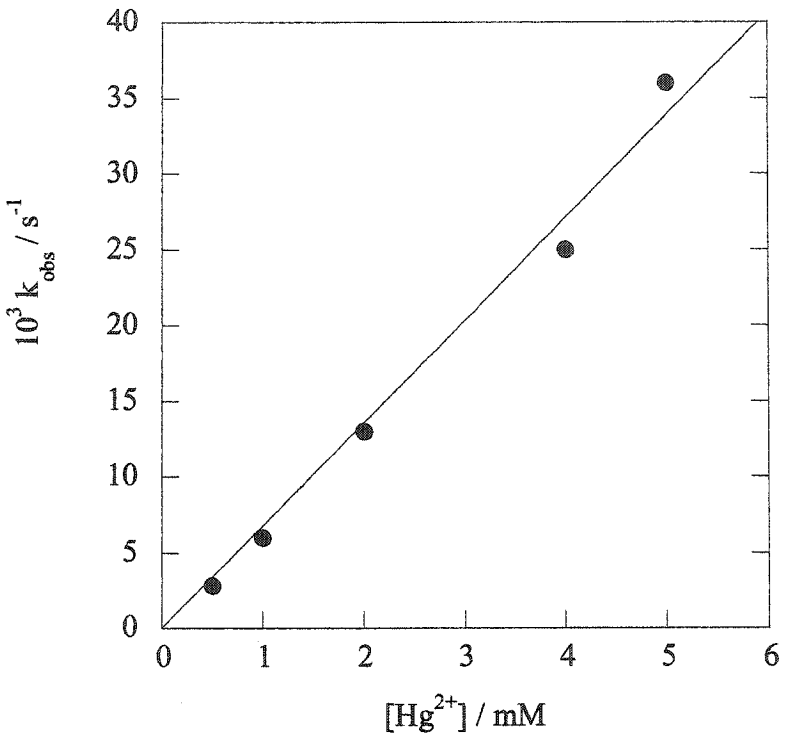

$k_{obs} = k * [MeCo(dmg)_2H_2O]$	
k	6.8 ± 0.2
Chisq	0.0000107
R	0.9944

Figure 4. 8 Dependence of the pseudo-first-order rate constants k_{obs} for the reaction of $MeCo(dmg)_2H_2O$ on the concentration of excess $Hg^{2+}_{(aq)}$, at pH 1.5 (HNO_3) and 21.1°C.

In Figure 4.9, the experimental data are shown fitted to eq 10 to give $k'[Hg^{2+}] = (0.125 \pm 0.005)\ s^{-1}$ and $K = (4.6 \pm 0.5)$ at 21.1°C and 1.0 M ionic strength ($NaClO_4$). We note that the rate constant is several orders of magnitude larger than the rate of decomposition of $MeCo(dmg)_2(H_2O)$ ($k_{1M} = 6.7 \times 10^{-5}\ s^{-1}$) (see above). Since $[Hg^{2+}] = 2.1$ mM, we calculate the intrinsic second-order rate constant $k' = (59 \pm 2)\ M^{-1}\ s^{-1}$. This value agrees well with those reported by Adin and Espenson, [36] $(65 \pm 2)\ M^{-1}\ s^{-1}$, and Abley et al., 54 $M^{-1}\ s^{-1}$, for the same reaction at 25°C. We note also that the value of K agrees with that determined by spectrophotometric titration for the protonation of $MeCo(dmg)_2(H_2O)$ (see above).

4.6 Effect of ionic strength

Although the pH dependence of the kinetics of methyl transfer from $MeCo(dmg)_2(H_2O)$ to Hg^{2+} have been previously studied, there is to our knowledge no report of the importance of ionic strength. We examined its influence under pseudo-first-order conditions at pH 1.5 (HNO_3) and 21.1°C in solutions with ionic strengths varying from 0.030 to 1.0 M ($HNO_3/NaClO_4$). The pseudo-first-order rate constants increase with ionic strength, Table 4.3.

The kinetic salt effect on rate constants is a well-known phenomenon. Based on Debye-Hückel theory, increasing ionic strength should cause the rate of reaction between ions of the same sign to accelerate, while the rate of reaction between ions of opposite

Table 4.2 Pseudo-first-order rate constants[a] for the reaction of 0.10 mM $MeCo(dmg)_2H_2O$ with 2.1 mM $Hg^{2+}_{(aq)}$ at 21.1°C and 1.0 M ionic strength ($NaClO_4$) as a function of $[H^+]$ (HNO_3)

$[H^+]$ M	pH	k_{obs} s^{-1}
0.001	3.00	0.124 ± 0.003
0.005	2.30	0.122 ± 0.005
0.01	2.00	0.119 ± 0.006
0.03	1.52	0.110 ± 0.001
0.10	1.00	0.083 ± 0.002
0.20	0.70	0.073 ± 0.005
0.30	0.52	0.056 ± 0.007
0.60	0.22	0.031 ± 0.004
1.00	0.00	0.020 ± 0.009

[a] Errors obtained from nonlinear curve fits to the integrated first-order rate equation.

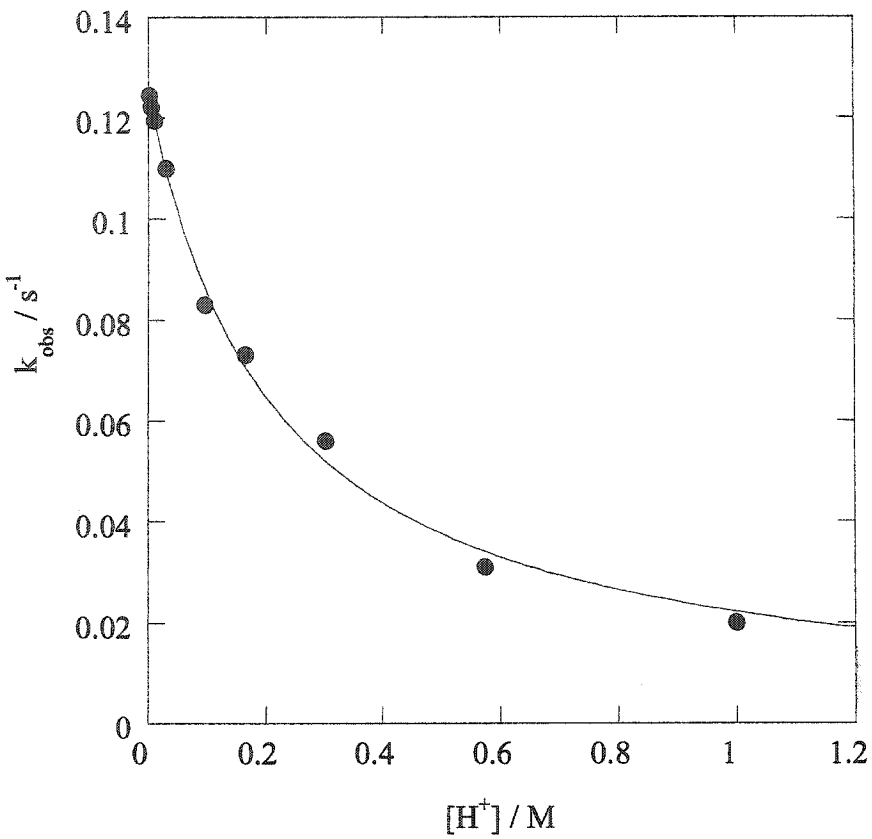

$k_{obs} = k' * [Hg^{2+}] / (1 + K [H^+])$	
$k' [Hg^{2+}]$	0.125 ± 0.005
K	4.6 ± 0.5
R	0.9957

Figure 4. 9 Dependence of the pseudo-first-order rate constants for the reaction of $MeCo(dmg)_2H_2O$ with 2.1 mM $Hg^{2+}_{(aq)}$ at 21.1°C and 1.0 M ionic strength ($NaClO_4$) on the concentration of H^+. The solid line is the curve fit of the experimental data to eq 10 (see text).

sign decreases. [44] This is the primary salt effect. In this case, the relationship between the rate constant and ionic strength is shown in eq 11:

$$\log k = \log k_0 + 2 z_A z_B A \mu^{1/2} / (1 + \mu^{1/2}) \quad (11)$$

where A is a theoretical constant (A = 0.509 for water at 25°C), μ is the ionic strength and z_A and z_B are the charges on the species in a given bimolecular reaction. [45] If a reaction involves collision between uncharged molecules, or between an ion and a neutral molecule, one should observe only a small positive or negative primary salt effect. [46]

The ionic strength can also affect the kinetics of a reaction by changing the concentration of a reactant as a result of changes in inter-ionic forces. [47] This is considered to be a secondary salt effect. For example, a secondary salt effect may arise from a change in the concentration of $MeCo(dmg)_2H_2O$ as a result of a change in its protonation constant with ionic strength, eq 12:

$$MeCo(dmg)_2H_2O + H_2O \leftrightarrows MeCo(dmg)(dmgH)H_2O^+ + OH^- \quad (12)$$

Also, the strength of Co-C bond is considerably affected by the nature of the axial base. [11,13,48] Drago reported the formation constant of $MeCo(dmg)_2CN^-$ as 10^8, eq 13: [11]

$$MeCo(dmg)_2H_2O + CN^- \leftrightarrows MeCo(dmg)_2CN^- \quad (13)$$

Table 4. 3 Pseudo first-order rate constants[a] for the reaction of $MeCo(dmg)_2H_2O$ with 1.5 mM $Hg^{2+}_{(aq)}$ at 21.1°C and 0.030 M HNO_3, at various ionic strengths ($HNO_3/NaClO_4$)

Ionic strength M	k_{obs} s^{-1}
0.030	0.014 ± 0.002
0.040	0.015 ± 0.005
0.13	0.021 ± 0.004
0.45	0.039 ± 0.003
0.88	0.067 ± 0.008
1.02	0.075 ± 0.005

[a] Errors obtained from nonlinear curve fits to the integrated first-order rate equation.

In 1.0 M $NaClO_4$, the formation of $MeCo(dmg)_2ClO_4^-$ could elongate and weaken the Co-C bond (trans-steric influence) [11,48,49] as well as making the methylcobaloxime negatively charged. Under these conditions, its reaction with positively charged mercury ions should be accelerated by ionic strength. However, there are two problems with this hypothesis: perchlorate is an extremely weak base (essentially non-coordinating) and the spectrum of methylcobaloxime does not change in the presence of 1 M perchlorate, arguing against its coordination.

The effect of the ionic strength on the rate law for the reaction of $MeCo(dmg)_2(H_2O)$ with Hg^{2+} can be expressed as following, eq. 14:

$$\text{Rate} = k_0 a_{Hg} [MeCo] = k_0 f_{Hg} [Hg^{2+}][MeCo] = k [Hg^{2+}] [MeCo] \quad (14)$$

where k_0 is the rate coefficient for infinitely diluted solutions, a_{Hg} is the activity of Hg^{2+} ions, f_{Hg} is the activity coefficient and $k = k_0 f_{Hg}$

The activity coefficient at 25°C depends on the ionic strength μ and the ionic charge z, eq. 15[44]:

$$\ln f = 1.174\, z\, \mu^{1/2} \quad (15)$$

Combining eq. 14 and eq 15 we find, eq.16:

$$\ln k = \ln k_0 + 1.174 \times 2 \times \mu^{1/2} = \ln k_0 + 2.348\, \mu^{1/2} \quad (16)$$

Based on our experimental data, the slope of the plot of lnk vs $\mu^{1/2}$, Figure 4.10, is 2.05 ± 0.01 which is comparable with 2.348 that would be expected from the primary salt effect, for 25°C eq. 16.

4.7 Effect of chloride

In the presence of chloride, Hg(II) forms a series of chloride complexes, Figure 4.11. In 1.0 M aqueous KCl, the predominant mercury species is $HgCl_4^{2-}$. This species absorbs strongly in the UV (λ_{max} 232 nm, $\varepsilon = 3.0 \times 10^4$ M^{-1} cm^{-1}), but negligibly at 440 nm, Figure 4.12.

The reaction between 0.26 mM $MeCo(dmg)_2H_2O$ and 3.5 mM Hg(II) in 0.030 M $HClO_4$ and 30.0°C was studied at $[Cl^-]$ = 0.01 and 1.0 M. The kinetic profile in the absence of chloride is shown in Figure 4.13 for comparison. Even small amounts of chloride shut down the reaction completely. The expected product of demethylation, $ClCo(dmg)_2(H_2O)$, does not absorb at 440 nm. [31]

Dealkylation of alkylcobaloxime complexes by Hg^{2+} follow an S_E2 mechanism, with inversion at carbon (S_Ei mechanism): [33,34,36,50]

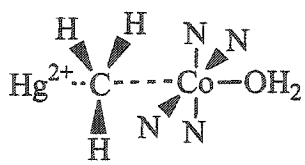

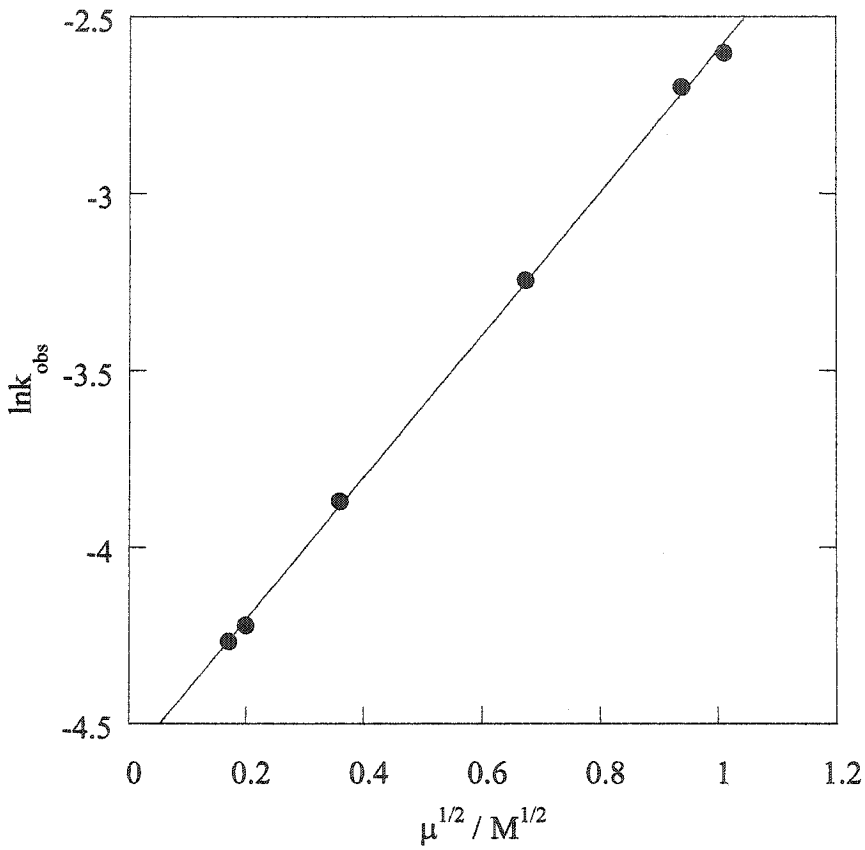

Figure 4. 10 Dependence of the $\ln k_{obs}$ on $\mu^{1/2}$ for the reaction of $MeCo(dmg)_2H_2O$ with 1.5 mM $Hg^{2+}_{(aq)}$ at 21.1°C and 0.030 M HNO_3.

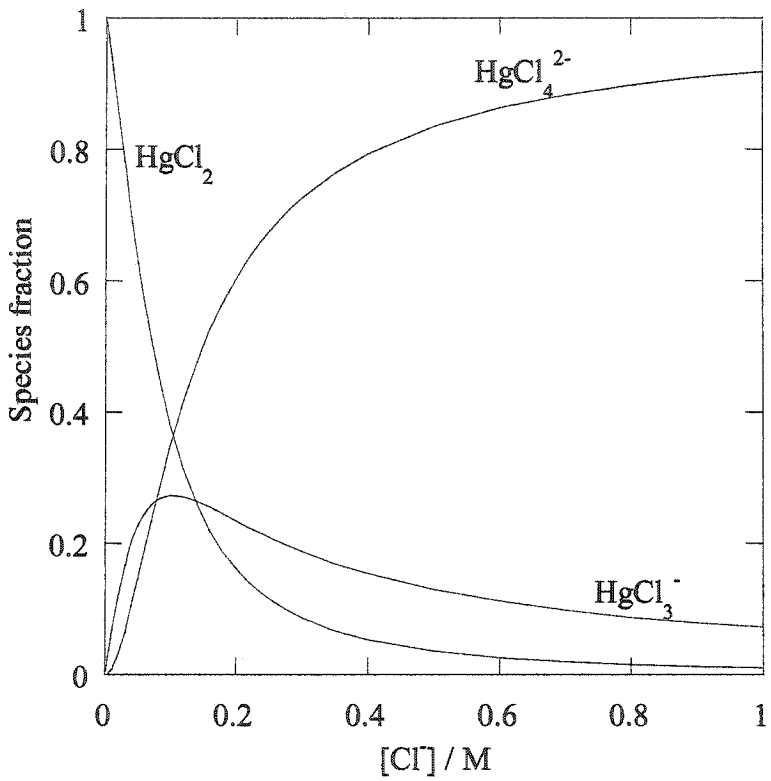

Figure 4. 11 Speciation of the mercuric ion in the presence of chloride, at pH 1.5.

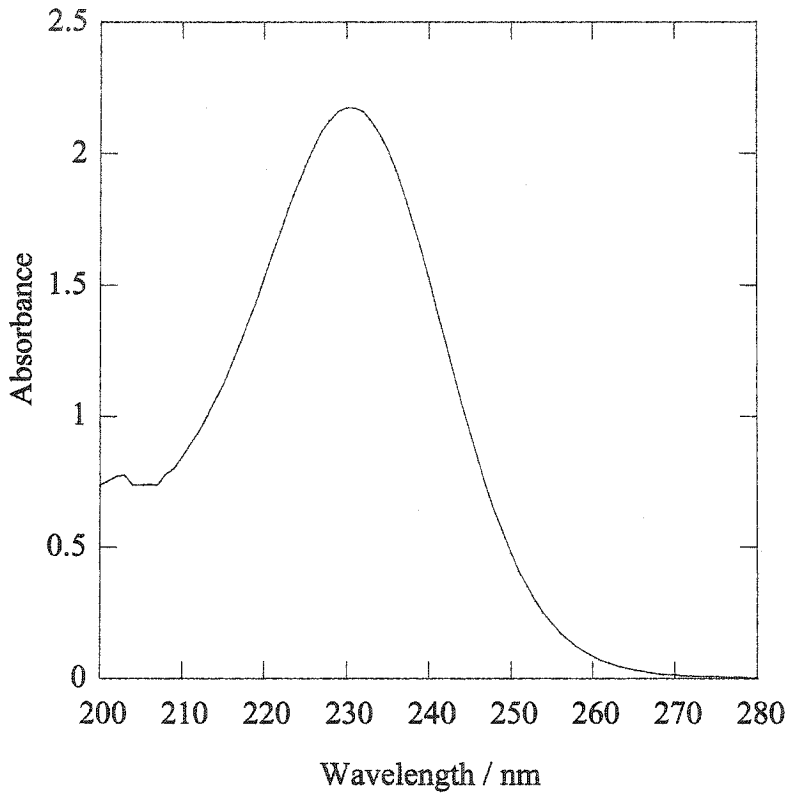

Figure 4. 12 UV spectrum of 0.07 mM Hg(II) in the presence of 1.0 M Cl^- at pH 1.5 ($HClO_4$).

The reaction rate depends on the electrophilicity of the attacking species. The presence of chloride results in the formation of less electrophilic species, such as $HgCl_2$ and $HgCl_4^{2-}$, which are incapable of inducing methyl transfer.

4.8 Conclusion

Methyl(aqua)bis(dimethylglyoximato)cobalt(III) is readily demethylated by Hg^{2+} in acidic aqueous solution. The main products of this reaction are methylmercury and bis(aqua)bis(dimethylglyoximato)cobalt(III). Our experiments confirm an earlier conclusion that the kinetics of the reaction are strongly pH-dependent since only the unprotonated form of methylcobaloxime reacts with Hg^{2+}. For this reason the reaction becomes faster at higher pH. The rate constant also depends on ionic strength, being significantly larger in higher ionic strength solutions. Finally, the presence of chloride completely inhibits the reaction. Since methyl(aqua)bis(dimethylglyoximato)cobalt(III) is known to mimic the chemistry of methylcobalamin, our study shows that abiotic methylation of mercury by methylcobalamin could be a source of methylmercury formation in fresh waters which have low pH and low chloride concentration. If the ionic strength of a certain aquatic environment should increase due to anthropogenic activities, the rate of methylation may increase significantly, but only if the ionic strength results from a non-coordinating anion. Also, at higher ionic strength solutions, the portion of mercury present as aqueous mercuric ion is higher, even in high pH and so, higher the methylation rate. Methylcobalamin cannot methylate Hg(II) in seawater due to the high chloride concentration in this environment.

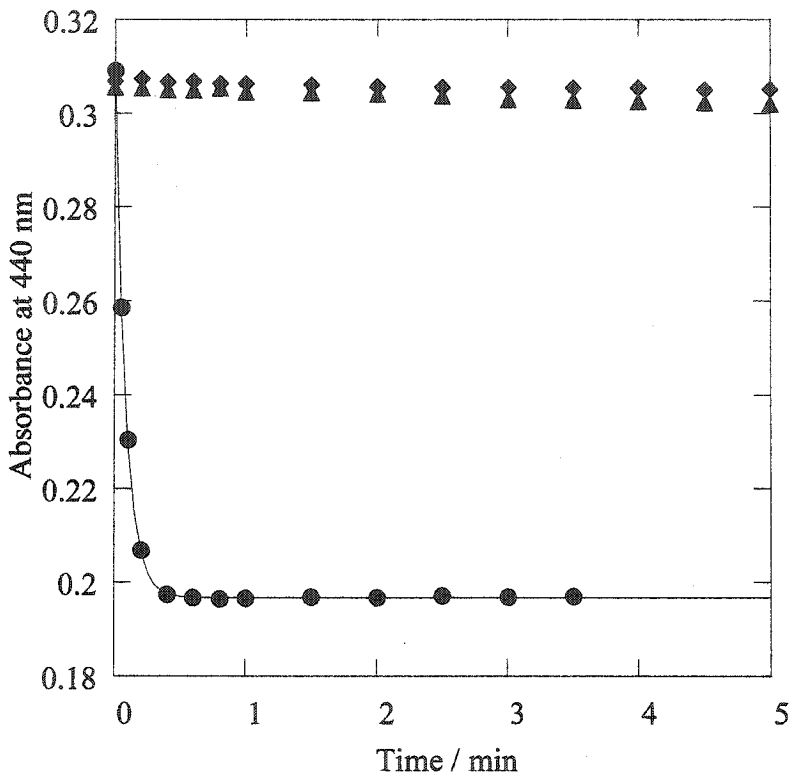

Figure 4. 13 Kinetic profiles for the reaction of 0.26 mM $MeCo(dmg)_2H_2O$ with 3.5 mM Hg(II) in 0.030 M $HClO_4$ at 30.0°C and 1.0 M ionic strength ($NaClO_4$/KCl). Reactions were conducted in the presence of 1.0 M KCl (◆); 0.01 M KCl (■) and in the absence of KCl (●). The solid line is the curve fit to the integrated first-order rate equation.

References

(1) Halpern, J.; Maher, J. P. *J. Am. Chem. Soc.* **1964,** *86*, 2311.

(2) Wood, J. M.; Kennedy, F. S.; Rossen, C. G. *Nature* **1968,** *220*, 173-174.

(3) Bertilsson, L.; Neujahr, H. Y. *Biochemistry* **1971,** *10*, 2805-2808.

(4) Nobumasa, I.; Eiji, S.; Shoe-Kung, P.; Kiyoshi, N.; Jong-Yoon, K.; Kwan, T.; Tyunosin, U. *Science* **1971,** *172*, 1248-1249.

(5) DeSimone, R. E.; Penley, M. W.; Charboneau, L.; Smith, S. J.; Wood, J. M.; Jill, H. A. O.; Pratt, J. M.; Ridsdale, S.; Williams, R. J. P. *Biochim. Biophys. Acta* **1973,** *304*, 851-863.

(6) Yamamoto, H.; Yokoyama, T.; Chen, J.-L.; Kwan, T. *Bull. Chem. Soc. Jpn.* **1975,** *48*, 844-847.

(7) Hintelman, H.; Keppel-Jones, K.; Evans, R. D. *Environ. Toxicol. Chem.* **2000,** *19*, 2204-2211.

(8) Hintelmann, H.; Evans, R. D. *Fresen. J. Anal. Chem.* **1997,** *358*, 378-385.

(9) Jordan, R. B. In Reaction mechanisms of inorganic and organometallic systems; Oxford University Press: Oxford, 1991.

(10) Brown, K.; Evans, R. D.; Zubkowski, J. D.; Valente, E. J. *Inorg. Chem.* **1996,** *35*, 415-423.

(11) Drago, R. S. *J. Organomet. Chem.* **1996,** *512*, 61-68.

(12) Rossi, M.; Glusker, J. P.; Randaccio, L.; Summers, M. F.; Toscano, P. J.; MArzilli, L. G. *J. Am. Chem. Soc.* **1985,** *107*, 1729 -1738.

(13) Balt, S.; Bolster, M. W. G.; Garderen, C. J. V.; Herk, A. M. V.; Lammers, K. R.; Valde, E. G. V. d. *Inorg. Chim. Acta* **1985,** *106*, 43-47.

(14) Elliot, C. M.; Hershenhart, E.; Finke, R. G.; Smith, B. L. *J. Am. Chem. Soc.* **1981,** *103*, 5558-5566.

(15) Schrauzer, G. N.; Lee, L. P.; Sibert, J. W. *J. Am. Chem. Soc.* **1970,** *92*, 2997-3005.

(16) Pratt, J. M.; Aron, J.; Chemaly, S. M.; Marques, H. M. In The biological alkylation of heavy elements; Craig, P. J., Glockling, F., Eds.; Royal Society of Chemistry: London, 1987.

(17) Filippelli, M.; Baldi, F. *Appl. Organomet. Chem.* **1993,** *7*, 487-493.

(18) Hill, H. A. O.; Pratt, J. M.; Ridsdale, S.; Williams, F. R.; Williams, R. J. P. *Chem. Commun.* **1970,** *6*, 341-342.

(19) Smith, E. L.; Mervyn, L.; Johnson, A. W.; Shaw, N. *Nature* **1962,** *194*, 1175.

(20) Wood, J. M. In *The Biological Alkylation of Heavy Elements*; Craig, P. J., Glockling, F., Eds.; Royal Society of Chemistry: London, 1987.

(21) Fanchiang, Y.-T.; Pignatelo, J. J.; Wood, J. M. *Organometallics* **1983,** *2*, 1748-1751.

(22) Fanchiang, Y.-T.; Pignatelo, J. J.; Wood, J. M. *Organometallics* **1983,** *2*, 1752-1754.

(23) Fanchiang, Y.-T.; Wood, J. M. *J. Am. Chem. Soc.* **1981,** *103*, 5100.

(24) Schrauzer, G. N.; Windgassen, R. J. *J. Am. Chem. Soc.* **1966,** *20*, 3738-3743.

(25) Schrauzer, G. N. *Acc. Chem. Res.* **1968,** *1*, 97-103.

(26) Bigotto, A.; Zangrado, E.; Randaccio, L. *J. Chem. Soc. Dalton Trans.* **1975,** *5*, 96-104.

(27) Brown, K.; Lyles, D.; Pencovici, M.; Kallen, R. *J. Am. Chem. Soc.* **1975,** *97*, 7338-7346.

(28) Asaro, F.; Dreos, R.; Geremia, S.; Nardin, G.; Pellizer, G.; Randaccio, L.; Tauzher, G.; Vuano, S. *J. Organomet. Chem.* **1997,** *548*, 211-221.

(29) Mestroni, G.; Zassinovich, G.; Camus, A.; Costa, G. *Transition Met. Chem.* **1975,** *1*, 32-36.

(30) Crumblis, A.; Gaus, P. L. *Inorg. Chem.* **1975,** *14*, 486-490.

(31) Adin, A.; Espenson, J. H. *Inorg. Chem.* **1972,** *11*, 686-688.

(32) McHatton, R. C.; Espenson, J. H.; Bakac, A. *J. Am. Chem. Soc.* **1986,** *108*, 5885-5890.

(33) Abley, P.; Dockal, E. R.; Halpern, J. *J. Am. Chem. Soc.* **1973,** *95*, 3166-3170.

(34) Fritz, H. L.; Espenson, J. H.; Williams, D. A.; Molander, G. A. *J. Am. Chem. Soc.* **1974,** *96*, 2378-2381.

(35) Jong-Yoon, K.; Nobumasa, I.; Tyunoshin, U.; Kwan, T. *Bull. Chem. Soc. Jpn.* **1971,** *44*, 300.

(36) Adin, A.; Espenson, J. H. *Chem. Commun.* **1971,** *13*, 653-654.

(37) Randaccio, L.; Furlan, M.; Geremia, S.; Slouf, M.; Srnova, I.; Toffoli, D. *Inorg. Chem.* **2000,** *39*, 3403-3413.

(38) Dash, K. C. *J. Indn. Chem. Soc.* **1994,** *71*, 227-238.

(39) Finke, R. G.; Smith, B. L.; McKenna, W. A.; Christian, P. A. *Inorg. Chem.* **1981,** *20*, 687-693.

(40) Choi, S.-C.; Bartha, R. *Appl. Environ. Microbiol.* **1993,** *59*, 290-295.

(41) Pak, K. R.; Bartha, R. *Appl. Environ. Microbiol.* **1998,** *64*, 1987-1990.

(42) Pak, K. R.; Bartha, R. *Appl. Environ. Microbiol.* **1998,** *64*, 1013-1017.

(43) Chu, V. C. W.; Gruenwedel, D. W. *Bioinorg. Chem.* **1977,** *7*, 169-186.

(44) Winn, J. S. Physical chemistry; HarperCollins: New York, 1995.

(45) Espenson, J. H.; Ryan, D. A. *J. Phys. Chem.* **1981,** *85*, 3658-3660.

(46) Warner, J. C.; Stitt, F. B. *J. Am. Chem. Soc.* **1933,** *55*, 4807-4812.

(47) Bronsted, J. N.; King, C. V. *J. Am. Chem. Soc.* **1925,** *47*, 2523-2531.

(48) Hansen, L. M.; Kumar, P. N. V. P.; Marynick, D. S. *Inorg. Chem.* **1994,** *33*, 728-735.

(49) Geremia, S.; Calligaris, M.; Randaccio, L. *Eur. J. Inorg. Chem* **1999**, 991-992.

(50) Jensen, F. R.; Rickborn, B. Electrophilic substitutions of organomercurials; McGraw Hill: New York, 1968.

Chapter 5

Rates and mechanisms of mercury methylation by methyltin compounds

5.1 Introduction

Organotin compounds are now among the most studied organometallic systems in terms of industrial and agricultural applications.[1] Some of these compounds have been found to be active hydrophobic agents for building materials (limestone, bricks and concrete), for cellulosic substrates (cotton, paper and wood) and, when mixed with an alkylglycoside, have shown to be effective as ore flotation agents.[2] Methyl- and butyltin compounds are widely used as stabilizers in the industrial production of polymers, as industrial catalysts, and as agricultural chemicals such as fungicides, insecticides, molluscides and bacteriocides, and timber preservatives.[3,4] One of the most common uses of n-butyltin compounds is as antifouling agents in paints.[5]

The increased use of organotin compounds has led to their presence in natural waters and sediments from where they find their way to biota and, eventually, to the human food chain.[5-7] Elemental or inorganic compounds of tin have only negligible toxic effects in humans or wildlife, while some organotin compounds have been shown to have a significant impact on different physiological processes of biota.[4,8,9] Methyltin compounds, especially trimethyltin, show high mammalian toxicity and can be hazardous to humans.[6]

Methyltin species represent up to 90% of the total concentration of organotin compounds in the aquatic environment.[10] Their presence is not only a result of man-

made pollution, but also of natural methylation reactions which occur in this environment.[11-15] Environmental reactions resulting in tin methylation include oxidative addition, nucleophilic attack, redistribution and disproportionation reactions.

The wide industrial and agricultural use of organotin compounds, their increased concentrations in the environment and their toxic effects have initiated a number of studies of their chemical, physical and biological attributes. Since the biological activity of toxic organotin compounds is believed to be due to their ability to bind to certain proteins, a number of studies have focused on the stability of organotin complexes with S, N and O donor ligands, especially with carboxylic acids, amino acids and related ligands.[16-19] Organotin compounds in the aquatic environment hydrolyze to products with different biological and environmental properties. For this reason, a number of studies have focused on the hydrolysis of organotins.[1-3,20-26]

Environmental concentrations of alkyltins vary widely, being higher in high salinity waters. Hamasaki et al. reviewed the concentrations of mono-, di- and trimethyltin compounds in water, sediments and biota.[6] The highest water concentrations are found for monomethyltin (up to 1200 ng Sn L^{-1} in seawater and up to 680 ng Sn L^{-1} in fresh water), followed by dimethyltin (up to 500 ng Sn L^{-1} in sea water and up to 260 ng Sn L^{-1} in fresh water) and trimethyltin (up to 20 ng Sn L^{-1} in seawater and not more than 8 ng Sn L^{-1} in freshwater). Methyltin concentrations in aquatic organisms are, in general, higher than their concentrations in water, suggesting that bioaccumulation might occur in the aquatic environment.[6]

Methyltin compounds are considered to be potential methylators of inorganic mercury in natural waters.[27-29] Levels of total mercury in the aquatic environment are

much lower than those of methyltin compounds. They are reported to range from 0.3 to 1.0 ng L^{-1} in non-contaminated river waters, 0.2 to 2.0 ng L^{-1} in non-contaminated coastal areas and up to 1.3 ng L^{-1} in ocean waters.[30] Reactions may be initiated between mercuric ions and methyltin compound, under specific conditions (pH, chloride concentration, temperature, etc.) to produce significant amounts of toxic methylmercury. Previous studies have presented strong evidence that such reactions can happen and may be a significant abiotic source of methylmercury in the aquatic environment.[15,29,31-34] However, the results from different groups are conflicting and the mechanism of this transmethylation reaction is still obscure.

In this chapter, we investigate the reactions of the mercuric ion with mono-, di- and trimethyltin. We show that methylmercury is a quantitative product of these reactions and that the reaction rates depend both on the speciation of mercury and methyltin reagents, determined by the pH and chloride concentrations. We also discuss the mechanism of the methyl transfer reactions and the relevance of our findings to the abiotic methylation of mercuric ions by methyltin compounds.

5.1 Speciation of methyltin(IV) compounds

Hydrolysis and speciation of methyltin complexes in aqueous media are of special interest from a biological and environmental point of view, since the different forms which exist in solutions of various pH and chloride concentration[3,20,21] may vary widely in their chemical and biological properties. Although methyltin chloride stock solutions with concentrations from 10 to 40 mM are stable, they have natural pH values less than 4

due to spontaneous hydrolysis which generates aqua and hydroxo complexes.[35,36] At high concentrations (ca. 0.1 M), oligomers are formed via Sn-O-Sn bridges.[36] Potentiometry and ^{119}Sn NMR have been used to measure the equilibrium constants for hydrolysis of methyltin(IV) halides in aqueous ionic media.[3,20,21] The principal reactions and their equilibrium constants are shown in Table 5.1, corrected for 1.0 M ionic strength.

Trimethyltin speciation at 0.2 mM in 1.0 M KCl (typical of solutions used in kinetics experiments), calculated as a function of pH, is shown in Figure 5.1a. In aqueous solution, Me_3SnCl readily aquates to $Me_3Sn(H_2O)_2^+$. This ion is believed to have a trigonal bipyramidal structure, with the Me groups occupying the equatorial positions and the water ligands in the axial positions.[16,23,37] The cation has a low affinity for chloride relative to oxygen donor ligands. It undergoes hydrolysis to the hydroxo complex, $[Me_3Sn(OH)(H_2O)]$.[22] The latter species is believed to have a distorted trigonal bipyramidal structure, although it is often represented as simply as Me_3SnOH.[24] In fact, from hereon in this chapter, coordinated water molecules will generally be omitted for simplicity. At pH 10 and [Cl-] = 1.0 M, Me_3SnOH represents 99.9% of total Me_3Sn(IV).

Me_2SnCl_2 also aquates in aqueous solution, giving $Me_2Sn(H_2O)_n^{2+}$. Its structure is most likely four-coordinate[18] and it hydrolyzes readily to hydroxo complexes.[1,24,25] At pH 10 in 1.0 M KCl, $Me_2Sn(OH)_2$ makes up 38.5% and $Me_2Sn(OH)_2Cl^-$ 56.9% of total Me_2Sn(IV), Figure 5.1b. $Me_2Sn(OH)_3^-$ is present as a minor species (4.6%).

Table 5.1 Thermodynamic constants for methyltin speciation at 1.0 M ionic strength and 25°C.

Equilibria in trimethyltin solutions[21]	-log β
$Me_3Sn^+ + H_2O \leftrightarrows Me_3Sn(OH) + H^+$	6.29
$2\ Me_3Sn^+ + H_2O \leftrightarrows (Me_3Sn)_2(OH)^+ + H^+$	5.28
$2\ Me_3Sn^+ + 2\ H_2O \leftrightarrows (Me_3Sn)_2(OH)_2 + 2\ H^+$	13.46
$Me_3Sn^+ + Cl^- \leftrightarrows Me_3SnCl$	0.60
Equilibria in dimethyltin solutions[3]	**-log β**
$Me_2Sn_2^+ + H_2O \leftrightarrows Me_2Sn(OH)^+ + H^+$	3.09
$Me_2Sn_2^+ + 2\ H_2O \leftrightarrows Me_2Sn(OH)_2 + 2\ H^+$	8.47
$Me_2Sn_2^+ + 3\ H_2O \leftrightarrows Me_2Sn(OH)_3^- + 3\ H^+$	19.6
$2\ Me_2Sn_2^+ + 2\ H_2O \leftrightarrows (Me_2Sn)_2(OH)_2^{2+} + 2\ H^+$	5.22
$2\ Me_2Sn_2^+ + 3\ H_2O \leftrightarrows (Me_2Sn)_2(OH)_3^+ + 3\ H^+$	9.71
$Me_2Sn_2^+ + Cl^- \leftrightarrows Me_2SnCl^+$	-0.55
$Me_2Sn_2^+ + 2\ Cl^- \leftrightarrows Me_2SnCl_2$	-0.53
$Me_2Sn_2^+ + Cl^- + H_2O \leftrightarrows Me_2SnClOH + H^+$	3.0
$Me_2Sn_2^+ + Cl^- + 2\ H_2O \leftrightarrows Me_2SnCl(OH)_2^- + 2\ H^+$	9.1
Equilibria in monomethyltin solutions[20]	**-log β**
$MeSn^{3+} + H_2O \leftrightarrows MeSn(OH)^{2+} + H^+$	1.68
$MeSn^{3+} + 2\ H_2O \leftrightarrows MeSn(OH)_2^+ + 2\ H^+$	3.98
$MeSn^{3+} + 3\ H_2O \leftrightarrows MeSn(OH)_3 + 3\ H^+$	9.71
$MeSn^{3+} + 4\ H_2O \leftrightarrows MeSn(OH)_4^- + 4\ H^+$	21.45
$2\ MeSn^{3+} + 5\ H_2O \leftrightarrows (MeSn)_2(OH)_5^+ + 3\ H^+$	8.85
$MeSn^{3+} + H_2O + Cl^- \leftrightarrows MeSn(OH)Cl^+ + H^+$	1.96

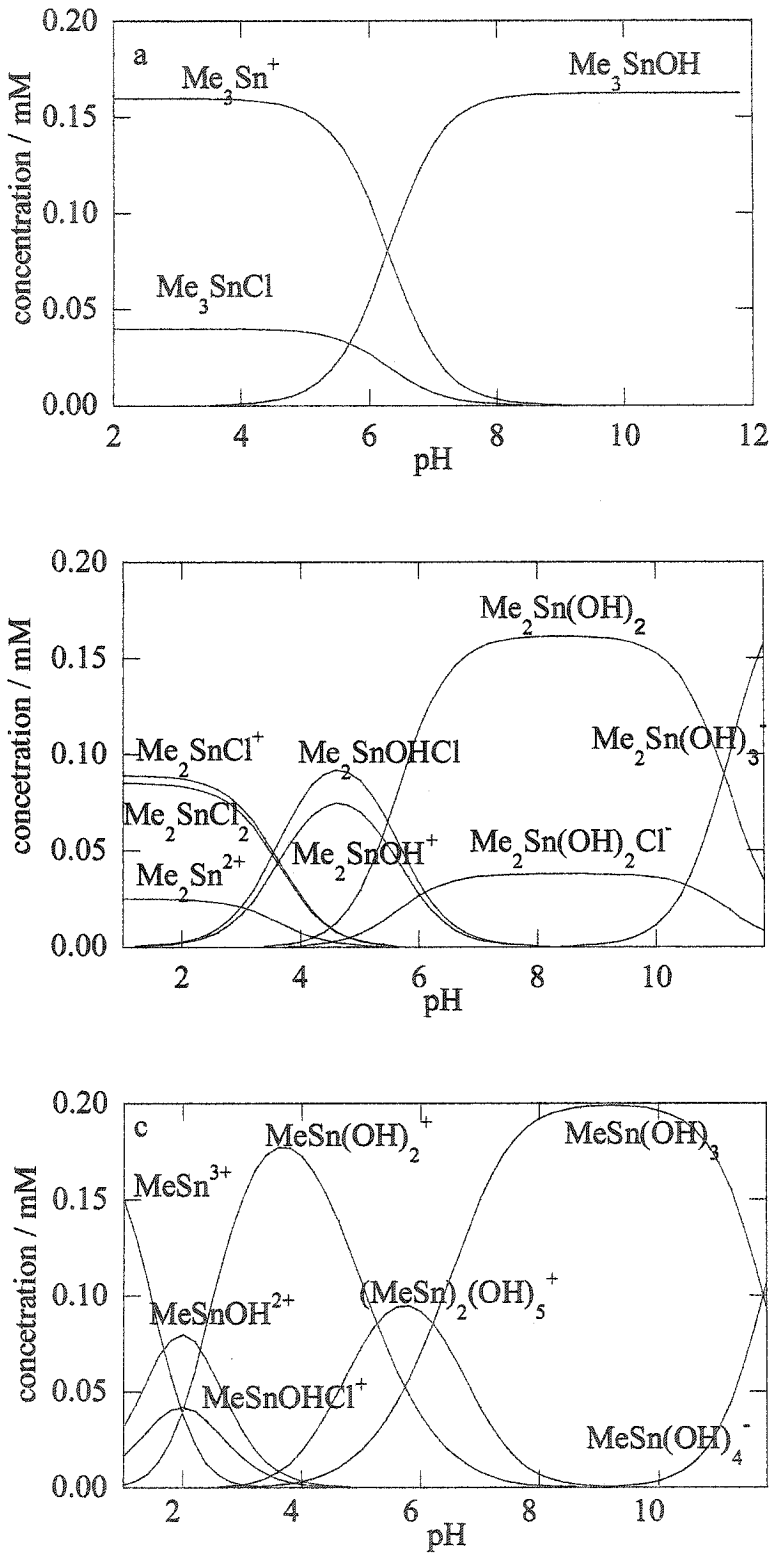

Figure 5.1 . Speciation of 0.20 mM solutions of (a) $Me_3Sn(IV)$; (b) $Me_2Sn(IV)$; and (c) MeSn(IV) in 1.0 M KCl.

Dissolution of $MeSnCl_3$ in 1.0 M KCl produces hydroxo and hydroxo-chloride species where the octahedral geometry at tin appears to be preferred.[2] At pH 10 and1.0 M KCl, $MeSn(OH)_3$ makes up 98.2% of total MeSn(IV), Figure 5.1c.

5.2 Titrations of methyltin(IV) solutions

5.2.1 Spectrophotometric titration of trimethyltin(IV)

When an acidic (pH 2.5) aqueous solution of trimethyltin(IV) in 1.0 M KCl at 20°C is made basic by dropwise addition of 0.10 M NaOH, a peak at 207 nm appears, Figure 5.2a. The absorbance at 207 nm is shown as a function of pH in Figure 5.2b. The absorbance change is ascribed to the formation of Me_3SnOH from the initially nonabsorbing mixture of Me_3Sn^+ and Me_3SnCl. The spectrophotometric titration curve was fitted to eq (1):

$$Abs/l = \varepsilon\,[Me_3SnOH] = \varepsilon\,[Sn]\,K_a / ([H^+] + K_a + [H^+]\,[Cl^-]\,K_{Cl}) \qquad (1)$$

where Me_3SnOH is the sole absorbing species at 207 nm, with extinction coefficient ε, [Sn] is the total concentration of trimethyltin species, K_a is the acid hydrolysis constant for Me_3Sn^+ and K_{Cl} is its chloride affinity. Using the published value of $K_{Cl} = 0.25$,[21] the fit yields $K_a = (4.9 \pm 0.8) \times 10^{-7}$, in agreement with the more accurate value measured by potentiometry of $(5.01 \pm 0.02) \times 10^{-7}$ at 25°C in 1.0 M KCl.[21] The effect of chloride is to decrease the effective concentration of the species undergoing hydrolysis, Me_3Sn^+.

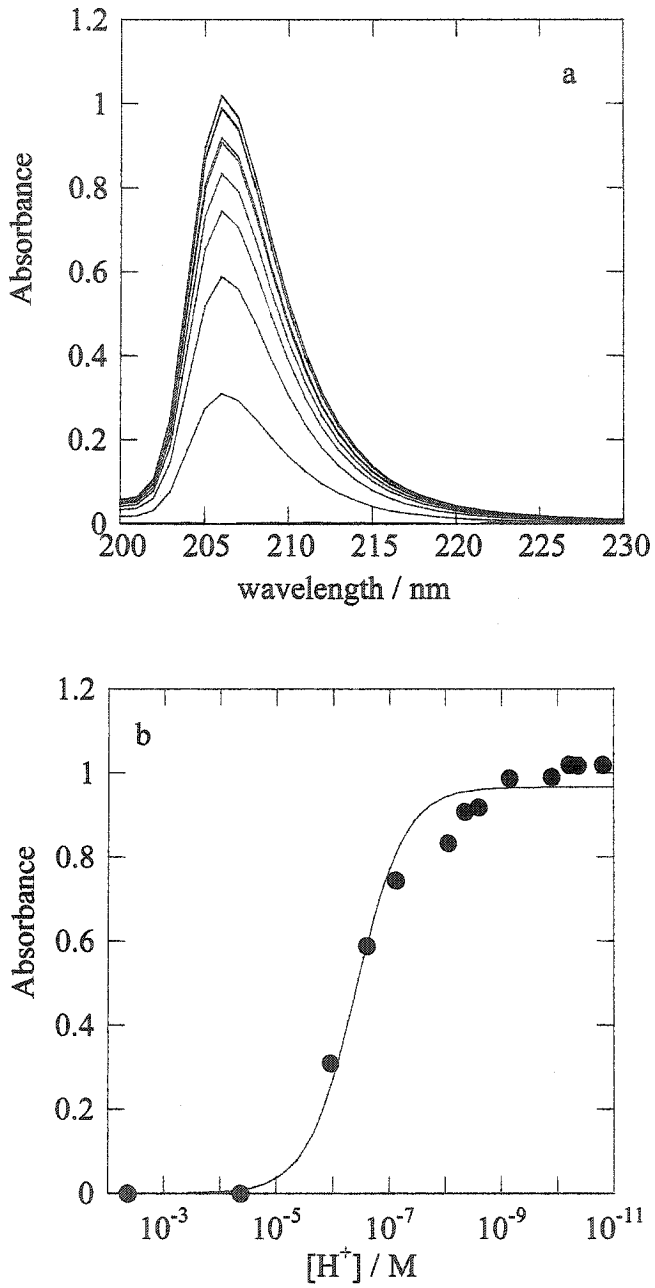

Figure 5.2 (a) Evolution of the UV spectrum of aqueous trimethyltin(IV) at 20.1°C in the presence of 1.0 M KCl, as the solution is made progressively more basic; (b) pH profile of the absorbance at 207 nm.

5.2.2 Spectrophotometric titration of dimethyltin(IV)

When an acidic (pH 3.5) aqueous solution of dimethyltin(IV) chloride in 1.0 M KCl is made basic by the dropwise addition of 0.10 M NaOH, a peak at 207 nm appears, Figure 5.3a. The absorbance as a function of pH is shown in Figure 5.3b. As it is shown in Figure 5.1b, the main species at initial pH 3.5 are Me_2Sn^{2+}, Me_2SnCl^+, Me_2SnCl_2, $Me_2Sn(OH)^+$ and $Me_2Sn(OH)Cl$. When the solution is made more basic (at pH ca 5) the predominant species in solution are $Me_2Sn(OH)^+$ and $Me_2Sn(OH)Cl$. With further addition of NaOH, the more basic species such as $Me_2Sn(OH)_2$, $Me_2Sn(OH)_2Cl^-$ and $Me_2Sn(OH)_3^-$ should be formed. In our experiments, the absorbance changes are ascribed to sequential formation of Me_2SnOH^+ /$Me_2Sn(OH)Cl$ and $Me_2Sn(OH)_2$ / $Me_2Sn(OH)_2Cl^-$/ $Me_2Sn(OH)_3^-$ from the initial non-absorbing mixture of Me_2Sn^+/Me_2SnCl^+/Me_2SnCl_2.

The absorbance at each point of the spectrophotometric titration curve is given by eq. 2:

$$Abs/l = \varepsilon_1 [Me_2Sn(OH)]^+ + \varepsilon_2 [Me_2Sn(OH)_2] + \varepsilon_3 [Me_2Sn(OH)_3]^- + \varepsilon_4 [Me_2Sn(OH)Cl] + \varepsilon_5 [Me_2Sn(OH)_2Cl]^-$$

$$= [Sn] (\varepsilon_1 \beta_{a1} [H^+]^2 + \varepsilon_2 [H^+] \beta_{a2} + \varepsilon_3 \beta_{a3} + \varepsilon_4 [H^+]^2 [Cl^-] \beta_{ab1} + \varepsilon_5 [H^+] [Cl^-] \beta_{ab2}) / ([H+]^3 (1 + \beta_{b1} [Cl^-] + \beta_{b2} [Cl^-]^2) + [H^+]^2 (\beta_{a1} + \beta_{ab1} [Cl^-]) + [H^+] (\beta_{a2} + \beta_{ab2} [Cl^-]) + \beta_{a3})$$

$$= (Abs_1 \beta_{a1} [H^+]^2 + Abs_2 [H^+] \beta_{a2} + Abs_3 \beta_{a3} + Abs_4 [H^+]^2 [Cl^-] \beta_{ab1} + Abs_5 [H^+] [Cl^-] \beta_{ab2}) / ([H^+]_3 (1 + \beta_{b1} [Cl^-] + \beta_{b2} [Cl^-]^2) + [H^+]^2 (\beta_{a1} + \beta_{ab1} [Cl^-]) + [H^+] (\beta_{a2} + \beta_{ab2} [Cl^-]) + \beta_{a3}) \quad (2)$$

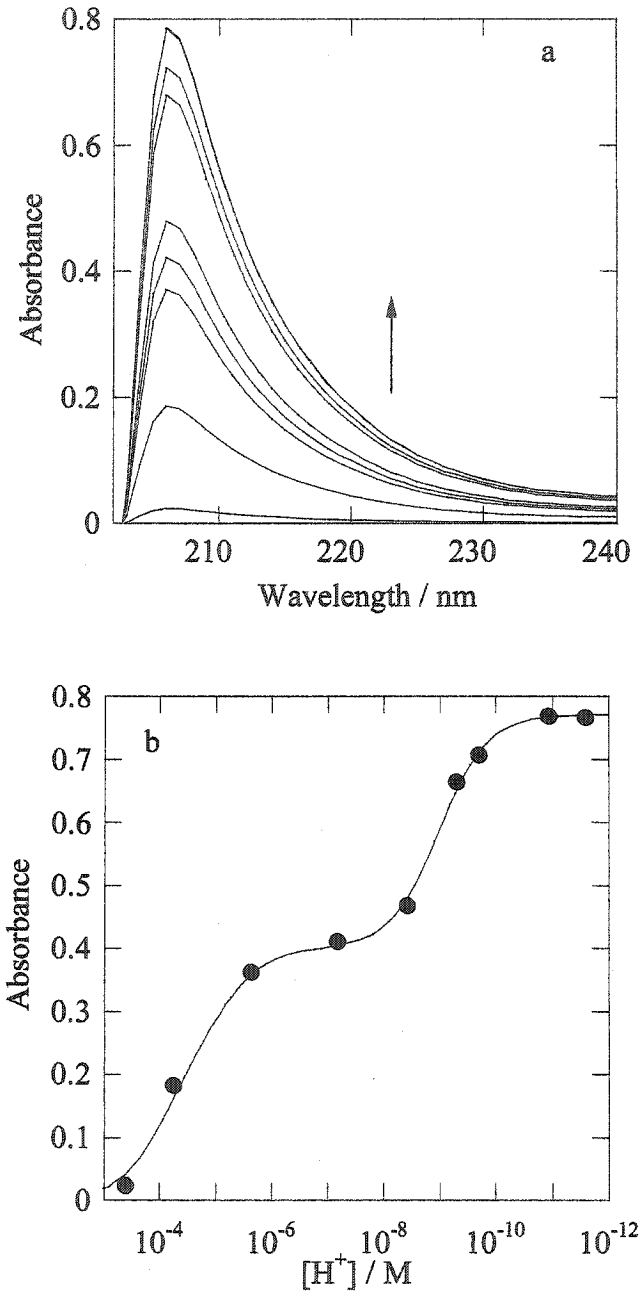

Figure 5.3 (a) Evolution of the UV spectrum of aqueous dimethyltin(IV) at 20.1°C in the presence of 1.0 M KCl, as the solution is made progressively more basic; (b) pH profile of the absorbance at 207 nm. Solid line is the nonlinear regression fit of experimental data to eq. 2 (see text)

where [Sn] is the total concentration of dimethyltin species and ε_1, ε_2, ε_3, ε_4 and ε_5 are the extinction coefficients of $Me_2Sn(OH)^+$, $Me_2Sn(OH)_2$, $Me_2Sn(OH)_3^-$, $Me_2Sn(OH)Cl$ and $Me_2Sn(OH)_2Cl^-$ respectively, β_{ai} (i = 1,2,3) are the hydrolysis constants of Me_2Sn^{2+}, β_{b1} and β_{b2} are the formation constants of Me_2SnCl^+ and Me_2SnCl_2 respectively, and β_{ab1} and β_{ab2} are the hydrolysis constants of Me_2SnCl^+. Using β_{b1} = 3.55, β_{b2} =3.39, β_{ab1} = 1.0 x 10^{-3} and β_{ab2} = 7.9 x 10^{-10} [3] and [Cl-] = 1M, the fit to eq. 13 gives β_{a2} ca. 4 x 10^{-9} and β_{a3} ca. 5 x 10^{-18}. Due to the limited number of the experimental data the values of the other parameters couldn't be determined and the values of β_{a2} and β_{a3} have a considerable error. However, the β_{a2} value is determined to have the same order of magnitude as the value reported from deStefano et. al.[3] while β_{a3} is much higher, most probably due to the presence of CO_3^{2-} in our experiments, run in presence of air.

6.2.3 Spectrophotometric titration of monomethyltin(IV)

An acidic (pH 2.5) aqueous solution of monomethyltin(IV) in 1.0 M KCl has a peak at 207 nm in its UV spectrum, attributed to $MeSn(OH)^{2+}$ and $MeSnOHCl^+$ which are present in the initial solution, together with $MeSn^{3+}$, Figure 5.1c. When this solution is made basic by the dropwise addition of 0.10 M NaOH, the absorbance at 207 nm increases, Figure 5.4a. The absorbance as a function of pH is shown in Figure 5.4b. The absorbance changes are ascribed to the sequential formation of $MeSn(OH)_2^+$ $MeSn(OH)^{2+}$, and $MeSn(OH)_3$, from $MeSn^{3+}$ present initially in the solution. The spectrophotometric titration curve is described by eq. 3:

$$Abs/l = \varepsilon_1 [MeSn(OH)^{2+}] + \varepsilon_2 [MeSn(OH)_2^{+}] + \varepsilon_3 [MeSn(OH)_3] + \varepsilon_4 [MeSnOHCl]$$

$$= [Sn] (\varepsilon_1 \beta_{a1} [H^+]^2 + \varepsilon_2 \beta_{a2} [H^+] + \beta_{a3} + \varepsilon_4 \beta_{ab1} [H^+]^2) / ([H^+]^3 + (\beta_{a1} + \beta_{ab1}) [H^+]^2 + \beta_{a2} [H^+] + \beta_{a3})$$

$$= ([H^+]^2 (Abs_1 \beta_{a1} + Abs_5 \beta_{ab1}) + Abs_2 \beta_{a2} [H^+] + Abs_3 \beta a3) / ([H^+]^3 + (\beta_{a1} + \beta_{ab1}) [H^+]^2 + \beta_{a2} [H^+] + \beta_{a3}) \quad (3)$$

where ε_1, ε_2, ε_3 and ε_4 are the extinction coefficients of $MeSn(OH)^{2+}$, $MeSn(OH)_2^{+}$ $MeSn(OH)_3$ and MeSnOHCl respectively, [Sn] the total concentration of monomethyltin(IV) solution, β_{ai} (i= 1,2,3) are the hydrolysis constant of $MeSn^{3+}$ and β_{ab1} is the hydrolysis constant of $MeSnCl^{2+}$. Fitting our experimental values to eq 3, we find the stepwise hydrolysis constants of $MeSn^{3+}$, $K_{a1} = (1.1 \pm 0.4) \times 10^{-3}$, $K_{a2} = (1.2 \pm 0.3) \times 10^{-7}$ and $K_{a3} = (3.8 \pm 0.9) \times 10^{-10}$. These values are very close to those reported from deStefano et al, Table 5.1.[20]

In these calculations we did not consider the formation of dinuclear species $(MeSn)_2(OH)_5^{+}$ which is reported from deStefano[20]. However, the formation of these species is still debatable: Blunden at al[2] did not recognized any polynuclear group of compounds by ^1H and ^{119}Sn NMR spectroscopy for pH up to 10 and [MeSn(IV)] up to 0.5M, while deStefano et al[20] realized that the formation of this species is highly dependent on MeSn(IV) concentration. However, the good agreement between our values of acidity constants and the more accurate ones published by deStefano et.al. [20] demonstrates that the formation of dinuclear species in not relevant in our experimental conditions.

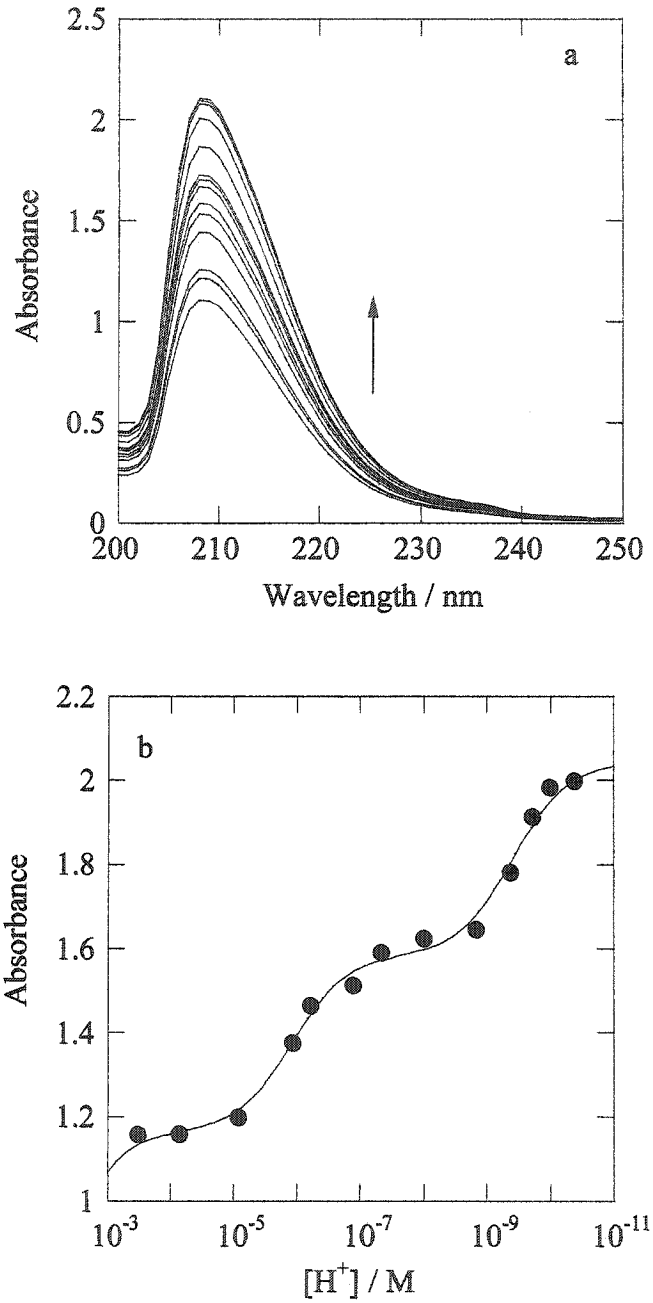

Figure 5.4 (a) Evolution of the UV spectrum of aqueous monomethyltin(IV) at 20.1°C in the presence of 1.0 M KCl, as the solution is made progressively more basic; (b) pH profile of the absorbance at 207 nm. Solid line is the nonlinear regression fit of experimental data to eq. 3 (see text)

5.3 Aqueous speciation of the mercuric ion in the presence of chloride

The hexaaquamercuric ion, $Hg(H_2O)_6^{2+}$, exists in acidic aqueous solution only in the presence of non-coordinating anions such as perchlorate.[38] It does not absorb appreciably in the UV above 220 nm, Figure 5.5. As the solution is made progressively more basic, hydrolysis leads to the formation of less soluble hydroxo complexes, eq. 4-5:[39]

$$Hg(H_2O)_6^{2+} + H_2O \leftrightarrows Hg(H_2O)_nOH^+ + H_3O^+ \qquad K_{h1} = 3.98 \times 10^{-4} \qquad (4)$$

$$Hg(H_2O)_nOH^+ + H_2O \leftrightarrows Hg(OH)_2 + H_3O^+ \qquad K_{h2} = 1.59 \times 10^{-3} \qquad (5)$$

In the presence of chloride, mercuric ions form stable chloro complexes, with the stability constants at 25°C and 1M ionic strength presented with eq 6-9: [39]

$$Hg^{2+} + Cl^- \leftrightarrows HgCl^+ \qquad K_{HgCl} = 5.3 \times 10^6 \qquad (6)$$

$$HgCl^+ + Cl^- \leftrightarrows HgCl_2 \qquad K_{HgCl2} = 3.2 \times 10^6 \qquad (7)$$

$$HgCl_2 + Cl^- \leftrightarrows HgCl_3^- \qquad K_{HgCl3} = 9.3 \qquad (8)$$

$$HgCl_3^- + Cl^- \leftrightarrows HgCl_4^{2-} \qquad K_{HgCl4} = 12.6 \qquad (9)$$

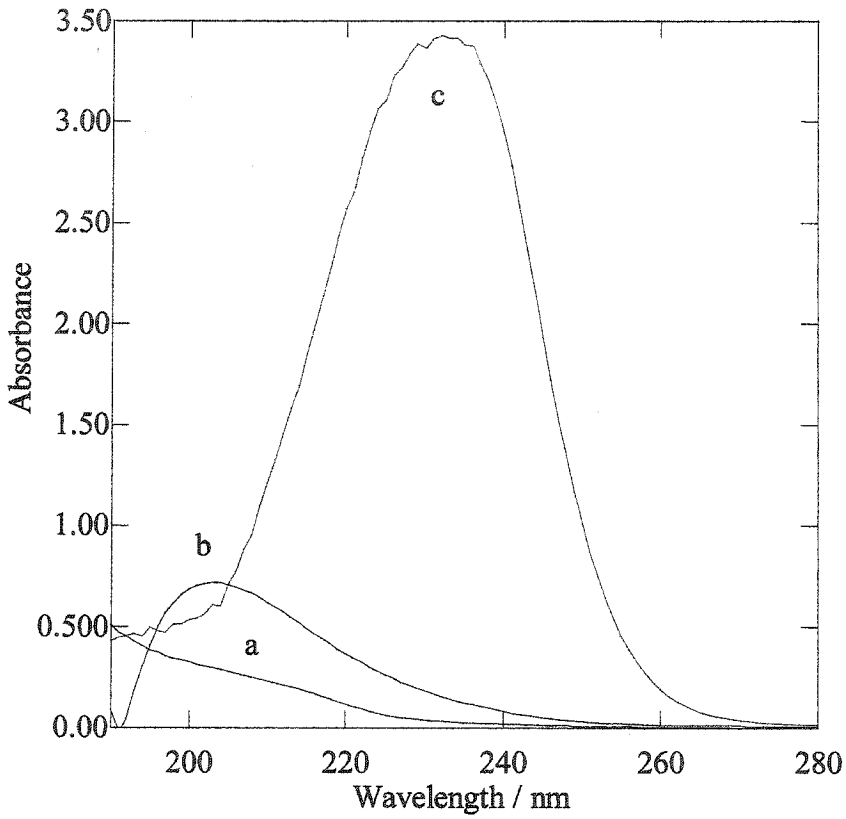

Figure 5.5 UV absorption spectra of 0.10 mM aqueous solutions of (a) Hg^{2+} at pH 1.5; (b) Hg^{2+} at pH 1.5 and pCl 2 (90.5% $HgCl_2$, 8.4% $HgCl_3^-$ and 1.1% $HgCl_4^{2-}$) and (c) Hg^{2+} at pH 1.5 and pCl 0 (91.9% $HgCl_4^{2-}$, 7.3% $HgCl_3^-$ and 0.8% $HgCl_2$).

$HgCl_2$ and $HgCl_4^{2-}$ absorb at λ_{max} 207 nm ($\varepsilon = 6.8 \times 10^3$ M^{-1} cm^{-1}) and λ_{max} 232 nm ($\varepsilon = 3.0 \times 10^4$ M^{-1} cm^{-1}), respectively, Figure 5.5. The spectrum of $HgCl_2$ remains unchanged up to pH 6.5 and that of $HgCl_4^{2-}$ up to pH 10. Because of the small formation constant for $HgCl_3^-$, $K_{HgCl2} >> K_{HgCl3} < K_{HgCl4}$, the addition of chloride to a solution of $HgCl_2$ results mostly in formation of $HgCl_4^{2-}$.

Complexation by chloride results in increased solubility of mercury at less acidic pH values. Using the formation constants shown above,[39] speciation of the mercuric ion was determined as a function of pH and pCl, Figure 5.6. The major species in aqueous mercuric solutions at pH 10 and $[Cl^-] = 1.0$ M are $HgCl_4^{2-}$ (90.2%), $HgCl_3^-$ (7.2%) and HgOHCl (1.2% of total mercury).

5.4 Yield of methylmercury

Howell et al. studied reactions of methyltins with $HgCl_2$ and demonstrated that MeHgCl is the stoichiometric product.[27] Woggon et al.[28] showed that the yield of methylmercury from the reactions of mono-, di-, and trimethyltin solutions with $HgCl_2$ added in deionized water and in natural water samples depends on methyltin species, pH and the sample matrix; higher methylmercury yields were detected in samples with higher pH, and in sterilized natural water samples. Also they showed that monomethyltin reacts faster then dimethyltin and trimethyltin.

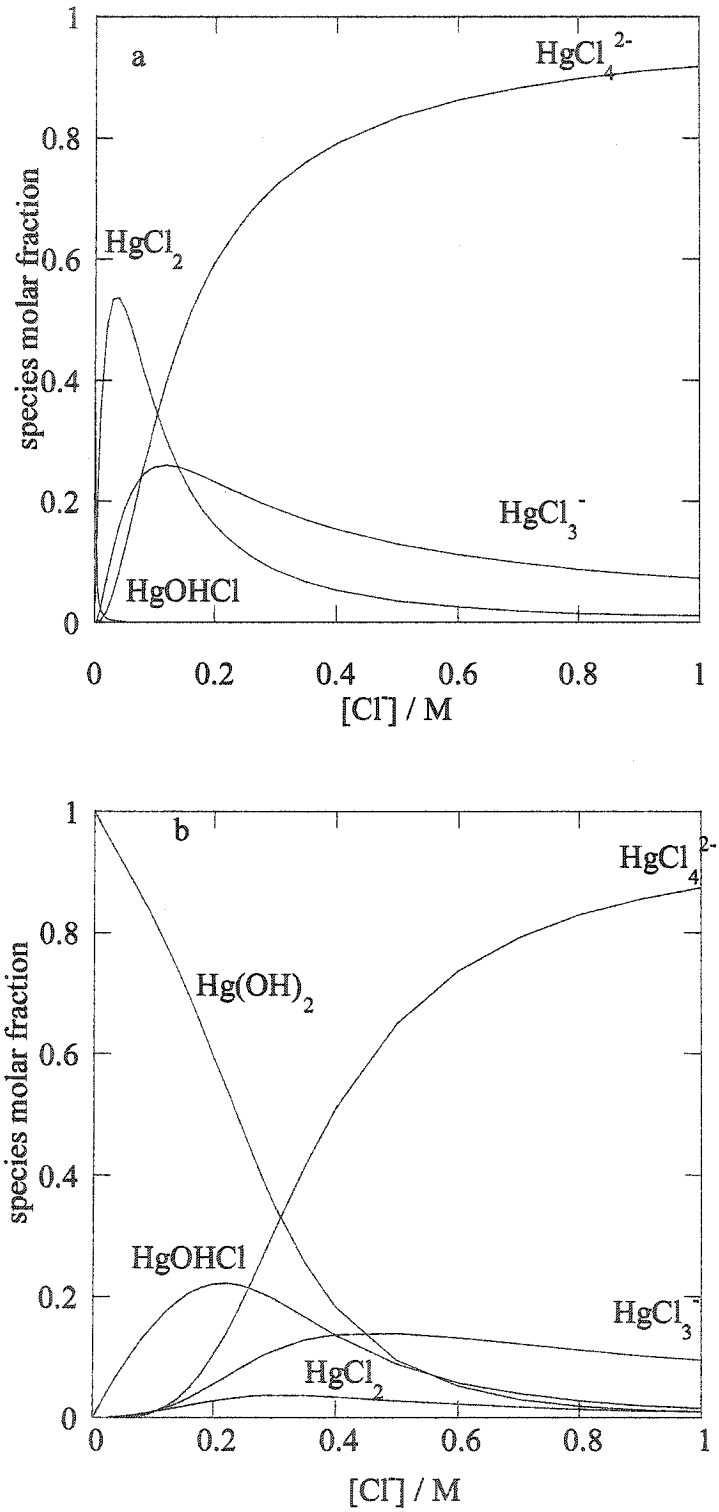

Figure 5.6 Chloride-dependent speciation diagram for 0.020 mM Hg(II) at (a) pH 7.5 and (b) pH 10.0

Also, Jewett, Bellama and Brinkman[32-34] have shown that methylmercury is the stoichiometric product of the reaction of mercuric ions with methyltin compounds.

A reaction mixture containing 0.20 mM trimethyltin and 0.020 mM $HgCl_4^{2-}$ at pH 10.0 and $[Cl^-]$ = 1.0 M was allowed to react at 40°C for 2 hours and then analyzed for methylmercury. The yield was (0.015 ± 0.002) mM $MeHg^+$ (average of 3 experiments), or (75 ± 9) % based on mercury. Similarly, the yield of methylmercury was (82 ± 5) % in the reaction with 0.20 mM dimethyltin and (80 ± 7) % in the reaction with monomethyltin, both measured at pH 10 and 1 M KCl solutions, after 1 hour at 20°C. Therefore transfer of methyl from tin to mercury is deemed to be quantitative, eq. 10:

$$Me_nSn(IV) + HgCl_4^{2-} \rightarrow Me_{n-1}Sn(IV) + MeHgCl \qquad (10)$$

5.5 Kinetics of the reaction of mercury with trimethyltin

Reactions of tetraalkyltin compounds R_4Sn with mercuric chloride are typical examples of electrophilic cleavage of alkylmetals by mercury complexes, eq. 11:[40-42]

$$R_4Sn + HgX_2 \rightarrow RHgX + R_3SnX \qquad (11)$$

Their kinetics, mechanisms and activation parameters in water-methanol mixtures have been thoroughly studied.[43-45] Less is known about the kinetics and mechanism of reactions of other alkyltins with mercury complexes. Jewett et al. studied the rate of transmethylation from trimethyltin to the mercuric ion in water as a function of pH,

chloride concentration and ionic strength by monitoring the change in concentration of trimethyltin species.[34] Methyl transfer from both Me_3Sn^+ and Me_3SnCl was inferred to occur to both $HgCl_2$ and $HgCl_3^-$. Methylation was inferred to occur by bimolecular electrophilic substitution, eq. 12:[32-34]

$$(CH_3)_3Sn(IV) + Hg(II) \leftrightarrows (CH_3)_2Sn(IV) + CH_3Hg(II) \qquad (12)$$

The measured second-order rate constants were acknowledged to depend on the speciation of both trimethyltin and mercury, but the relationships were not specified in detail.

Cerrati et al. also studied the kinetics of methylation of $HgCl_2$ by mono-, di- and trimethyltin in seawater by monitoring the concentration of methylmercury formed.[29] Under pseudo-first-order conditions, the relative rates of methylmercury formation at pH 8 showed an unusual and unexplained ordering: $Me_3Sn^+ > Me_2Sn^{2+} < MeSn^{3+}$. However, the authors didn't take into account the speciation of $HgCl_2$ and methyltin species as a function of pH.

5.5.1 Rate law

In this study, the kinetics of mercury methylation were investigated under pseudo-first-order conditions using trimethyltin(IV) as the excess reagent. Mercuric halide complexes show relatively strong absorption bands in the UV due to ligand-to-metal charge transfer.[46] We followed the kinetics of mercury methylation by trimethyltin species via

the loss of absorbance of $HgCl_4^{2-}$ at 232 nm, or the loss of absorbance of $HgCl_2$ at 207 nm. When 0.20 mM trimethyltin in 1.0 M KCl at pH 10.0 and 44.8°C is mixed with 0.020 mM $HgCl_4^{2-}$, the absorbance due to the latter at 232 nm decreases, Figure 5.7a. The kinetic profile is pseudo-first-order, Figure 5.7b. The observed rate constants, summarized in Table 5.2, depend linearly on the concentration of the trimethyltin reagent, Figure 5.7c, with an intercept insignificantly different from zero. Under these conditions, the pH-dependent second-order rate constant k_{app} is (0.93 ± 0.03) M^{-1} s^{-1}.

5.5.2 Effect of pH

The observed rate constants for the reaction of trimethyltin(IV) with Hg^{2+} in 1.0 M KCl are highly pH-dependent, Table 5.3. At 44.8°C, the measured rate constant k_{app} decreases with increasing pH, Figure 5.8a. Since the spectrum of $HgCl_4^{2-}$ is invariant over the range of pH investigated, the effect is ascribed to hydrolysis of the trimethyltin(IV) reagent. The rate law is described by eq. 13-14:

$$-d[HgCl_4^{2-}]/dt = k1\ [HgCl_4^{2-}]\ [Me_3SnOH] \quad (13)$$

$$k_{app} = k_1 K_a\ [Sn] / ([H^+] + K_a + [H^+]\ [Cl^-]\ K_{Cl}) \quad (14)$$

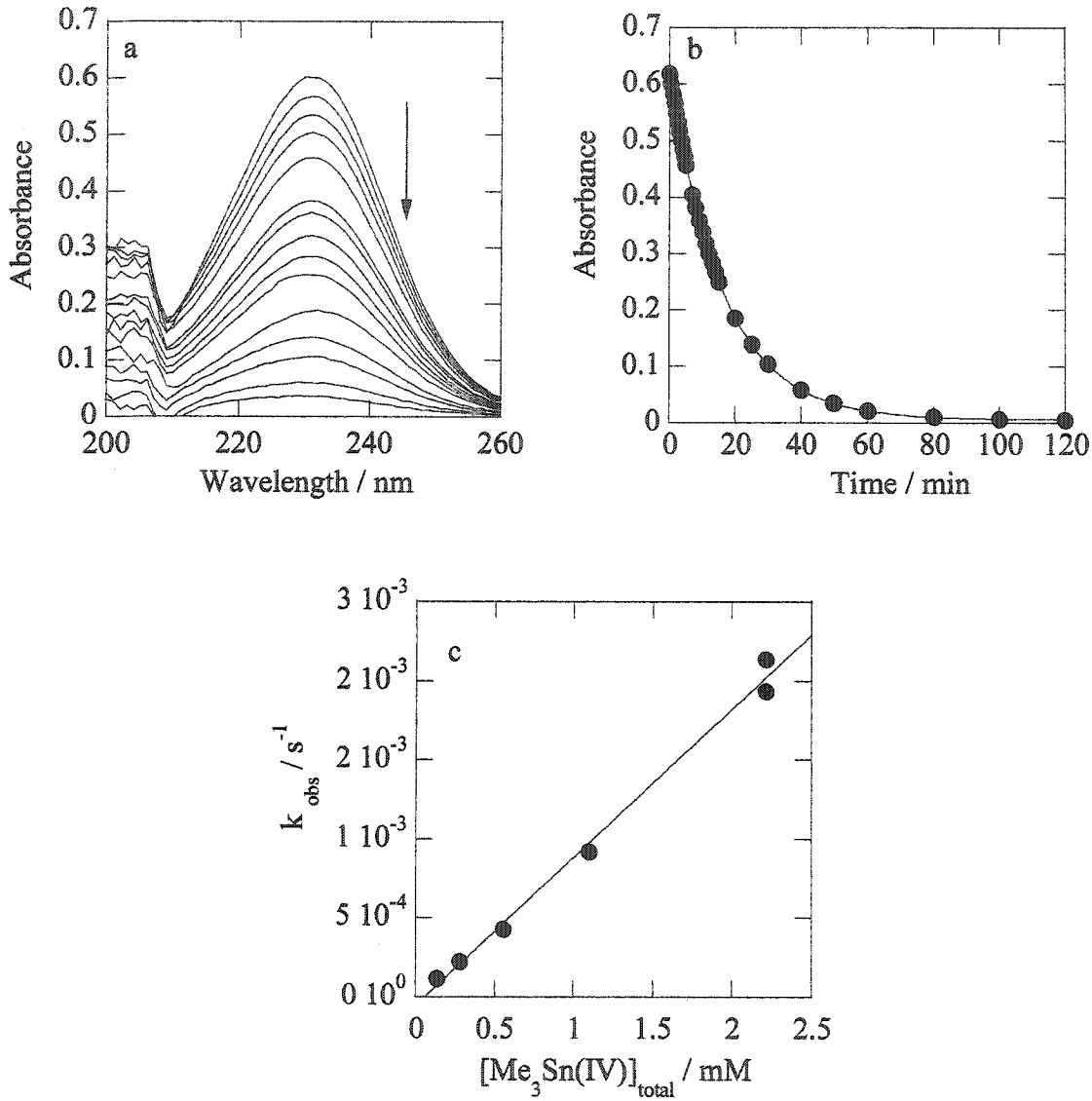

Figure 5.7 (a) Evolution of the UV spectrum of an aqueous solution of 0.020 mM $HgCl_4^{2-}$ upon addition of 0.20 mM $Me_3Sn(IV)$ at pH 10.0 and 44.8°C in the presence of 1.0 M Cl^-. Spectra recorded over 120 min. (b) Kinetic profile of the reaction at 232 nm. The solid line is the single exponential fit to the experimental data. (c) Dependence of the pseudo-first-order rate constants measured at pH 10.0 and 44.8°C on the concentration of the excess reagent, $Me_3Sn(IV)$.

Table 5.2. Observed rate constants for the reaction of excess trimethyltin with 0.020 mM Hg^{2+} at pH 10.0, 1.0 M KCl and 44.8°C

$[Me_3SnOH]$ mM	10^4 kobs s^{-1}
0.137	1.17 ± 0.04
0.280	2.21 ± 0.06
0.557	4.27 ± 0.05
1.09	9.18 ± 0.03
2.21	21.3 ± 0.9
2.21	19.3 ± 0.7

Table 5.3 pH dependence of the observed rate constants for the reaction of 2.0 mM $Me_3Sn(IV)$ with 0.20 mM Hg(II) in 1.0 M KCl at 44.8°C

pH ± 0.01	$10^4 k_{obs}$ s^{-1}
2.36	-[a]
4.63	0.40 ± 0.02
5.95	3.16 ± 0.04
6.59	5.93 ± 0.02
6.89	6.88 ± 0.06
7.14	9.93 ± 0.05
8.05	15.3 ± 0.1
8.34	16.3 ± 0.6
8.42	16.7 ± 0.3
9.14	17.5 ± 0.6
9.43	17.8 ± 0.4
9.89	18.0 ± 0.4
10.17	17.3 ± 0.2
10.36	17.3 ± 0.3
10.73	17.7 ± 0.4

a No reaction detected.

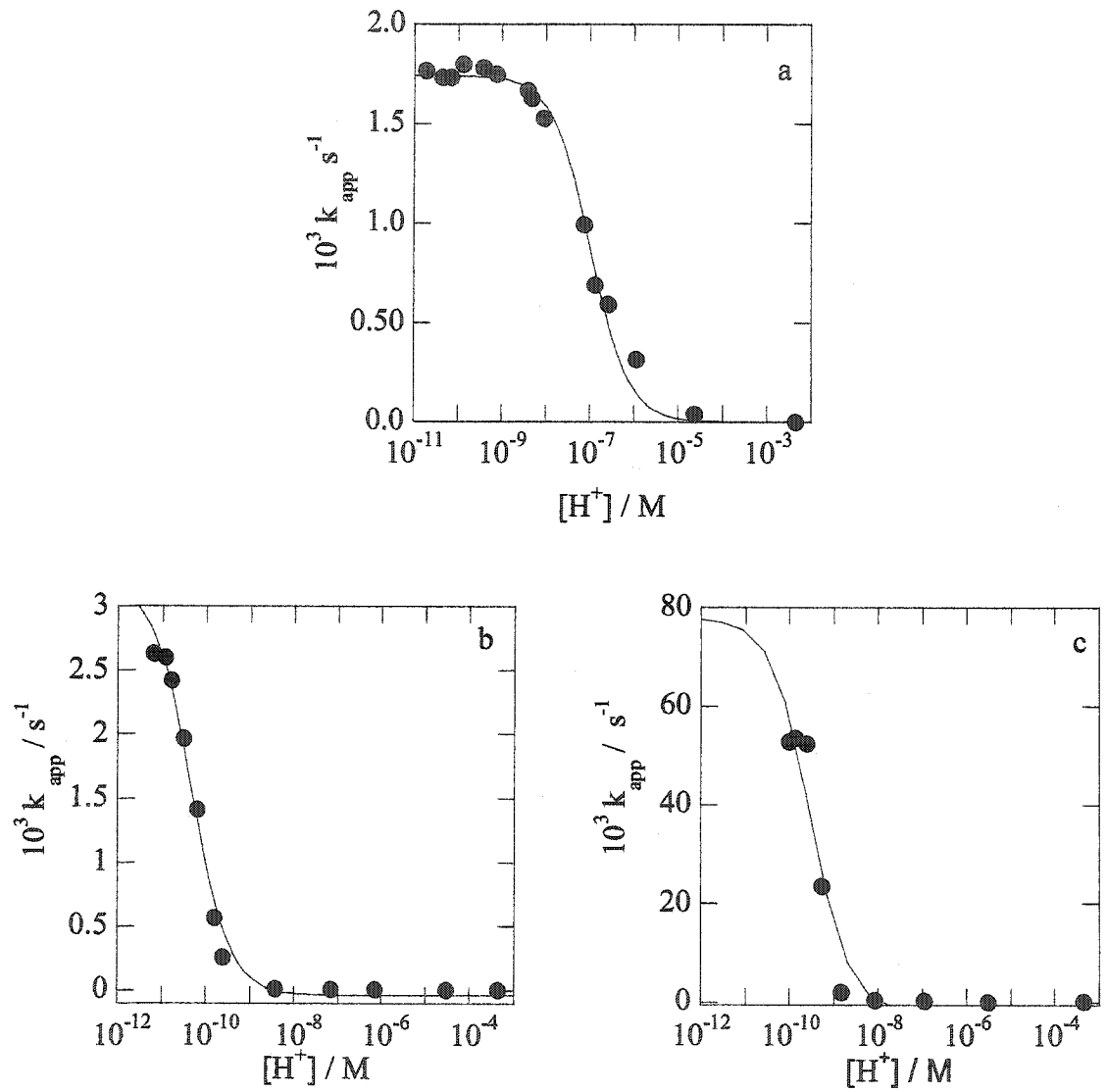

Figure 5.8 pH Dependence of the apparent rate constant k_{app} for the reaction of 0.020 mM Hg2+ at pH 10.0 and 1.0 M KCl with (a) 0.2 mM $Me_3Sn(IV)$ at 44.8°C; (b) 0.2 mM $Me_2Sn(IV)$ at 30.1°C; and (c) 0.1 mM MeSn(IV) at 30.2°C.

The experimental values of k_{app} were fitted to eq. 15 using $K_{Cl} = 0.25$ for 1.0 M ionic strength and 25°C.[21] The fit yields $k_1 = (0.87 \pm 0.01)\ M^{-1}\ s^{-1}$ and $Ka = (1.3 \pm 0.1) \times 10^{-7}$ for the pH independent rate constant and acidity constant at 45°C.

5.5.3 Effect of chloride concentration

At pH 7.5, trimethyltin exists in aqueous solution predominantly (> 90%) as Me_3SnOH, even in the presence of 1.0 M KCl, Figure 5.1a. Decreasing the amount of chloride to 0.10 M changes only the speciation of Hg(II), Figure 5.6. The distribution of Hg(II) species in this range is given by eq.15-17:

$$\alpha(HgCl_2) = 1 / (1 + K_{HgCl3}\,[Cl^-] + K_{HgCl3}\,K_{HgCl4}\,[Cl^-]^2) \quad (15)$$

$$\alpha(HgCl_3^-) = K_{HgCl3}\,[Cl^-] / (1 + K_{HgCl3}\,[Cl^-] + K_{HgCl3}\,K_{HgCl4}\,[Cl^-]^2) \quad (16)$$

$$\alpha(HgCl42\text{-}) = K_{HgCl3}\,K_{HgCl4}\,[Cl^-]^2 / (1 + K_{HgCl3}\,[Cl^-] + K_{HgCl3}\,K_{HgCl4}\,[Cl^-]^2) \quad (17)$$

where K_{HgCl3} and K_{HgCl4} are the sequential formation constants of $HgCl_3^-$ and $HgCl_4^{2-}$, respectively.[39] The observed rate constants increase with chloride concentration at constant ionic strength, Table 5.4 and Figure 5.9. The chloride dependence of k_{app} is expressed in eq. 18:

$$k_{app} = [Sn]\,(k_2 + k_3\,K_{HgCl3}\,[Cl^-] + k_4\,K_{HgCl3}\,K_{HgCl4}\,[Cl^-]^2) / (1 + K_{HgCl3}\,[Cl^-] + K_{HgCl3}\,K_{HgC4}\,[Cl^-]^2) \quad (18)$$

Table 5.4 Chloride-dependent pseudo-first-order rate constants for the reaction of 0.20 mM Hg^{2+} with 2.5 mM $Me_3Sn(IV)$ at 44.8°C, pH 7.5 and ionic strength 1.0 M ($NaClO_4$)

$[Cl^-]$ M	$10^3 k_{obs}$ s^{-1}
0.0035	0.058 ± 0.004
0.0055	0.088 ± 0.005
0.0125	0.142 ± 0.003
0.0325	0.308 ± 0.005
0.0425	0.563 ± 0.002
0.0725	0.992 ± 0.008
0.1025	1.18 ± 0.03
0.2525	1.21 ± 0.05
0.5025	1.25 ± 0.06
1.0025	1.27 ± 0.06

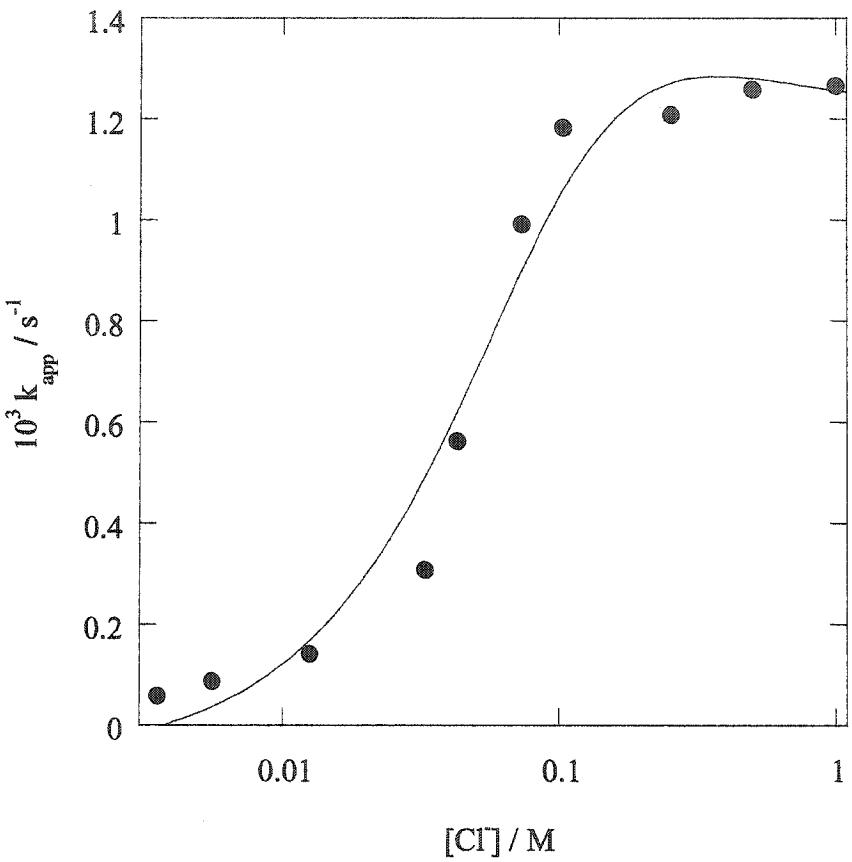

Figure 5.9 Chloride dependence of the second-order rate constant k_{app} for the reaction of Hg(II) with Me_3SnOH at pH 7.5, 44.8°C and 1.0 M ionic strength ($KCl/NaClO_4$). The solid line is the non-linear curve fit to eq 18 (see text).

where $k_{app} = k_{obs} / [Sn]$. Fitting the experimental data to eq. 19 yields k_2 insignificantly different from zero, $k_3 = (0.8 \pm 0.1)\ M^{-1}\ s^{-1}$ and $k_4 = (0.48 \pm 0.04)\ M^{-1}\ s^{-1}$. $HgCl_3^-$ is almost twice as reactive as $HgCl_4^{2-}$.

5.5.4 Effect of ionic strength

The kinetics of the reaction of 0.20 mM Hg(II) with 2.5 mM trimethyltin were measured at pH 7.5, $[Cl^-] = 0.07$ M and 44.8°C in solutions with ionic strengths varying from 0.12 M to 1.0 M ($NaClO_4$). Under these conditions, Hg(II) is distributed as $HgCl_2$ (34%), $HgCl_3^-$ (34%) and $HgCl_4^{2-}$ (32%). Me_3Sn(IV) is distributed as Me_3SnOH (52%), Me_3Sn^+ (26%) and Me_3SnCl (22%). The rate constants are invariable over this range of ionic strength, Table 5.5, consistent with one of the reactants being uncharged (i.e., Me_3SnOH).

5.6 Reaction of mercury(II) with dimethyltin(IV)

5.6.1 Kinetics

When a 0.20 mM dimethyltin(IV) solution was mixed with a 0.020 mM Hg(II) solution at pH 10, 1.0 M KCl and (20.1± 0.1)°C, the absorbance of $HgCl_4^{2-}$ at 232 nm decreased, Figure 5.10a. The kinetic profiles are pseudo-first-order, Figure 5.10b and the observed rate constants, summarized in Table 5.6, depend linearly on the total concentration of

Table 5.5. The effect of ionic strength ($NaClO_4$) on observed rate constants for the reaction of 2.5 mM $Me_3Sn(IV)$ with 0.20 mM Hg^{2+} in 0.07 M KCl, pH 7.5 and 44.8°C

Ionic strength M	$10^3 k_{obs}$ s^{-1}
0.12	0.981 ± 0.003
0.29	0.965 ± 0.005
0.46	0.976 ± 0.006
0.62	0.988 ± 0.008
1.00	0.992 ± 0.008

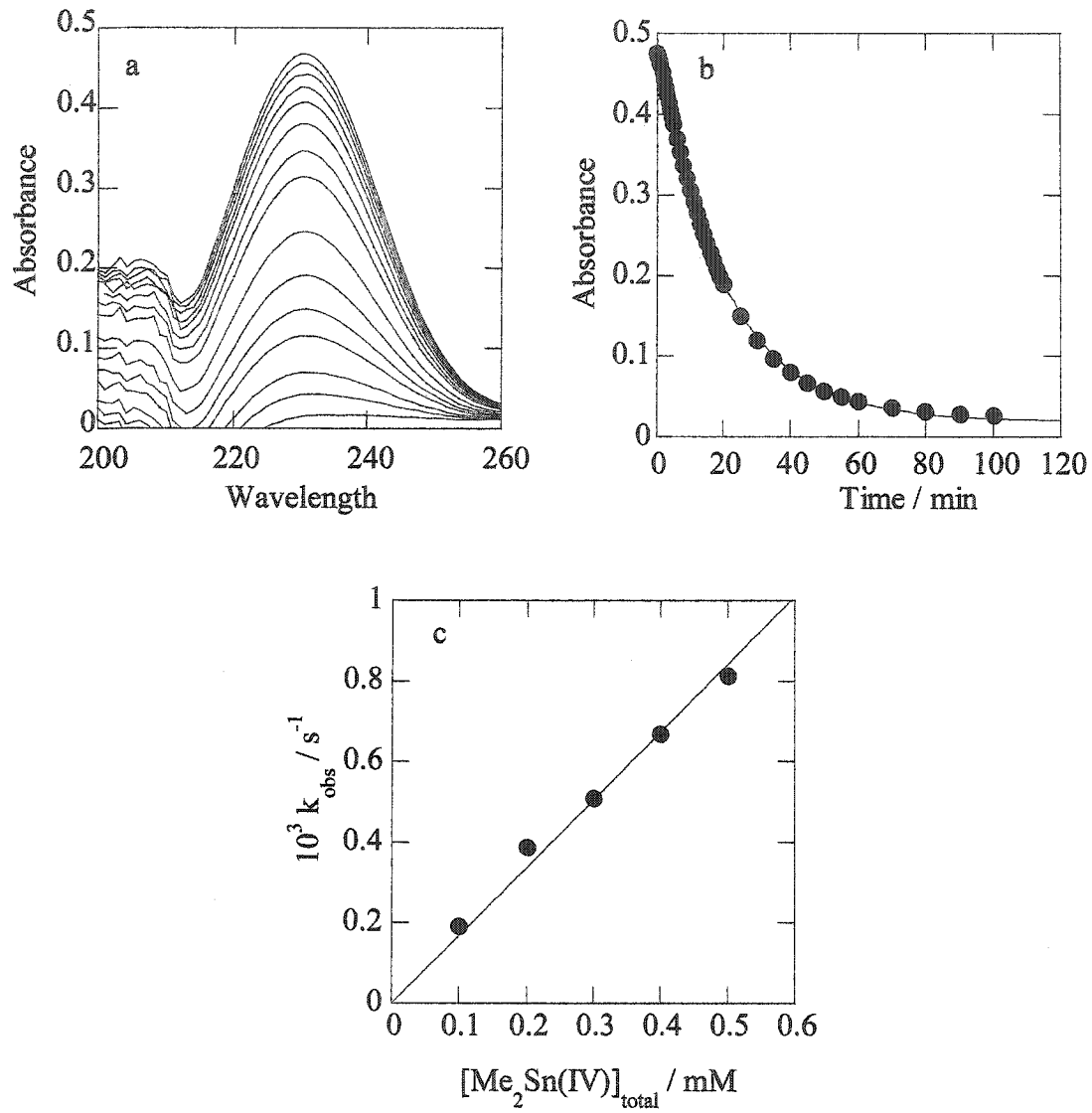

Figure 5.10 (a) Evolution of the UV spectrum of an aqueous solution of 0.020 mM $HgCl_4^{2-}$ upon addition of 0.20 mM $Me_2Sn(IV)$ at pH 10.0 and 20.1°C in the presence of 1.0 M Cl^-. Spectra recorded over 100 min. (b) Kinetic profile of the reaction at 232 nm. The solid line is the single exponential fit to the experimental data. (c) Dependence of the pseudo-first-order rate constants measured at pH 10.0 and 20.1°C on the concentration of the excess reagent, $Me_2Sn(IV)$.

Table 5.6 Observed rate constants for the reactions of dimethyl tin with 0.02 mM Hg^{2+} at pH 10, 1M KCl and 20.1°C

$[Me_2Sn(IV)]$ mM	$10^4 k_{obs}$ s^{-1}
0.100	1.93 ± 0.01
	1.93 ± 0.02
0.200	3.87 ± 0.03
	3.90 ± 0.02
0.301	5.13 ± 0.03
	5.08 ± 0.02
0.401	6.68 ± 0.05
	6.72 ± 0.04
0.501	8.28 ± 0.08
	8.00 ± 0.05

dimethyltin(IV), Figure 5.10c. Under these conditions, the pH-dependent second-order rate constant k_{app} is (1.68 ± 0.03) M^{-1} s^{-1}.

5.6.2. Effect of pH

The observed rate constants for the reaction of dimethyltin(IV) with Hg^{2+} in 1.0 M KCl are highly pH-dependent, Table 5.7. At 30.1°C, the measured rate constant k_{app} increases with increasing pH, Figure 5.8b due to the hydrolysis of the dimethyltin(IV) reagent. The rate constants increase sharply when pH increases from ca. 7 to ca. 10, which corresponds to the transformation of $Me_2Sn(OH)_2$ to $Me_2Sn(OH)_3^-$, Figure 5.1b. Then, the apparent rate constant is, eq 19:

$$k_{app} = (k_1 [H^+] + k_2 K_{a3}) / ([H^+] + K_{a3}) \quad (19)$$

where k_1 and k_2 are the rate constants for the reaction of $Me_2Sn(OH)_2$ and $Me_2Sn(OH)_3^-$ respectively and K_{a3} is the hydrolysis constant of $Me_2Sn(OH)_2$. Fitting the experimental data to eq. 19, we find that the rate constant for $Me_2Sn_2(OH)_2$ is insignificantly different from zero, and the rate constants for the reaction of $Me_2Sn(OH)_3^-$ at pH 10, 1M KCl and 30.1°C is (6.34 ± 0.03) M^{-1} s^{-1}. The acidity constant determined from this experiment is (4.7 ± 0.7) x 10^{-11}, is comparable with the value 7.9 x 10^{-12} reported from deStefano et.al., for this constant at 25°C, Table 5.1[3], shows that the presence of OH group significantly increases the rate of the reaction of $Me_2Sn(IV)$ with mercuric ions in 1M KCl solutions..

Table 5.7 pH dependence of the observed rate constants for the reaction of 0.5 mM $Me_2Sn(IV)$ with 0.10 mM Hg(II) in 1.0 M KCl at 30.1°C

pH ± 0.01	$10^3 k_{obs}$ s^{-1}
3.35	-[a]
4.53	(2.38 ± 0.02) x 10^{-3}
6.14	5.83 ± 0.05) x 10^{-3}
7.16	9.50 ± 0.06) x 10^{-3}
8.42	1.35 ± 0.03) x 10^{-2}
9.62	0.256 ± 0.005
9.80	0.567 ± 0.005
10.20	1.42 ± 0.01
10.53	1.97 ± 0.02
10.79	2.42 ± 0.05
10.93	2.60 ± 0.03
11.20	2.63 ± 0.01

[a] No reaction detected.

5.7 Reaction of mercury(II) with monomethyltin(IV)

5.7.1 Kinetics

The kinetics of mercury methylation by monomethyltin(IV) was monitored by following the absorbance (at 232 nm) of a 0.010 mM Hg(II) solution at pH 10, and 1M KCl after addition of 0.10 mM MeSn(IV) at (20.1 ± 0.1°C), Figure 5.11a. The kinetic profiles are pseudo-first-order, Figure 5.11b and the observed rate constants, summarized in Table 5.8, depend linearly on the total concentration of monomethyltin(IV), Figure 5.11c. Under these conditions, the H-dependent second-order rate constant k_{app} is 15.9 ± 0.6 M^{-1} s^{-1}.

5.7.2. Effect of pH

The observed rate constants for the reaction of monomethyltin(IV) with Hg^{2+} in 1.0 M KCl are highly pH-dependent, Table5.9. At (30.2 ± 0.1)°C, the measured rate constant k_{app} decreases with increasing pH, Figure 5.8c due to the hydrolysis of the monomethyltin(IV) reagent. The rate constants increase sharply when pH increases from ca. 9 to ca. 11, which corresponds to the formation of $MeSn(OH)_4^-$ from $MeSn(OH)_3$, Figure 5.1c. Then, the apparent rate constant is, eq 20:

$$k_{app} = (k_1 [H^+] + k_2 K_{a4}) / ([H^+] + K_{a4}) \quad (20)$$

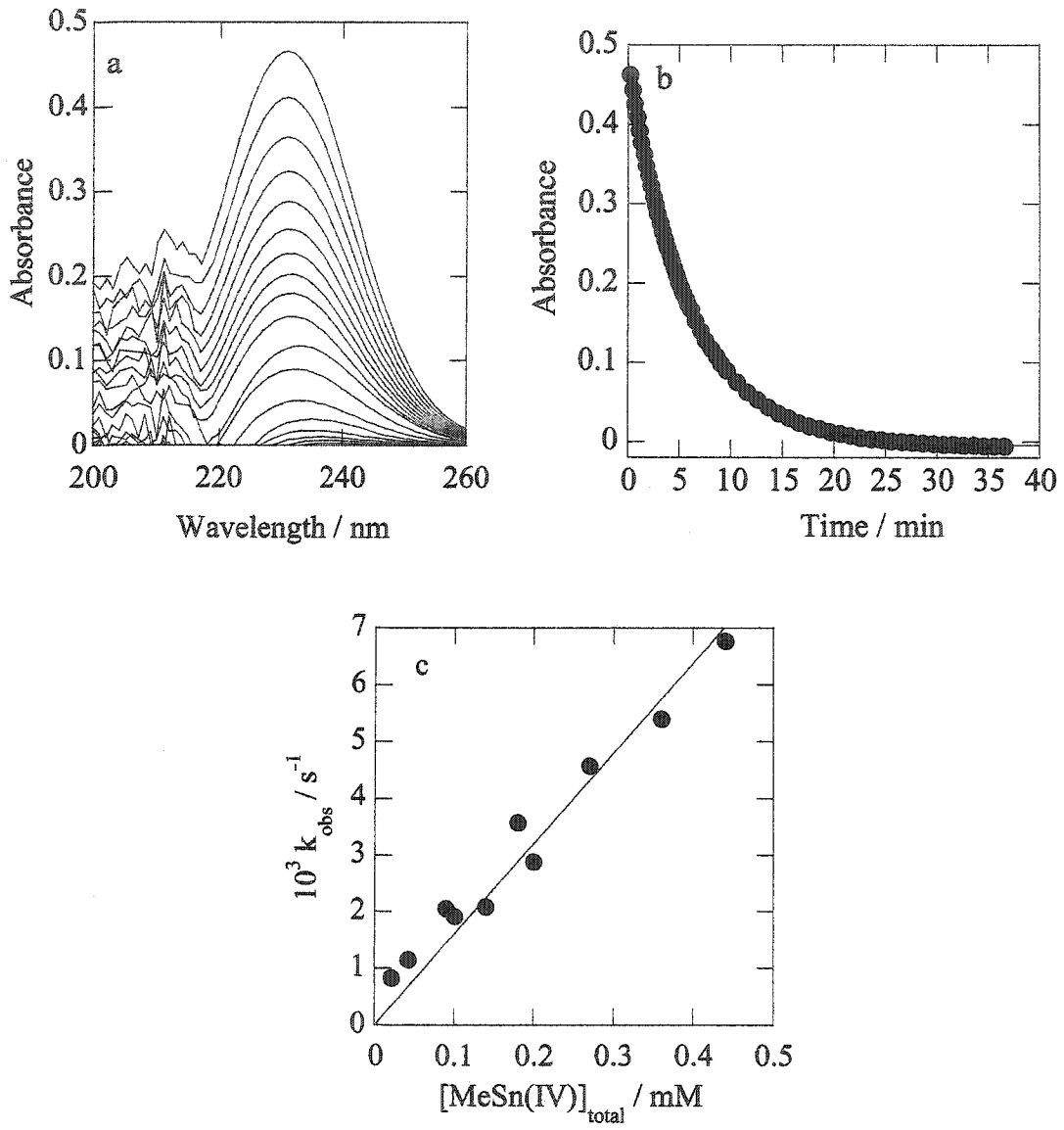

Figure 5.11 (a) Evolution of the UV spectrum of an aqueous solution of 0.020 mM $HgCl_4^{2-}$ upon addition of 0.20 mM MeSn(IV) at pH 10.0 and 20.1°C in the presence of 1.0 M Cl^-. Spectra recorded over 40 min. (b) Kinetic profile of the reaction at 232 nm. The solid line is the single exponential fit to the experimental data. (c) Dependence of the pseudo-first-order rate constants measured at pH 10.0 and 20.1°C on the concentration of the excess reagent, MeSn(IV).

Table 5.8 Observed rate constants for the reactions of monomethyl tin with 0.02 mM Hg^{2+} at pH 10, 1M KCl and 20.1°C

[MeSn(IV) mM	$10^3 k_{obs}$ s^{-1}
0.021	0.832 ± 0.003
0.042	1.15 ± 0.02
0.09	2.05 ± 0.03
0.10	1.92 ± 0.05
0.14	2.08 ± 0.03
0.18	3.56 ± 0.06
0.20	2.88 ± 0.03
0.27	4.57 ± 0.05
0.36	5.40 ± 0.04
0.44	6.77 ± 0.06

Table 5. 9 pH dependence of the observed rate constants for the reaction of 0.5 mM MeSn(IV) with 0.05 mM Hg(II) in 1.0 M KCl at 30.1°C

pH ± 0.01	$10^3 k_{obs}$ s^{-1}
3.35	-[a]
5.51	-
6.95	0.282 ± 0.005
8.08	0.395 ± 0.002
8.83	1.97 ± 0.01
9.27	23.7 ± 0.2
9.62	52.3 ± 0.3
9.87	53.5 ± 0.5
10.02	52.7 ± 0.4

[a] No reaction detected.

where k_1 and k_2 are the rate constants for the reaction of $MeSn(OH)_3$ and $MeSn(OH)_4^-$ respectively and K_{a4} is the hydrolysis constant of $MeSn(OH)_3$. Fitting the experimental data to eq. 20, we find that the rate constant for the reaction of $MeSn(OH)_4^-$ is (156 ± 3) M^{-1} s^{-1}. The acidity constant determined from this experiment, (2.9 ± 1.5) x 10^{-10} is comparable with 1.82 x 10^{-12} reported from deStefano et.al., Table 5.1 for hydrolysis at 25°C.[20]

5.8. Effect of temperature

The dependence of the intrinsic (pH-independent) rate constants on temperature can be used to calculate the activation enthalpy $\Delta H^{\ddagger}$ and activation entropy $\Delta S^{\ddagger}$ for the methylation reaction.[47] As expected, the rate constants increase with temperature. The results for experiments in 1.0 M KCl, and pH 10.0 are summarized in Table 5.10. The Eyring plot should be linear, eq 21:

$$\ln(k/T) = \ln(k_B/h) + \Delta S^{\ddagger}/R - \Delta H^{\ddagger}/(RT) \qquad (21)$$

where k_B is the Boltzmann constant, h is Planck's constant and R is the gas constant. The activation parameters, determined from the slope and intercept of Eyring plots, Figure 5.12, are $\Delta H^{\ddagger}$ = (70 ± 2) kJ/mol and $\Delta S^{\ddagger}$ = - (27 ± 1) J/K.mol, $\Delta H^{\ddagger}$ = 57 ± 1 kJ/ mol and $\Delta S^{\ddagger}$ = (- 46 ± 3) J/K.mol and $\Delta H^{\ddagger}$ = (88 ± 5) kJ/mol and $\Delta S^{\ddagger}$ = (57 ± 11) J/K.mol for the reaction of Hg(II) with $Me_3Sn(IV)$, $Me_2Sn(IV)$ and MeSn(IV) respectively. The errors in the activation parameters are calculated from the error propagation formula and the errors

Table 5.10. Temperature-dependence of the rate constants for reactions of methyltin compounds with Hg(II) solutions at pH 10.0, 1.0 M KCl

MeSn(IV)		$Me_2Sn(IV)$		$Me_3Sn(IV)$	
T	k	T	K	T	k
°C	$M^{-1} s^{-1}$	°C	$M^{-1} s^{-1}$	°C	$M^{-1} s^{-1}$
5.6	2.51 ± 0.05	10.5	0.66 ± 0.02	10.5	0.025 ± 0.001
11.5	4.68 ± 0.03	10.8	0.68 ± 0.03	11.3	0.031 ± 0.002
11.7	4.16 ± 0.07	20.5	1.61 ± 0.04	21	0.078 ± 0.005
20.5	17.4 ± 0.2	22.4	1.85 ± 0.02	23.2	0.084 ± 0.003
20.7	24.9 ± 0.5	29.9	3.50 ± 0.04	29.8	0.19 ± 0.02
29.7	56.1 ± 0.2	30.2	3.85 ± 0.02	30.2	0.19 ± 0.01
29.9	67.6 ± 0.8	38.9	6.80 ± 0.01	38.6	0.43 ± 0.05
38.2	130 ± 10	38.9	6.87 ± 0.04	47.2	0.89 ± 0.04
38.9	123 ± 12	48.9	13.1 ± 0.2		

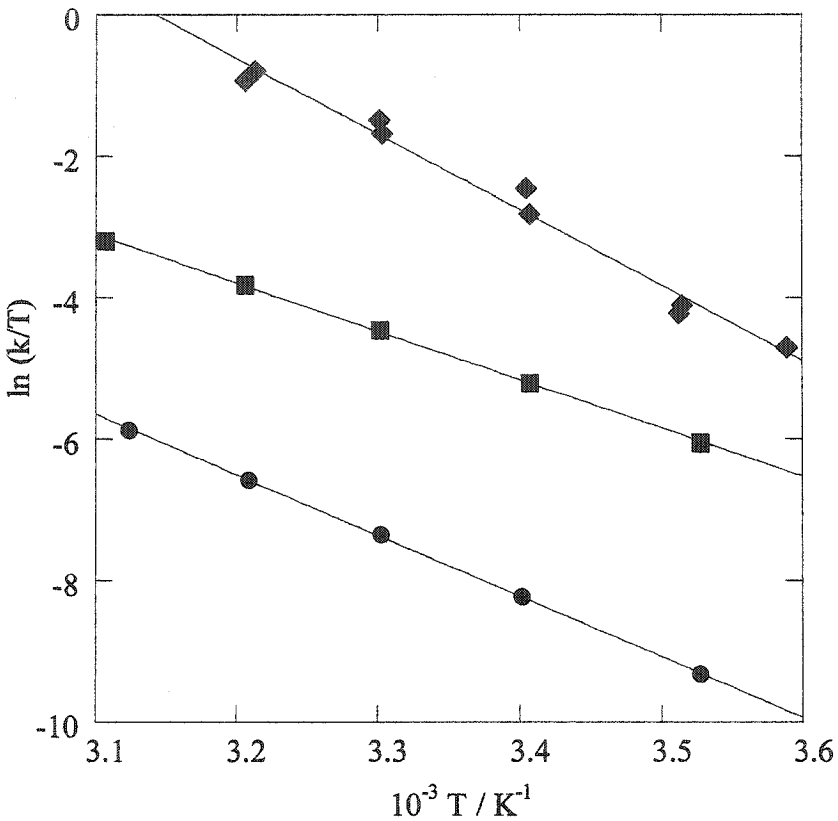

Figure 5.12 Eyring plots for the reaction of (●) $Me_3Sn(IV)$, (■) $Me_2Sn(IV)$ and (◆) MeSn(IV) with Hg(II) at pH 10.0 and 1.0 M KCl.

in temperature (±0.1K) and rate constants (from non-liner regression analysis).[48]

5.9 Mechanistic analysis

Kinetics of reactions with excess of methyltin compound is pseudo-first-order and the observed rate constants depend linearly on methyltin concentration, allowing the determination of second-order rate constants. We found that, for reactions at 20°C, pH 10 and 1M KCl the order of the second-order rate constants is MeSn(IV) > $Me_2Sn(IV)$ > $Me_3Sn(IV)$, Figure5.13.

The second order rate constants are strongly depended on the pH, mainly due to the pH effect on methyltin species distribution. For reactions run in 1M KCl, the predominant form of Hg(II) is $HgCl_4^{2-}$ for pH 1 to 10.5 while hydroxide forms predominate the methyl tin speciation. Controversially to other studies where the reactions of $HgCl_4^{2-}$ or $Me_nSn(OH)^{4-n}$ are considered to be irrelevant to the overall kinetics,[33,34] we show that instead, the contribution of these species is the most important one. Based on our results the rate law in these conditions is, eq.22:

$$-d[Hg^{2+}]/dt = (k_{HgCl4}\,[HgCl_4^{2-}] + k_{HgCl3}\,[HgCl_3^{-}])\,[Me_nSn(OH)^{4-n}] \qquad (22)$$

The reaction rates were close to zero in acid solutions where the hydroxides concentrations are close to zero and become faster when increasing the pH up to 10.5.

Also, the involvement of hydroxide-methyl tin species in these reactions means that the order of the second-order rate constants cannot be explained with the charge of

the ionic species $MeSn^{3+}$, Me_2Sn^{2+} and Me_3Sn^{+}. Most probably, the rate constants of these reactions will increase for compounds with weaker $C^{\delta-} - Sn^{\delta+}$ bonds. According to Neuman[36] the bond polarization $C^{\delta-} - Sn^{\delta+}$, which is there in principle may be changed by substitution at C and/or Sn: the presence of electron-donor groups will increase the rate of scission of the C – Sn bond. This complies with the result of our experiments that the rate of mercury methylation by methyltin compounds increases when the number of electron-donating groups such as OH^- increases. Going from trimethyltin to dimethyltin and monomethyltin, the number of Me^- groups decreases and the number of OH^- groups increases leading to higher rate constants of the reaction of MeSn(IV) with Hg^{2+} as compared to $Me_2Sn(IV)$ and $Me_3Sn(IV)$ complexes.

The effect of chloride concentration on kinetics of $Me_3Sn(OH)$ with Hg(II) demonstrates the consequences of mercury speciation in the reaction rate and mechanism. Our results show that $HgCl_2$ is the least active species (rate constant is insignificantly different from zero), followed by $HgCl_4^{2-}$ ($k_{HgCl4} = 0.46 \pm 0.04\ M^{-1}\ s^{-1}$) and the fastest $HgCl_3^-$ ($k_{HgCl3} = 1.0 \pm 0.1\ M^{-1}\ s^{-1}$). This trend coincides with the trend of formation constants of these chloride mercuric complexes: the more stable the complex, the less active it is in the reaction with tri methyl tin hydroxide. This aspect suggests that the mechanism of the reaction involves the cleavage of the chloride ion from Hg – Cl bond during the slowest step of the reaction. The Hg – Cl bond is stronger at $HgCl_2$ ($K_{HgCl2} = 3.2 \times 10^6$), followed by $HgCl_4^{2-}$ ($K_{HgCl4} = 12.6$) and the weakest $HgCl_3^-$ ($K_{HgCl3} = 9.3$).

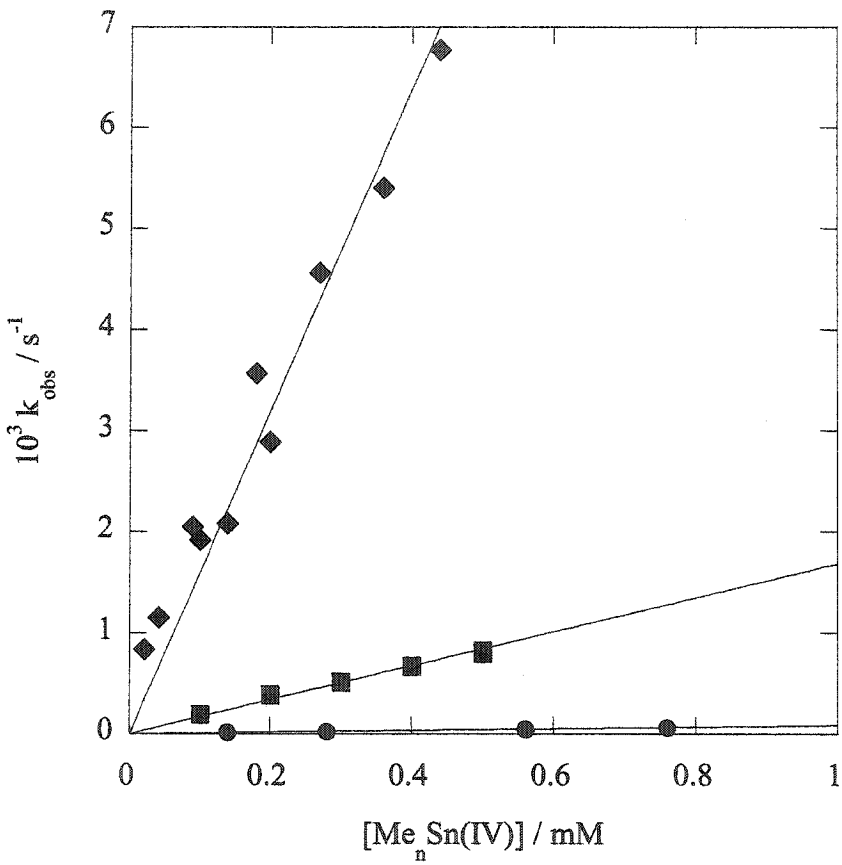

Figure 5.13 Dependence of the observed rate constant from total concentration of (●) $Me_3Sn(IV)$, (■) $Me_2Sn(IV)$ and (◆) MeSn(IV) for their reaction with 0.02 mM Hg^{2+} at pH 10, 1.0 M KCl and 20.1°C

The activation parameters, determined for the reaction of a Hg(II) solution at pH 10.0 and 1 M KCl with mono-, di-, and tri- methyl tin hydroxides, show that the differences in activation enthalpies are not very large but the differences in activation entropies are quite evident. The high negative values of $\Delta S^{\ddagger}$ for the reactions of $Me_3Sn(IV)$ and $Me_2Sn(IV)$ suggest a bimolecular reaction with a highly organized transition state, similar with mechanism proposed for the S_E2 reactions of R_4Sn compounds with chloride mercuric complexes: [44]

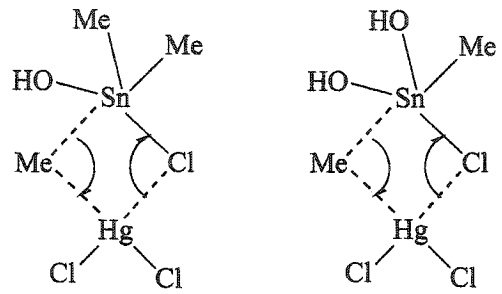

The positive value of $\Delta S^{\ddagger}$ for the reaction of MeSn(IV) suggests a one molecular mechanism. The presence of three OH groups may account for a high polarizability of the C – Sn bond and formation of "separate" moieties of $Me^{-\delta}$ and $Sn^{+\delta}(OH)_3^2$. Then, the unstable $Me^{-\delta}$ reacts readily with Hg^{2+} explaining the high rate constants of the reaction of MeSn(IV) at pH 10.5 and 1M KCl, with Hg^{2+}.

5.10. Conclusion

The results of this work demonstrate quite clearly that methyl tin compounds are a source of abiotic methylation of inorganic mercury in the aquatic environment. Since the

reactions are faster in high pH and chloride concentrations, their contribution to methyl mercury formation will be more important in seawater. Speciation calculations of sea water[49] show that Hg(II) exist 100% as $HgCl_4^{2-}$ even in the presence of 1μM fulvic acid as complexing agent. Also, Donard and Weber[50] have concluded that in simulated seawater methyl tin compounds are mostly as neutral hydroxide species. Taking into account this information, the average concentrations of methyltins, and the rate constant for pH 8 and 25°C (ca. 0.8 M^{-1} s^{-1}) which is typical for seawaters, we calculate the half time of mercury in seawater, due to its reaction with mono methyl tin (which is the fastest and the most abundant of methyltin compounds) is 2.8 years. The rate of methylmercury formation in these conditions is ca. 0.4pg L^{-1} day^{-1}. Considering that about 85% of inorganic mercury is converted from this reaction to methylmercury, makes clear that this reaction is an important one in mercury methylation in the aquatic environment.

References

(1) Arena, G.; Purrello, R.; Rizzarelli, E.; Gianguzza, A.; Pellerito, L. *J. Chem. Soc. Dalton Trans.* **1989**, 773-777.

(2) Blunden, S. J.; Hill, R. *Inorg. Chim. Acta* **1990**, *177*, 219-223.

(3) deStefano, C.; Foti, C.; Gianguzza, A.; Martino, M. *J. Chem. Eng. Data* **1996**, *41*, 511-515.

(4) Dahab, O. A.; El-Sabrouti, M. A.; Halim, Y. *Environ. Pollut.* **1990**, *63*, 329-344.

(5) Ranke, J. *Environ. Sci. Technol.* **2002**, *36*, 1539-1545.

(6) Hamasaki, T.; Nagase, H.; Yoshioka, Y.; Sato, T. *Crit. Rev. Environ. Sci. Technol.* **1995**, *25*, 45-91.

(7) Thompson, J. A.; Sheffer, M. G.; Pierce, R. C.; Chau, Y. K.; Cooney, J. J.; Cullen, W. R.; Maguire, R. J. "Organotin compounds in the aquatic environment," NRCC/CNRC, 1985.

(8) Alzieu, C.; Thibaud, Y. *Bull. Acad. Nat. Med.* **1983**, *167*, 473-482.

(9) Laughlin, R. B.; Linden, O. S. *Ambio* **1985**, *14*, 88-94.

(10) Donard, O. F. X.; Rapsomanikis, S.; Weber, J. H. *Anal. Chem.* **1986**, *58*, 772-777.

(11) Craig, P. J.; Rapsomanikis, S. *Environ. Sci. Technol.* **1985**, *19*, 726-730.

(12) Hamasaki, T.; Nagase, H.; Sato, T.; Kito, H.; Ose, Y. *Appl. Organomet. Chem.* **1991**, *5*, 83-90.

(13) Lee, D. S.; Weber, J. H. *Appl. Organomet. Chem.* **1988**, *2*, 435-440.

(14) Rapsomanikis, S.; Weber, J. H. *Environ. Sci. Technol.* **1985**, *19*, 352-356.

(15) Chau, Y. K.; Wong, P. T. S.; Mojesky, C. A.; Carty, A. J. *Appl. Organomet. Chem.* **1987**, *1*, 235-239.

(16) Hynes, M. J.; O'Dowd, M. *J. Chem. Soc. Dalton Trans.* **1987**, 563-566.

(17) Sousa, G. F. d.; Filgueiras, C. A. L.; Darensbourg, M. Y.; Reibenspies, J. H. *Inorg. Chem.* **1992**, *31*, 3044-3049.

(18) Farrer, H. N.; McGrady, M. M.; Tobias, R. S. *J. Am. Chem. Soc.* **1965**, 5019-5025.

(19) Ahmet, M. T.; Houlton, A.; Frampton, C. S.; Miller, J. R. *J. Chem. Soc. Dalton Trans.* **1993**, 3085-3092.

(20) deStefano, C.; Foti, C.; Gianguzza, A.; Marrone, F.; Sammartano, S. *Appl. Organomet. Chem.* **1999**, *13*, 805-811.

(21) deStefano, C.; Foti, C.; Gianguzza, A.; Millero, F. J.; Sammartano, S. *J. Solution Chemistry* **1999**, *28*, 959-972.

(22) Hynes, M. J.; Keely, J. M.; McManus, J. *J. Chem. Soc. Dalton Trans.* **1991**, 3427-3429.

(23) Takahashi, A.; Natsume, T.; Koshino, N.; Funahashi, S.; Inada, Y.; Takagi, H. D. *Can. J. Chem.* **1997**, *75*, 1084-1092.

(24) Barbieri, R.; Silvestri, A. *Inorg. Chim. Acta* **1991**, *188*, 95-98.

(25) Natsume, T.; Aizawa, S.-i.; Hatano, K.; Funahashi, S. *J. Chem. Soc. Dalton Trans.* **1994**, 2749-2753.

(26) Beckman, J.; Henn, M.; Jurkschat, K.; Schurmann, M.; Dakternieks, D.; Duthie, A. *Organometallics* **2002**, *21*, 192-202.

(27) Howell, G. N.; O'Conor, M. J.; Bond, A. M.; Hudson, H. A.; Hanna, P. J.; Strother, S. *Aust. J. Chem.* **1986**, *39*, 1166-1175.

(28) Woggon, H.; Klein, S.; Jehle, D.; Zydek, G. *Nahrung* **1984**, *28*, 851-862.

(29) Cerrati, G.; Bernhard, M.; Weber, J. H. *Appl. Organomet. Chem.* **1992**, *6*, 587-595.

(30) Horvat, M.; Covelli, S.; Faganeli, J.; Logar, M.; Mandic, V.; Rajar, R.; Sirca, A.; Zagar, D. *Sci. Total Environ,* **1999**, *237/238*, 43-56.

(31) Rosenkranz, B.; Bettmer, J.; Buscher, W.; Breer, C.; Cammann, K. *Appl. Organomet. Chem.* **1997**, *11*, 721-725.

(32) Brinckman, F. E., Ed. *Environmental inorganic chemistry of main group elements with special emphasis on their occurrence as methyl derivatives*; VCH: Deerfield Beach, Fla., 1985.

(33) Bellama, J. M.; Jewett, K. L.; Nies, J. D. In *Environmental inorganic chemistry*; Irgolic, K. J., Martell, A. E., Eds.; VCH: Deerfield Beach, Fla., 1985; pp 239- 247.

(34) Jewett, K. L.; Brinckman, F. E.; Bellama, J. M. In *Organometals and organometalliods: Occurrence and fate in the environment*; Brinckman, F. E., Bellama, J. M., Eds.; American Chemical Society: Washington, D.C., 1978; Vol. 82, pp 158 -185.

(35) Davies, A. *Organotin chemistry*; VCH: New York, 1997.

(36) Neuman, W. P., Ed. *The organic chemistry of tin*; Wiley: Toronto, 1970.

(37) Tobias, R. S. In *Organometals and organometalloids: Occurrence and fate in the environment*; Brinckmann, F. E., Bellama, J. M., Eds.; American Chemical Society: Washington, D.C., 1978; Vol. 82.

(38) Grant, G. J., Ed. *Mercury: Inorganic and coordination chemistry*; Wiley: Chichester, New York, 1994; Vol. 4.

(39) Smith, R. M.; Martell, A. E. *Critical stability constants*; Plenum Press: New York, 1976; Vol. 4.

(40) Fukuzumi, S.; Kochi, J. K. *J. Phys. Chem.* **1981**, *85*, 648-654.

(41) Fukuzumi, S.; Kochi, J. K. *J. Am. Chem. Soc.* **1980**, *102*, 7290-7297.

(42) Kashin, A. N.; Beletskaya, I. P.; Reutov, O. A. *ZH Organ. Khim.* **1979**, *15*, 673-677.

(43) Abraham, M. H.; Johnston, G. F. *J. Chem. Soc.* **1970**, *A*, 188-192.

(44) Abraham, M. H.; Johnston, G. F. *J. Chem. Soc.* **1970**, *(A)*, 193-198.

(45) Abraham, M. H.; Irving, R. J.; Johnston, G. F. *J. Chem. Soc.* **1970**, *(A)*, 199-202.

(46) Templet, P.; McDonald, J. R.; McGlynn, S. P. *J. Chem. Phys.* **1973**, *56*, 5746.

(47) Espenson, J. H. *Chemical kinetics and reaction mechanisms*; 2nd ed.; McGraw-Hill, Inc.: New York, 1981.

(48) Morse, P. M.; Spencer, M. D.; Wilson, S. R.; Girolami, G. S. *Organometallics* **1994**, *13*, 1646-1655.

(49) Turner, D. R.; Whitfield, M.; Dickson, A. G. *Geochim. Cosmochim. Acta* **1981**, *45*, 855-862.

(50) Donard, O. F. X.; Weber, J. H. *Environ. Sci. Technol.* **1985**, *19*, 1104.

Chapter 6

Thesis Conclusions and Claims to Original Research

6.1 Conclusions

This study shows the importance of the abiotic pathway of mercury methylation in the aquatic environment. The amount of methylmercury formed and the rate of methylation are dependent on several environmental factors such as pH, temperature, and the presence of complexing agents, especially the presence of chloride. It also depends on mercury speciation in a certain environment and the chemical properties of the methylation agents.

Chapter 3 demonstrates the role that methyl iodide has in the biogeochemistry of mercury in the aquatic environment. Mercuric ions promote the hydrolysis of methyl iodide yielding mercuric iodide compounds (HgI^+ and HgI_2) and methanol. Hg^0, which is found in appreciable amounts in natural water, reacts with methyl iodide giving about 1% methyl mercury iodide. Considering that the natural systems are not in equilibrium and the inputs of mercury in the aquatic environment are continuous, the methylation of Hg^0 by methyl iodide can have an important impact in the total burden of methyl mercury in the water column.

Chapter 4 shows that methylation of mercuric ions by methylcobalamine is not an enzymatic reaction. The methylmercury formation is almost quantitative while the reaction rate is highly dependent on experimental condition. The rate constant almost doubles when the $[H^+]$ concentration decreases 10 times. Increasing the ionic strength

using non-coordinating ions, increases significantly the rate constant, while the presence of chloride slows down the reaction when $HgCl^+$ is formed and upon formation of $HgCl_2$ the reaction shuts down completely.

Reactions of mercuric ions with methyl tin compounds, presented in chapter 5 demonstrate the importance of these compounds as very active methyl donors towards mercury. These transmethylation reactions are fast and methyl mercury yield is almost quantitative. MeSn(IV) reacts faster then $Me_2Sn(IV)$ and $Me_3Sn(IV)$. We conclude that the hydroxo-complexes of methyl tin compounds are more active than ionic forms or chloride compounds. Also the reactivity of $HgCl_2$ is smaller that of $HgCl_4^{2-}$, while $HgCl_3^-$ is the fastest in the reaction with $Me_3Sn(IV)$. The optimum conditions for these reactions are high pH and chloride concentration which make them suitable for methylation of mercury in the seawater environment.

Finally, we conclude that the chemical methylation of mercury is highly dependent on the specific environmental conditions. The mechanisms of the reaction and the rates laws presented in this thesis will allow a better understanding of the methylmercury formation in the aquatic environment.

6.2 Claims to the original research

Formation of methylmercury in the aquatic environment is a dilemma that have puzzled environmental chemists for a long time now. The general cliché is that methylmercury is formed biologically from certain strains of bacteria, mainly by sulfate reducing bacteria. The chemical formation of methylmercury is only recently considered as a possible

pathway and still the results are scarce and quite controversial. For the first time in this thesis we accomplished a comprehensive study of the mechanisms of the reactions of chemical methylation of mercury by some of the methyl donors known to be present in natural waters. The rate laws of these reactions accomplished in different experimental conditions are presented for the first time in this thesis. They will allow a general estimation of the chemical methylation of mercury in known environments under specific conditions of pH, ionic strength, chloride and other complexing agent presence.

We show that, under certain conditions such as the presence of methyl iodide Hg^0 can be a source of methyl mercury formation in the aquatic environment.

pH, ionic strength and the presence of chloride in natural waters have a great role in the chemical methylation of mercury. Changing the experimental conditions can either facilitate the reactions so that they become instantaneous and give quantitative yields of methylmercury or can stop them completely. We show for the first time that the importance of the abiotic methylation and the role of different methyl donors can only be evaluated under specific environmental conditions.

APPENDIX

A-1. Derivation of pH-dependent rate constants formula

The rate law for the reaction of $[Hg^{2+}]$ with the methylation reagent B, eq. 1:

$$[Hg^{2+}] + B \rightarrow \text{products} \quad (1)$$

is, eq. 2:

$$\text{rate} = k\,[Hg^{2+}]\,[B] \quad (2)$$

where, k is the rate constant and $[Hg^{2+}]$ and [B] the concentrations of mercuric ion and the methylating agent respectively. Increasing the pH promotes the hydrolysis of $[Hg^{2+}]$, eq. 3-4:

$$Hg^{2+} + H_2O \leftrightarrows HgOH^+ + H^+ \qquad K_{a1} = [HgOH^+]\,[H^+] / [Hg^{2+}] \quad (3)$$

$$HgOH^+ + H_2O \leftrightarrows Hg(OH)_2 + H^+ \qquad K_{a2} = [Hg(OH)_2]\,[H^+] / [HgOH^+] \quad (4)$$

The total concentration of mercuric ions in solution is, eq.5:

$$C_{Hg} = [Hg^{2+}] + [HgOH^+] + [Hg(OH)_2] \quad (5)$$

Substituting eq. 3 and 4 to eq. 5, the total concentration of mercuric ions is, eq. 6:

$$C_{Hg} = [Hg^{2+}] (1 + K_{a1} / [H^+] + K_{a1} K_{a2} / [H^+]^2) \quad (6)$$

In the experimental conditions when only C_{Hg} is known, the rate law is written as, eq.7:

$$\text{rate} = k_{measured} C_{Hg} [B] = k_{measured} [Hg^{2+}] (1 + K_{a1} / [H^+] + K_{a1} K_{a2} / [H^+]^2) [B] \quad (7)$$

Comparing eq.2 and eq. 7, we find this equation for the dependence of the measured rate constants from pH and the calculation of the pH-independent rate constant k, eq. 8-9:

$$k = k_{measured} (1 + K_{a1} / [H^+] + K_{a1} K_{a2} / [H^+]^2) \quad (8)$$

$$k_{measured} = k [H^+]^2 / ([H^+]^2 + K_{a1} [H^+] + K_{a1} K_{a2}) \quad (9)$$

A-2 Derivation of Cl-dependent rate constants formula

The addition of chloride will affect the speciation of mercuric-chloride complexes present in the solution, eq. 10-13:

$$Hg^{2+} + Cl^- \leftrightarrows HgCl^+ \qquad K_1 = [HgCl^+] / [Hg^{2+}] [Cl^-] \quad (10)$$

$$HgCl^+ + Cl^- \leftrightarrows HgCl_2 \qquad K_2 = [HgCl_2] / [HgCl^+] [Cl^-] \quad (11)$$

$$HgCl_2 + Cl^- \leftrightarrows HgCl_3^- \qquad K_3 = [HgCl_3] / [HgCl_2] [Cl^-] \quad (12)$$

$$HgCl_3^- + Cl^- \leftrightarrows HgCl_4^{2-} \qquad K_4 = [HgCl_4^{2-}] / [HgCl_3^-] [Cl^-] \quad (13)$$

The total concentration of mercuric ion in presence of chloride is, eq. 14:

$$C_{Hg} = [Hg^{2+}] + [HgCl^{+}] + [HgCl_2] + [HgCl_3^{-}] + [HgCl_4^{2-}]$$

$$= [Hg^{2+}] (1+ K_1 [Cl^{-}] + K_1 K_2 [Cl^{-}]^2 + K_1 K_2 K_3 [Cl^{-}]^3 + K_1 K_2 K_3 K_4 [Cl^{-}]^4) \quad (14)$$

Assuming that all mercury- chloride complexes react with the methylating agent B, the rate law is, eq. 15:

$$\text{rate} = (k_0 [Hg^{2+}] + k_1 [HgCl^{+}] + k_2 [HgCl_2] + k_3 [HgCl_3^{-}] + k_4 [HgCl_4^{2-}]) [B]$$

$$= [Hg^{2+}] (k_0 + k_1 K_1 [Cl^{-}] + k_2 K_1 K_2 [Cl^{-}]^2 + k_3 K_1 K_2 K_3 [Cl^{-}]^3 + k_4 K_1 K_2 K_3 K_4 [Cl^{-}]^4) [B] \quad (15)$$

where k_0, k_1, k_2, k_3 and k_4 are the rate constants for the reaction of the methylating agent B with Hg^{2+}, $HgCl^{+}$, $HgCl_2$, $HgCl_3^{-}$ and $HgCl_4^{2-}$ respectively. Using the total concentration of mercury in solution in the rate law, we find, eq. 16:

$$\text{rate} = k_{meas} C_{Hg} [B] = k_{meas} [Hg^{2+}] (1+ K_1 [Cl^{-}] + K_1 K_2 [Cl^{-}]^2 + K_1 K_2 K_3 [Cl^{-}]^3 + K_1 K_2 K_3 K_4 [Cl^{-}]^4) [B] \quad (16)$$

Comparing equation 15 with equation 16, yields eq. 17:

$$k_{meas.} = k_0 + k_1 K_1 [Cl^{-}] + k_2 K_1 K_2 [Cl^{-}]^2 + k_3 K_1 K_2 K_3 [Cl^{-}]^3 + k_4 K_1 K_2 K_3 K_4 [Cl^{-}]^4 \quad (17)$$

A-3 Temperature dependence of rate constants - Eyring plots

The classical way of expressing the effect of temperature on the rate constants is the Arrhenius theory. The basic formula of this theory is the Arrhenius equation, eq 18:

$$k = A \exp(-E_a / RT) \tag{18}$$

where, k is the rate constant, A is the Arrhenius pre-exponential coefficient, E_a the activation energy, R the gas constant and T the temperature.

Latter Eyring showed the way to calculate the Arrhenius pre-exponential parameter and expressed the activation energy in terms of the free energy of activation $\Delta G^{\ddagger}$, eq. 19:

$$k = k_B T / h \exp(-\Delta G^{\ddagger} / RT) \tag{19}$$

where k_B and h are the Boltzman and Planck's constants respectively. Knowing the relationship of the free energy of activation $\Delta G^{\ddagger}$ with the enthalpy and enthropy of activation ($\Delta H^{\ddagger}$ and $\Delta S^{\ddagger}$ respectively), eq 20:

$$\Delta G^{\ddagger} = \Delta H^{\ddagger} - T \Delta S^{\ddagger} \tag{20}$$

one can find the equation of the Eyring plot, eq. 21:

$$\ln(k/T) = \ln(k_B/h) + \Delta S^{\ddagger}/R - \Delta H^{\ddagger}/(RT) \quad (21)$$

The slope and intercept of the linear Eyring plots are used for the calculation of the activation parameters